Vibrational Spectroscopy of Carboranes and Parent Boranes and Its Capabilities in Carborane Chemistry

L. A. LEITES

Institute of Organo-Element Compounds, Russian Academy of Sciences, Moscow, Russia

Received July 10, 1991 (Revised Manuscript Received December 9, 1991)

Contents

0009-2665/92/0792-0279$10.00/0

Larissa A. Leites born in Moscow, graduated from the Chemical Department of Moscow State University. Her Ph.D. dissertation (1965) was devoted to the vibrational spectra of Si-, Ge-, and Sn-containing compounds and the problem of $\sigma-\pi$ conjugation. From 1965 up to the present she has been working at the Laboratory of molecular spectroscopy of the Nesmeyanov Institute of Organo-Element Compounds (previously USSR Academy of Sciences) and is the coauthor of more than 170 publications. In 1987 she received the Dr.Sci. degree for the study of the vibrational spectra of carboranes. Her main research interests are in the area of the vibrational spectroscopy of organoelement and organometallic compounds (with a current emphasis on Raman spectroscopy) where she is solving the puzzles of their structure, bonding nature, and intermolecular interactions.

I. Introduction

Vibrational spectroscopy at its present level encompasses not only infrared (IR) but necessarily also Raman spectra and takes into account not only band frequencies but also intensities, states of polarization, half-widths, and contours. In combination with group theoretical considerations, it is a powerful tool in the elucidation molecular structures and can provide valuable information on intra- and intermolecular interactions as well.

However, an analysis of the current literature on carborane chemistry reveals that the main physical methods used in this field are NMR and X-ray diffraction, while vibrational spectroscopy serves only as a subsidiary, second-grade technique. As a rule, only IR spectra in a limited region are utilized, and the frequencies are presented in the experimental sections of synthetic papers merely as a set of boring figures. Since vibrational spectra can be approached through both IR and Raman methods, with the Raman spectrum of a molecule being complementary to and often even more informative than the IR spectrum, the high potential of vibrational spectroscopy has been left virtually unused.

Meanwhile the modern developments of laser Raman and Fourier-transformed Raman instrumentation enable Raman spectra to be obtained for most samples; this is especially relevant for carboranes which are generally white solids.

This review is written with two aims in mind: to give the carborane chemists a chance to look at familiar objects from a new viewpoint, i.e. through the eyes of a vibrational spectroscopist, and to demonstrate the possibilities of this method.

The review covers all vibrational studies on carboranes and parent *closo*-boranes published after the beginning of carborane era in 1963 and available in Moscow in 1991. It is the first attempt to treat in a comprehensive fashion all spectroscopic information and includes those Russian papers which have sometimes proved unavailable abroad. Only a few lines were devoted to vibrational spectroscopy in the review by Onak[1] in 1982.

Synthetic papers in which the carboranes obtained are characterized by IR spectroscopy are not included. References to such papers can be found in the tables of the monograph by Grimes[2] and in some reviews.

The full vibrational spectra are now available for quite a few "large" icosahedral structures, namely, the *closo*-borate anions $B_{12}X_{12}^{2-}$ (X = H, D, Cl, Br, I), the *closo*-carboranes $C_2B_{10}H_{12}$ and $C_2H_2B_{10}Cl_{10}$, and several species containing heteroatoms, $CHB_{10}H_{10}P$ and $CHB_{10}H_{10}As$ as well as $B_{10}H_{10}Si_2Me_2$. Many monosubstituted icosahedral *closo*-carboranes of the type $C_2B_{10}H_{11}X$ with various substituents X have also been studied. The complete vibrational data on "medium" polyhedra are limited to the "Archimedian antiprisms" $B_{10}X_{10}^{2-}$ (X = H, Cl, Br, I) and 1,10-$C_2B_8H_{10}$. In the case of "small" polyhedra, the spectra have been obtained for the octahedral species $B_6X_6^{2-}$ and 1,6-$C_2B_4H_6$ and also for the *closo*-carboranes 1,5-$C_2B_3H_5$ and 2,4-$C_2B_5H_7$. The data on *nido*-carboranes are scanty and involve 4,5-$C_2B_4H_8$ as well as several isomers of $C_2B_9H_{12}^-$ and their derivatives. Also, the spectra of a few π-dicarbollyl complexes of transition metals are available.

However, it is not the author's intention merely to enumerate spectral data impassively but to focus on the peculiar vibrational properties of caged systems caused by their specific electronic structures. The cluster rigidity, which clearly manifests itself in the vibrational spectrum, leads to some curious consequences, which significantly simplify the spectral interpretation and provide additional opportunities for using the spectra as an analytical aid.

The comparison of all the information available allows us to explore the spectral changes in the series $B_nX_n^{2-}$, n = 6, 10, 12; X = H, Cl, Br, I as well as $C_2B_{m-2}H_m$, m = 5–7, 10, 12 and to establish some general regularities.

In order to keep this survey to a reasonable size, analogies with other physical methods and quantum chemical results will not be discussed in detail.

To demonstrate the kind of novel information about carboranes that may be obtained by means of vibrational spectroscopy, two spectacular examples will be presented. The first example deals with the investigation of the molecular mobility and phase transitions of carboranes in the solid state and the second with the discovery of the ability of carboranes to serve as CH proton donors in hydrogen bonding.

The review has its roots in the author's long-term cooperation with the laboratories of the Moscow Institute of Organo-Element Compounds involved in carborane chemistry. Investigations of thousands of carborane-containing samples by Raman and IR

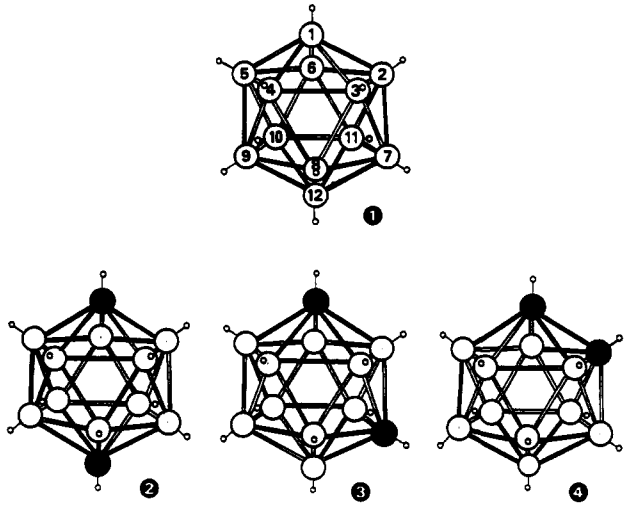

Figure 1. *closo*-Dodecaborate anion $B_{12}H_{12}^{2-}$ (1) and three isomers of dicarba-*closo*-dodecaborane $C_2B_{10}H_{12}$: 1,12-dicarba-*closo*-dodecaborane (*p*-carborane) (2), 1,7-dicarba-*closo*-dodecaborane (*m*-carborane) (3), 1,2-dicarba-*closo*-dodecaborane (*o*-carborane) (4). The symbols are as follows: ○, hydrogen atom; ●, carbon atom; ◯, boron atom.

methods have provided the experience necessary to accomplish this task.

II. Analysis of Vibrational Spectra of Icosahedral closo-Carboranes and Their "Precursors"—closo-Dodecaborate Anions

A. Peculiarities of Vibrational Spectra of the Three Isomers of Dicarba-*closo*-dodecaborane $C_2B_{10}H_{12}$

The most wide-spread carboranes are the icosahedral dicarba-*closo*-dodecaboranes $C_2B_{10}H_{12}$ (Figure 1; hereafter they will be referred to simply as "carboranes"). Their chemistry has been widely elaborated, their electronic structure has attracted much attention, and they find application in modern technology (see, e.g., the accompanying paper of Bregadze). For these reasons, the review will commence with a discussion of their vibrational spectra.

From the point of view of traditional vibrational spectroscopy, these compounds are not simple objects. Their molecules contain 24 atoms so, generally speaking, the spectra should consist of $3 \times 24 - 6 = 66$ fundamentals.

Among the three carborane isomers, the para isomer has the highest symmetry, its molecule belonging to the D_{5d} symmetry point group. According to the group theory, 66 normal modes of *p*-carborane are distributed among the symmetry species as follows:

$$\Gamma_{vib} = 6A_{1g} + 2A_{1u} + A_{2g} + 5A_{2u} + 6E_{2g} + 6E_{2u} + 7E_{1g} + 7E_{1u}$$

The selection rules for this spectrum are very strict. They permit 19 vibrations to show themselves only in the Raman spectrum and 12 others to appear only in the IR spectrum. In Raman, one should observe six polarized lines of A_{1g} species and 13 depolarized lines (seven of E_{1g} and six of E_{2g} species). "Ungerade" species should be active in IR. These are five parallel bands of A_{2u} species and seven perpendicular bands of E_{1u} species. In other words, the spectrum of the para isomer must obey the so-called "rule of mutual exclusion". Vibrations of A_{1u}, A_{2g}, and E_{2u} species are "silent", i.e. inactive either in the Raman or in the IR spectra. Such motions could, in principle, be detected by those methods, for which there are effectively no symmetry selection rules.

The molecules of *o*- and *m*-carboranes possess lower symmetries, belonging to the C_{2v} symmetry point group. Their 66 fundamentals are distributed among the symmetry species as follows:

$$\Gamma_{vib} = 21A_1 + 13A_2 + 16B_1 + 16B_2$$

The selection rules for their spectra are less strict, they allow all 66 vibrations to be active in the Raman spectra and all but the A_2 species in the IR spectra. Moreover, in this case the Raman activities need not be the reverse of the IR activities since neither structure has a center of inversion. Thus, theory predicts that on going from the carborane para isomer to the ortho and meta isomers the spectra must become significantly more complicated. However, these theoretical expectations are, in fact, not realized as is immediately seen from the experimental data.

The IR spectra of icosahedral carboranes (in a limited 700–3200-cm^{-1} region) were given merely as pictures or sets of frequency values in the first publications, devoted to the discovery of carboranes in 1963–1964, together with the first reasonable assignments.[3-7] The first Raman spectra of *o*- and *m*-carboranes were published in 1968 by Bukalov et al.[8] The spectra were obtained with a homemade Raman apparatus using a red laser and photoplates sensitive only up to 1500 cm^{-1}. The step by step progress in laser Raman technique enabled this group of investigators to gradually improve their results. Up to now they have studied the Raman spectra (beginning from 5 cm^{-1}) of the three carborane isomers in the solid state over the temperature range from 12 K to the melting point; polarization measurements have been carried out for the spectra of melts and solutions.[9-14] Complete IR spectra (from 50 cm^{-1}) were also obtained by the same authors for the three carborane isomers in the gaseous and solid phases as well as in solutions.[9-11,15]

The Raman and IR spectra of solid samples of *p*-, *m*-, and *o*-carborane at ambient temperature are presented in Figure 2. It is striking that the spectra of the three isomers are very similar: on going from the para isomer to less symmetrical ortho and meta isomers, one does not notice the actual symmetry lowering and the breakdown of the mutual exclusion rule because the spectral pattern does not *principally* change, it remains practically the same. Unexpectedly, some bands continue to be active only in the Raman and some others only in the IR. For instance, the most intense Raman line in the region of 760 cm^{-1} which corresponds to the totally symmetric polyhedron "breathing" mode has no IR analogue. Thus it is obvious that measurement of only the IR spectrum of a carborane (as chemists usually do) involves the loss of much information.

It is also of interest that the number of spectral features observed is much lower than predicted by group theory. This is true for the spectrum of the para isomer, where only 13 Raman lines are observed instead of the theoretical 19, and the more so for the meta and ortho

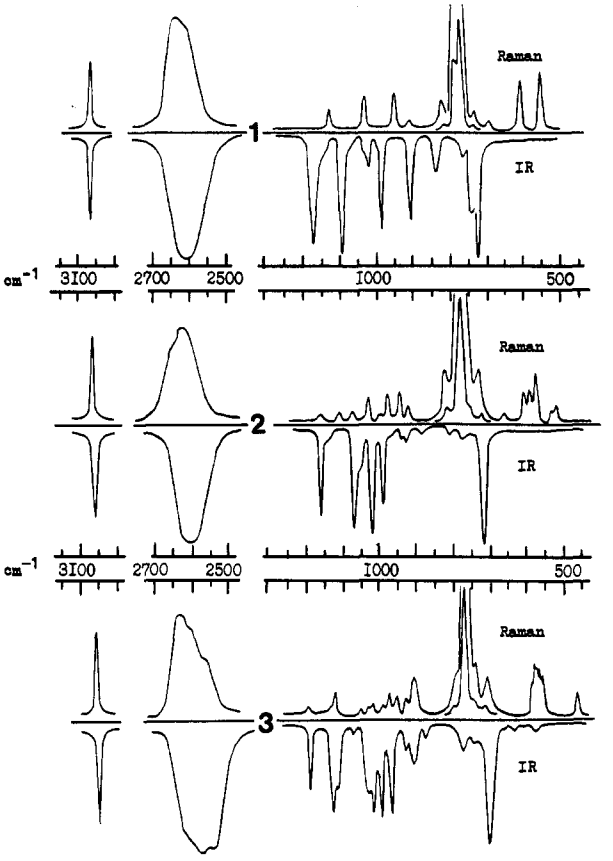

Figure 2. Vibrational (Raman and IR) spectra of three isomers of dicarba-*closo*-dodecaborane (solid samples, room temperature): 1, *p*-carborane; 2, *m*-carborane; 3, *o*-carborane. Low-frequency region is omitted because of the lack of spectral features.

isomers, which exhibit ca. 20 Raman lines instead of 66. The same is valid for their IR spectra.

The last but not least noteworthy feature of carborane vibrational spectra is the absence of low-frequency modes. The lowest experimentally observed band lies near 450 cm^{-1}. If this were really the case it would be of great importance, indicating the rigidity of the carborane cage. However, before making such a statement one must be sure that there are no low-frequency vibrations among the "silent" modes.

Thus, it is obvious that the vibrational spectra of icosahedral carboranes contravene the theoretical predictions. The vibrational behavior of carboranes seems to be unusual, as in other respects, and ideas extrapolated from classical views are only of limited use.

The authors[9,10] have suggested that the peculiarities observed are due to the higher effective symmetry of these molecules and that the key to rationalizing carborane spectra should be deduced from the spectrum of a regular icosahedron. It appears as though the carborane molecules "remember" that they are descended from this highly symmetrical polyhedron. Or, speaking more strictly, since the masses of B and C atoms and the B–B and B–C bond lengths are close in value and the bonding system is delocalized, some carborane vibrations do not "feel" the reduction of the polyhedron symmetry and continue to obey the selection rules of the I_h symmetry point group of an "average" icosahedron. The only possibility to verify this suggestion is a comparison of the spectrum of a carborane with that of the undistorted *closo*-dodecaborate anion $B_{12}H_{12}^{2-}$.

B. Analysis of Vibrational Spectra of *closo*-Dodecaborate Anions $B_{12}X_{12}^{2-}$ (X = H, D, Cl, Br, I)

The spectra of $B_{12}X_{12}^{2-}$ (the polyhedron is depicted in Figure 1) are very interesting not only as representatives of carborane parent compounds. These entities, which alone have the unique symmetry of a regular icosahedron, represent a challenging problem from the group theoretical point of view. Observation of the spectral changes in the series X = H, D, Cl, Br, I is very useful for a better understanding of the vibrational motions of two coaxial icosahedra. Normal coordinate analysis on these anions could provide force fields and normal mode eigenvectors and predict the frequencies of "silent" modes.

In addition, an analysis of the spectrum of $B_{12}H_{12}^{2-}$ should be useful in assigning the spectrum of elemental boron because some boron crystal modifications consist of boron icosahedra.[16]

Vibrational spectra of the undistorted anions $B_{12}H_{12}^{2-}$ and $B_{12}D_{12}^{2-}$ in aqueous solutions were obtained for the first time by Muetterties et al. in 1962 for sodium salts,[17] then in 1977 Raman spectra were published for potassium salts,[18] and finally, complete vibrational data[19] were presented in 1982 for the acid $(H_3O)_2B_{12}H_{12}$ as well as for aqueous solution of its potassium and cesium salts. The spectra of solid salts $M_2B_{12}H_{12}$ have been also published: the IR data for the salts with M = Ag, Cu, Hg, Na, K, Rb, Cs within the limited frequency range of 700–3700 cm^{-1} can be found in refs 20 and 21 and full vibrational data on $M_2B_{12}H_{12}$ and $M_2B_{12}D_{12}$ with M = K, Cs in ref 19.

As to the experimental results for halogenated *closo*-dodecaborate anions, only few data were available before 1982. Muetterties et al.[17] succeeded in obtaining only one line in the Raman spectrum of $Cs_2B_{12}Cl_{12}$ in aqueous solution; IR spectra of the solid salts $Cs_2B_{12}X_{12}$ with X = Cl, Br, I within a limited frequency range can be found in refs 22 and 23. In 1982 complete vibrational spectra of the salts $Cs_2B_{12}X_{12}$ in aqueous solutions and in the solid state were published.[19]

All the experimenters have proposed frequency assignments while, in a few other studies,[24-28] a group theoretical treatment of the icosahedron vibrations was carried out, normal coordinate analysis with various approximations of the force field was performed and the frequencies of inactive vibrations were predicted.

The analysis of the spectra of the undistorted icosahedra $B_{12}X_{12}^{2-}$ in the series X = H, D, Cl, Br, I will be given below on the basis of the most recent experimental[19] and theoretical[28] results.

For the 66 fundamentals of the $B_{12}X_{12}^{2-}$ icosahedron, belonging to I_h symmetry point group, the reduced representation is

$$\Gamma_{vib} = 2A_g + F_{1g} + 2G_g + 4H_g + 3F_{1u} + 2F_{2u} + 2G_u + 2H_u$$

where F denotes triply degenerate species and G and H refer to 4- and 5-fold degeneracy, respectively.

Only vibrations of species A_g and H_g are active in Raman while F_{1u} is the only species active in IR. Thus, in the Raman spectrum two polarized lines corresponding to the totally symmetrical vibrations of A_g species and four depolarized lines corresponding to the

TABLE I. Vibrational Spectra (ν, cm^{-1}) of $B_{12}H_{12}^{2-}$ and $B_{12}D_{12}^{2-}$ Anions in Aqueous Solutions

$M_2B_{12}H_{12}$					$M_2B_{12}D_{12}$				
Raman (solution in H_2O)			IR (solution in H_2O and D_2O*)		Raman (solution in D_2O)			IR (solution in D_2O)	
M = Na (ref 17)	M = K (ref 18)	M = K (ref 19)	M = Na (ref 17)	M = K (ref 19)	M = Na (ref 17)	M = K (ref 18)	M = K (ref 19)	M = Na (ref 17)	M = K (ref 19)
2158 s,p	2517 s,p	2517 s,p			1912 p	1910 s,p	1899 m,p		
			2480 s	2485 s				1882	1872 s
2475 m,dp	2472 m	2470 m,dp			1867	2864 s	1854 m,dp		
			1070 m	1072* m				932	928 w
949 w,dp	954 m	955 w,dp			888	896 m	891 w,dp		
770 sh,dp	774 m	770 m,sh,dp							
743 s,p	746 vs,p	745 s,p			736		736 w,p		
							728 w,p		
			720 m	719* m	716 p	718 vs,p	713 vs,p		
							657 vw,dp		
					620	622 m	616 s,dp		
584 m,dp	582 m	580 m,dp						596#	588# m
						542 w	531 w,dp		

*These data are taken from IR spectra of solid samples.

TABLE II. Comparison of Fundamental Frequencies of $B_{12}X_{12}^{2-}$ Icosahedra in the Series X = H, D, Cl, Br, I for Aqueous Solutions (ν, cm^{-1})[a]

symmetry species	number	$B_{12}H_{12}$	$B_{12}D_{12}$	$B_{12}Cl_{12}$	$B_{12}Br_{12}$	$B_{12}I_{12}$	proposed assignment[19]
A_{1g} (Raman,p)	ν_1	2517 s	1899 m	1075 w	984 vw	-	out-of-phase breathing mode $\nu_{BX}-\nu_{BB}$ with gradually increasing contribution of ν_{BB}
	ν_2	745 s	713 s	300 vs	193.5 vs	145 vs	in-phase breathing mode $\nu_{BX}+\nu_{BB}$ with gradually increasing contribution of ν_{BX}
H_g (Raman,dp)	ν_3	2470 m	1854 m	990 vvw	-	898 vvw?	analogue of ν_1
	ν_4	955 w	891 w	715 vw	-	654 w	
	ν_5	770 m	616 s	295 m	192 m	143.5 m	analogue of ν_2
	ν_6	580 m	531 w	127 m	84 m	70 m	mainly δ_{BBX}
F_{1u} (IR)	ν_7	2485 s	1872 s	1040 vs	983 s	(926) s	analogue of ν_1
	ν_8	1071 m	928 w	(540) s	(442) s	(379) s	
	ν_9	719 m	(588) m	(161) m	(111) m	-	mainly δ_{BBX}

[a] The frequencies taken from the IR spectra of solid salts are given in parentheses.

5-fold degenerate modes of H_g species should be observed, whereas the IR spectrum must exhibit only three triply degenerate F_{1u} modes. Hence, in this noteworthy case, the overall selection rules leave no doubt in assigning observed spectral features to symmetry species. Moreover, symmetry considerations show that the A_g modes may involve only stretching coordinates ν(BB) and ν(BX) while all the internal coordinates, ν(BB), ν(BX), and δ(BBX), may be involved in the H_g and F_{1u} species.

The experimental data on $B_{12}H_{12}^{2-}$ and $B_{12}D_{12}^{2-}$ anions in aqueous solutions, obtained by different groups of authors, are given in Table I.

The data for $B_{12}H_{12}^{2-}$ agree well. However, for the deuterated substance the frequency discrepancies are up to 13 cm^{-1}; this may be due to the different degrees of deuteration, the highest being achieved in ref 19, reaching 96.2% according to IR optical density measurements. The last value means that in ref 19 the content of $B_{12}D_{12}^{2-}$ species in the isotopic mixture was 63%, while in refs 17 and 18 it was about 30%, all the rest consisting of different $B_{12}D_nH_{12-n}^{2-}$ entities whose different frequencies lead to the overall band broadening and to the shift of the position of the band's center of gravity.

The slight contradiction between Muetterties et al.[17] and Abdul-Fattah and Butler[18] concerning the assignment of a fundamental of H_g species in the Raman spectrum of $B_{12}D_{12}^{2-}$ was definitely clarified by Leites et al.[19] in favor of ref 18 on the basis of polarization measurements and of better satisfaction of the Redlich–Teller rule.

All six lines were observed in the Raman spectrum of $B_{12}Cl_{12}^{2-}$ in aqueous solution.[19] It was found that one of the lines—a polarized one at 300 cm^{-1}—is 100 times more intense than all the others, the latter having been detected only after a substantial increase in the electron gain of the detector. A major aid in the search for weak bands was provided by the results of Weber and Thorpe[24] who had calculated in advance the vibrational frequencies of $B_{12}Cl_{12}^{2-}$.

In the Raman spectra of $B_{12}Br_{12}^{2-}$ and $B_{12}I_{12}^{2-}$ solutions, it was not possible to detect all the six of the allowed lines since some of them probably have a very low intensity[19] (vide infra).

The frequencies of the IR active modes situated lower than 600 cm^{-1}, i.e. in the region where both H_2O and D_2O absorb, were taken from the IR spectra of the solid salts.

The results[19] obtained for the nine allowed fundamentals of the icosahedra studied together with the assignments given are summarized in Table II. The assignments were made on the basis of the band frequency and intensity behavior in the series X = H, D, Cl, Br, I. A comparison of these values enabled the authors[19] to elucidate the vibration mechanism.

Let us first consider the Raman active modes ν_1 and ν_2 of A_g species. These are purely stretching because they may involve only ν(BB) and ν(BX) coordinates. The ν_2 mode at X = H manifests itself as a highly intense line at 745 cm^{-1}; as one goes from H to D, its frequency is shifted slightly to 713 cm^{-1}. Hence, this is a vibration with the ν(BB) coordinate being predominant. However, as one passes to halogenated anions the situation alters, which is not surprising since the masses of H and D atoms are smaller than that of the B atom while the masses of halogen atoms are greater. Evidently, the kinematics of the vibrational motion for X = Cl, Br, I must change completely as compared to that for X = H, D. Indeed, as one goes from X = H, D to X = Cl the ν_2 mode frequency sharply decreases down to 300 cm^{-1} and shows a further dependence on the X mass: 193.5 cm^{-1} for X = Br and 145 cm^{-1} for X = I.

The increasing intensity of the ν_2 line in the series studied is also worthy of note. For X = H the ν_2 intensity was comparable to that of other Raman lines in the spectrum, while in the case of halogenated anions it became enhanced by a factor of several hundred.

A remarkable behavior is exhibited also by the ν_1 mode. For X = H it manifests itself as an intense line at 2517 cm^{-1}, that is, in the usual region of B–H stretchings. As one passes to X = D it is shifted to 1899 cm^{-1}; the isotopic ratio of 1.32 also indicates that the B–X stretch is primarily involved in this vibration. However, on going to halogenated entities, the ν_1 frequency, having decreased to 1075 cm^{-1} with X = Cl, subsequently depends on the mass of X insignificantly. The ν_1 line intensity gradually decreases in the series studied; this feature changes from a very strong line for X = H into a very weak one for X = Br. In the Raman spectrum of the last member of the series, $B_{12}I_{12}^{2-}$, this line has not been detected even under most rigorous conditions of registration.

To explain the observed changes in the ν_1 and ν_2 frequencies and intensities, it was assumed[19] that the ν_2 and ν_1 modes were, respectively, in-phase and out-of-phase "breathing" vibrations of two coaxial polyhedra, composed of B and X atoms, with respect to one another. In other words, both modes are the following linear combinations of ν(BX) and ν(BB) coordinates:

$$\nu_2 = \alpha\nu(\mathrm{BX}) + \beta\nu(\mathrm{BB})$$

$$\nu_1 = \gamma\nu(\mathrm{BX}) - \delta\nu(\mathrm{BB})$$

For X = H, coefficients α and δ are small, ν_2 involves mainly B–B stretch, while ν_1 involves mainly B–H stretch. On going to halogenated anions, coefficients α and δ increase and ν(BB) and ν(BX) coordinates tend to mix more and more. The signs + and – in the expressions given above explain the increase in the intensity of the ν_2 line and the decrease in the intensity of the ν_1 line.

The data of Table II show that the frequency changes of the ν_3 and ν_7 modes in the series studied are similar to that of ν_1, while that of ν_5 is similar to that of ν_2; this means that they involve much the same combinations of internal coordinates, respectively.

The relative positions of the frequencies, $\nu_1 > \nu_7 > \nu_3$, clearly suggest that the missing line of the species A_g for X = I must lie in the vicinity of 930 cm^{-1}, whereas the ν_3 line of the species H_g for X = Br must be situated near 950 cm^{-1}.

Thus, the vibrations of $B_{12}X_{12}^{2-}$ icosahedra in solution are really governed by the selection rules of the I_h symmetry group. All the experimental findings given above have allowed the authors[24-28] to perform complete normal coordinate analysis on the icosahedral entities and to obtain the inactive frequency values, the potential energy distribution (PED), the force fields, and the mean amplitudes of the vibrations.

The first analysis of the vibrations of the X_{12} icosahedral cage model was made by Weber and Thorpe.[24] A complete set of symmetry coordinates for the icosahedral cage was published by Boyle and Parker.[25] The same problem was solved (using a different approach) by Cyvin and Cyvin,[26] while Cyvin et al.[27] extended the coordinate set to the $X_{12}Y_{12}$ double-icosahedron model. They developed a simple harmonic force field for $B_{12}H_{12}^{2-}$, which was based on the first experimental findings.[17,18] After these data were revised, and the full spectra of the whole series $B_{12}X_{12}^{2-}$ for X = H, D, Cl, Br, I, together with the assignments of the active fundamentals, were published,[19] Cyvin and Cyvin[28] extended their normal coordinate analysis to the whole series, including $B_{12}F_{12}^{2-}$ which has not yet been synthesized.

The latter authors used a simple force field in the Keating version. Only the stretching B–X force constant was varied, the bending ones were kept constant for all X. The force constants of the initial force field employed can be found in section VIII, where all force constants used in borane and carborane normal coordinate analyses are listed.

The calculated frequencies along with the PED data for $B_{12}H_{12}^{2-}$ and $B_{12}Cl_{12}^{2-}$ reported in refs 24 and 28 are reproduced in Table III. It is seen, that in general the calculated frequencies are in good agreement with the experimental data in all regions except for 800–1100 cm^{-1}, where the discrepancies sometimes reach 80 cm^{-1}. This seems to be related to the primitiveness of the force field chosen (the constant values of the bending force constants for all X).

The PED data[28] are very well compatible with the description of the normal modes proposed in ref 19. In particular, in regard to the A_g ν_1 and ν_2 modes, they are indeed almost completely separated as ν(BX) and ν(BB), respectively, for $B_{12}H_{12}^{2-}$; however, with the increase in mass of X these modes become more and more mixed. For X = Cl, they are mixed in equal portions (see Table III), while for $B_{12}Br_{12}^{2-}$ and $B_{12}I_{12}^{2-}$ the main contributions are reversed. In the extreme case of X = I, ν_1 is predominantly ν(BB) – 73r + 37s (designations of Table III), while ν_2 at 145 cm^{-1} is mainly ν(BI) – 28r + 64s.

The frequencies of the computed "silent" $B_{12}H_{12}^{2-}$ modes[28] are presented in Table IV. The knowledge of these frequencies is essential for analyses of the spectra of icosahedral carboranes because, on going from $B_{12}H_{12}^{2-}$ to molecules with lowered symmetry, some "silent" modes become active.

It is important to note that there really are no low-frequency modes among the $B_{12}H_{12}^{2-}$ anion fundamentals—neither among the active nor among the inactive ones. The lowest frequency (464 cm^{-1}) corresponds to an inactive cage deformation mode of the H_u

TABLE III. Raman- and IR-Active Frequencies (cm^{-1}) of $B_{12}X_{12}^{2-}$, X = H, Cl and PED Data

species	$B_{12}H_{12}^{2-}$ observed (ref 19)	calculated ref 24	calculated ref 27	PED[a] (ref 28)	$B_{12}Cl_{12}^{2-}$ observed (ref 19)	calculated ref 24	calculated ref 28	PED[a] (ref 28)
A_{1g}								
ν_1	2517	2491	2514	100 s	1075	1033	1082	54s + 53r
ν_2	745	759	774	100 r	300	289	301	47r + 46s
H_g								
ν_3	2470	2472	2497	111 s	990	1088	1069	58s + 55r
ν_4	955	968	980	58s + 42r	715	770	717	76r + 73r′ + 21s
ν_5	770	800	801	68 r + 41δ	295	284	286	54r′ + 34s
ν_6	580	582	570	125r′	127	135	125	96δ
F_{1u}								
ν_7	2485	2481	2504	131 s + 26δ	1040	1076	1068	91r + 59s
ν_8	1071	1065	1048	33 r + 33δ	540	552	533	61s + 28r
ν_9	719	700	719	105 r + 101δ	161	166	156	155δ + 29r

[a] Potential energy distribution terms, defined as 100 $L_{ik}^2 F_{ii}/\lambda_k$, referred to symmetry coordinates.[27] Abbreviations are as follows: r, B–B stretch; s, B–X stretch; δ, BBX bend. Terms below 15 are omitted.

TABLE IV. Inactive Vibrational Frequencies (cm^{-1}) and PED of $B_{12}H_{12}^{2-}$

species	calculated frequencies ref 24	calculated frequencies ref 27	PED[a] (ref 28)
F_{1g}	1011	1014	100δ
G_g	955	975	71δ
	671	618	96r + 38δ
F_{2u}	2470	2496	102s
	886	800	101r
G_u	859	922	82δ
	770	788	87r + 15δ
H_u	984	993	69δ
	520	464	123r + 62δ

[a] See footnote to Table III.

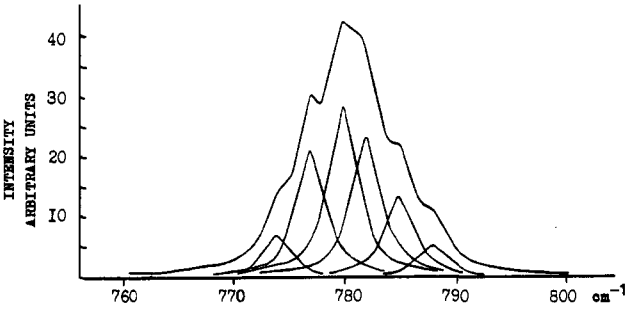

Figure 3. Computer simulation of the isotopic broadening of the $B_{12}H_{12}^{2-}$ band at ca. 780 cm^{-1}, corresponding to the A_g skeletal mode (on the assumption of Lorentzian contour and half-width of each component 3 cm^{-1}).

species. This means that icosahedron cage is, indeed, a rigid system. This fact will play a prominent role in understanding the spectra of substituted carboranes.

Preetz et al.[29] reported the Raman and IR spectra of solid cesium salts of monohalododecaborates $XB_{12}H_{11}^{2-}$, X = Cl, Br, I. The reduced symmetry of these anions relative to $B_{12}H_{12}^{2-}$ results in the appearance of new spectral features attributable to cage modes in the region 500–1200 cm^{-1}. In addition, the spectra exhibit two new characteristic bands in the region 175–380 cm^{-1}, which shift to low frequencies in the series X = Cl, Br, I. They are therefore assigned to (B_{12})–X stretching and bending vibrations.

C. Isotopic Broadening of Spectral Bands of Icosahedral Boranes and Carboranes

The natural abundance of ^{10}B and ^{11}B isotopes must lead to isotopic splitting or at least broadening of the vibrational bands, corresponding to the motions in which boron atoms participate. It is important to evaluate the limits of this effect for icosahedral boranes and carboranes, because it has to be taken into account, in particular, when studying band widths and shapes (e.g., in view of the molecular mobility problem, vide infra). This problem was elucidated in ref 30. Since the $B_{12}X_{12}^{2-}$ entity exhibits six main isotopomers, the normal modes computation[28] was extended to take this fact into account.[31] The results obtained show that isotopic splitting in this case cannot be detected experimentally because the spacing between the band maxima of the six main isotopomers is not more than 1–2 cm^{-1}. However, these results do allow us to estimate isotopic broadening. An example will be presented below.

Let us assume that a polarized Raman line at 780 cm^{-1} (calculated value of ν_2 for $B_{12}H_{12}^{2-}$) has an intrinsic half-width of 3 cm^{-1} and a Lorentzian contour. Then, taking account of the natural relative proportion of each isotopomer and computed ν_2 frequency values, we can deduce the resulting spectral curve which is a superposition of the six weighted lines. The resulting isotopically broadened band with a half-width about 10 cm^{-1} and a complicated contour is presented in Figure 3. Isotopic broadening of other bands is of the same order of magnitude. Thus, it is obvious that isotopic splitting in the spectra of icosahedral boranes and carboranes can be observed only in the crystal phase at very low temperatures when the band narrowing becomes significant, if at all.

D. Correlation between the Spectra of the Icosahedral Entities $B_{12}H_{12}^{2-}$ and $C_2B_{10}H_{12}$

The detailed analysis of the spectrum of the undistorted $B_{12}H_{12}^{2-}$ icosahedron provides a deeper rationale for $C_2B_{10}H_{12}$ spectra.

As mentioned above, the *p*-$C_2B_{10}H_{12}$ (*p*-carborane) molecule belongs to symmetry point group D_{5d} and the molecules of the meta and ortho isomers to the C_{2v} group. Both D_{5d} and C_{2v} groups are subgroups of the icosahedron I_h point group. Their correlation diagram is given in Figure 4 and shows that each degenerate mode of the icosahedron must split into several components in the spectra of carboranes and that some inactive vibrations must become active. But, in fact, this is not the case.

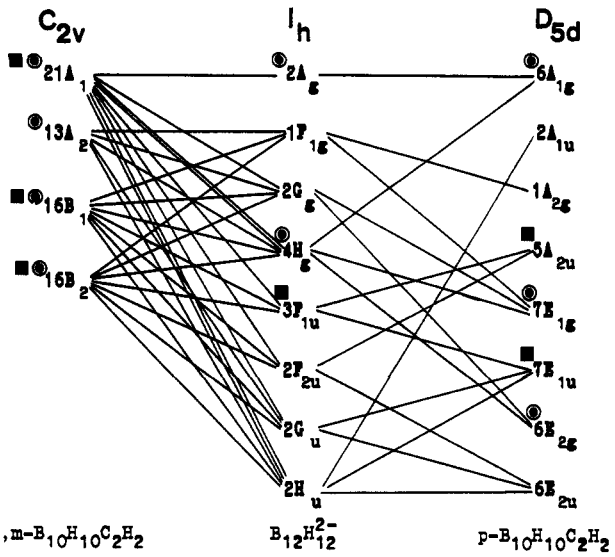

Figure 4. Correlation between symmetry species of icosahedral $B_{12}H_{12}^{2-}$ and $C_2B_{10}H_{12}$ molecules. The symbols are as follows: ■, IR-active modes; ◉, Raman-active modes.

Let us begin with the most symmetrical case of *p*-carborane. On going from $B_{12}H_{12}^{2-}$ to *p*-carborane, two boron atoms in the opposite vertices of the icosahedron are substituted by two carbon atoms and the polyhedron turns from a spherical top into a prolate symmetric top. The latter no longer has 3-fold symmetry axes and, of the six 5-fold axes, only one remains.

The correlation diagram (see Figure 4) shows the fate of each icosahedron mode on symmetry lowering. For instance, each Raman-active H_g 5-fold degenerate mode must split into three Raman-active modes: one totally symmetric A_{1g} mode and two doubly degenerate modes of E_{1g} and E_{2g} species. In other words, each depolarized line of $B_{12}H_{12}^{2-}$ spectrum must "generate" three lines in the Raman spectrum of *p*-carborane: one polarized and two depolarized. All the other *p*-carborane depolarized Raman lines of E_{1g} and E_{2g} species must originate from the inactive icosahedron modes G_g and F_{1g}.

The vibrational spectrum of *p*-carborane is shown in Figure 2, the assignments given in refs 9 and 30 are based on polarization measurements in the Raman, band envelopes in the gas-phase IR spectrum, and the data for deuterated molecules.

The results of group theoretical analysis are available[9] and show which *p*-carborane internal coordinates may participate in normal modes of a given symmetry species. It is a priori evident that the real normal modes are mixtures (to a greater or lesser extent) of several coordinates. For instance, the close values of the atomic masses of C and B suggest the mixing of B–B and B–C stretching coordinates; especially since these stretching frequencies are close in value even in the spectra of nonrelated compounds [cf. 745 cm^{-1} of $B_{12}H_{12}^{2-}$ ν(BB)[19] with 675 cm^{-1} of trimethylboron ν(BC)[32]].

Let us consider the transformation of the Raman spectrum of $B_{12}H_{12}^{2-}$ into that of *p*-carborane which is graphically outlined in Figure 5. The comparison shows that the two totally symmetric icosahedron vibrations, ν_1 at 2517 cm^{-1} and ν_2 at 745 cm^{-1}, have close analogies in the Raman spectrum of *p*-carborane. These are the intense polarized lines at 2620 cm^{-1} [corresponding to ν(BH)] and at 765 cm^{-1} ("breathing" motion of the polyhedron). The increase in the ν(B–H) frequency reflects a real increase in the K_{BH} force constant on going from the *closo*-borate anion to *p*-carborane.

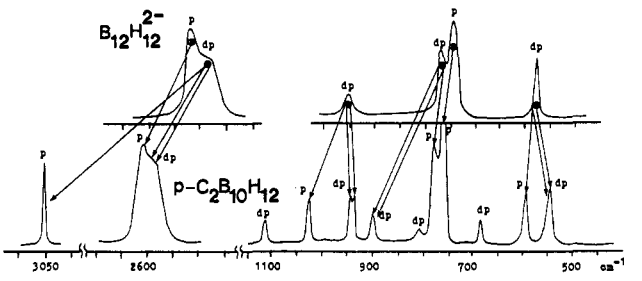

Figure 5. Correlation between Raman spectra of $B_{12}H_{12}^{2-}$ (in aqueous solution) and *p*-$C_2B_{10}H_{12}$ (solid plastic phase).

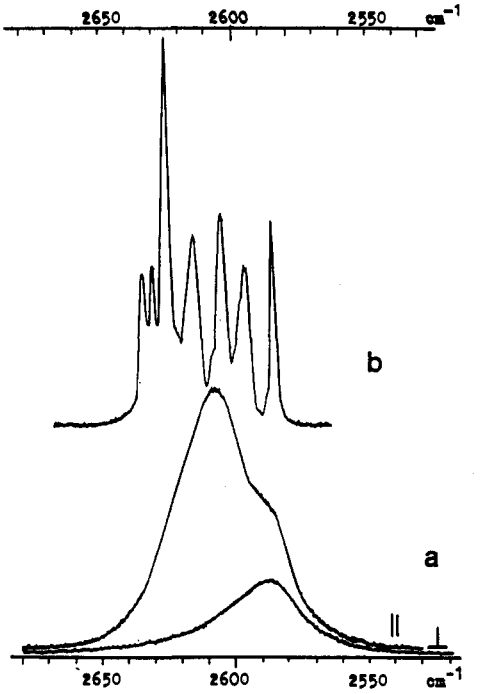

Figure 6. The ν(BH) band in the Raman spectrum of *p*-carborane: (a) polarization measurements (in CCl_4 solution); and (b) solid sample, 87 K.

There must be two more ν(BH) modes in the Raman spectrum of *p*-carborane, namely those of E_{1g} and E_{2g} species originating from the H_g mode of $B_{12}H_{12}^{2-}$ at 2470 cm^{-1}. However, only one depolarized feature at 2597 cm^{-1} is observed in this region (Figures 5 and 6).

The same phenomenon is seen for other degenerate modes of *p*-carborane, originating from the H_g modes of $B_{12}H_{12}^{2-}$. Only one depolarized line is observed instead of the two, corresponding to the E_{1g} and E_{2g} modes. To rationalize this curious situation, the authors[9,30] have assumed that this pair of related modes, E_{1g} and E_{2g}, has coincident or nearly coincident frequencies because of their close displacement eigenvectors. This assumption is substantiated by the only case in which it has been possible to identify both E_{1g} and E_{2g} modes as a depolarized split pair at 940/946 cm^{-1}, originating from the 955 cm^{-1} H_g mode of $B_{12}H_{12}^{2-}$ (Figure 5).

At the same time, new A_{1g} modes, originating from H_g species of $B_{12}H_{12}^{2-}$, are always easily identified as polarized lines in suitable regions.

The results[28] for silent $B_{12}H_{12}^{2-}$ modes (Table IV) are very useful for estimation of the spectral regions where

"new" active modes, arising from silent modes, should appear in the *p*-carborane spectrum. It is noticeable that the "new" bands have very low intensities and not all of them have been found experimentally, as if they "remember" their origin from inactive modes.

Thus, the spectral changes observed on going from $B_{12}H_{12}^{2-}$ to *p*-carborane can be explained only if the rather reasonable assumption is made that some carborane vibrations, in which the new fragments of the molecule (the CH groups) do not participate, continue to obey the selection rules effective for the I_h symmetry group, i.e. as if they do not "feel" the symmetry lowering.

The above comments are even more valid for *o*- and *m*-carboranes (their spectra are presented in Figure 2). The correlation diagram (Figure 4) shows that, since *o*- and *m*-carborane molecules have no symmetry axes higher than C_2, degeneracy is removed and the spectrum should become much more complicated. However, as already mentioned, this is not the case.[10] The bands which should be split appear not to be split, and silent modes which should now be active do not emerge in the spectrum. The former statement is confirmed by the "averaged" depolarization ratios observed for many Raman lines of *o*- and *m*-carborane (measured in solutions), which are due to the overlap of the bands, corresponding to respective symmetric and antisymmetric modes.

Thus, the similarity of the spectral patterns of the three $C_2B_{10}H_{12}$ isomers and the fact that some Raman lines of *o*- and *m*-carboranes have no IR counterparts and vice versa, as if the mutual exclusion rule continues to work, facts which seem puzzling at first sight, can be rationalized in terms of the higher effective symmetry of those carborane vibrations which do not involve CH groups. On going from $B_{12}H_{12}^{2-}$ to a carborane, these modes do not "feel" the symmetry lowering and continue to obey the icosahedron selection rules. This is why the spectra of the three icosahedral carborane isomers are so simple and so similar.

There are two papers in which the authors reported that they had carried out normal coordinate analysis on the three carborane isomers.[33,34] One of them published in 1974 was devoted to the IR spectra of *o*- and *m*-carboranes.[33] The aim of the authors was to determine if a calculation based on a simple valence force field could reproduce the vibrational frequencies and IR intensities of such unusual systems as the carboranes satisfactorily. The authors computed the vibrational frequencies with the help of a force field estimated on the basis of Lipscomb's quantum chemical results[35] and Gordy's relation.[36] The IR intensities were calculated in a valence optical approximation, using the data of Koetzle and Lipscomb[37] on charge distribution and dipole moments. In spite of using the so-called "zero-order approximation" force field which neglects off-diagonal force constants, the authors[33] succeeded in obtaining results which could serve as a rather good basis for the IR spectral interpretation (these authors did not take the Raman spectra into consideration).

It is important to note that, according to these results, many of fundamentals have nearly coinciding frequencies and many IR bands have very low intensities. It is amusing that this conclusion, based on theoretical calculations, is virtually identical to the inference[9,10] drawn later after examination of the experimental spectra, although the latter authors expressed it quite differently, viz. "some carborane vibrations obey the selection rules of higher effective (icosahedron) symmetry".

In a 1979 paper Gribov, Klimova, and Reichstatt reported on the quantum chemical examination of bonding in icosahedral borate anions and carboranes.[34] It was claimed there that the authors performed a normal coordinate analysis of the *p*-carborane molecule. They stated that they did not succeed in obtaining good results using an ordinary force field model based on the Gordy relation,[36] and that to reproduce *p*-carborane fundamentals it was necessary to make essential changes in the usual force field by significantly increasing the icosahedron edge stretching force constants or by introducing additional off-diagonal force constants which took into account the interactions of bonds having no common atoms. Furthermore, the force constants for the icosahedron "edges" appeared to be smaller than those of its "angles". According to ref 34, the new force field models, which are essentially different from those considered in earlier studies, reflect the specific character of chemical bonding in electron-deficient polyhedral molecules. Unfortunately, no numerical results are given in this paper, neither the force fields nor the frequencies and PED data obtained.

On comparing the conclusions of these papers,[33,34] having two authors in common, an inevitable question arises: why was it possible to reproduce the *o*- and *m*-carborane vibrations with a normal force field[33] while, for the analogous *p*-carborane molecule, the introduction of new force field models[34] became necessary? It is appropriate to remember here that Weber and Thorpe,[24] Cyvin et al.,[27,28] and also Bragin, Urevig, and Diem[38] succeeded in reproducing $B_{12}X_{12}^{2-}$ as well as $B_6H_6^{2-}$ and 1,6-$C_2B_4H_6$ vibrational spectra, respectively, by employing different but usual force field models.

It is well-known that the inverse vibrational problem, i.e. the problem of force field determination on the basis of experimental vibrational frequencies, belongs to the so-called "illegitimate problems", the difficulties met hereby being related to ambiguity and instability of solutions (see, e.g., ref 39). That is why the conclusion[34] that the peculiar bonding in cluster boranes and carboranes necessitates a special "reversed" type of force field seems to be not sufficiently proven, although tempting.

Finally, it is important to emphasize that carboranes really do not have low-frequency modes. This can now be affirmed with certainty. Indeed, all $B_{12}H_{12}^{2-}$ active mode frequencies lie above 450 cm^{-1}. Calculations[28] of $B_{12}H_{12}^{2-}$ silent mode frequencies show that the lowest one lies at 464 cm^{-1}. Substitution of two boron atoms by two carbon atoms can lead only to an increase in the polyhedron vibrational frequencies, because all the force constants associated with vibrational coordinates involving the carbon atom are always higher than those involving the corresponding boron atom, e.g. K_{CH} is higher than K_{BH}, K_{BC} is higher than K_{BB}, etc., while the mass difference between B and C atoms is small.

The absence of low-frequency modes in carborane spectra is a manifestation of the rigidity of the polyhedron and has very important consequences (see below).

TABLE V. CH Stretching Frequencies (cm^{-1}) in the Spectra of $C_2B_{10}H_{12}$ Carboranes

molecule	point symmetry group	species	ν(CH) CCl_4 solution Raman[a]	CCl_4 solution IR	solid, 293 K Raman	solid, 293 K IR
p-carborane	D_{5d}	ν^s A_{1g}	3064.4 ρ = 0.24	-	3058.1	-
		ν^{as} A_{2u}	-	3065.2	-	3958.8
m-carborane	C_{2v}	ν^s A_1	3070.0 ρ = 0.24	-	3063.5	-
		ν^{as} B_1	-	3070.7	-	3063.6
o-carborane	C_{2v}	ν^s A_1	3079.3 ρ = 0.26	-	3070.6	-
		ν^{as} B_1	-	3080.2	-	3070.8

[a] ρ stands for the depolarization ratio (±0.05).

E. Analytical Implications of the Spectra of Icosahedral Boranes and Carboranes

What can be said about these spectra now, after the theoretical analysis, from the point of view of using them in solving particular structural chemical problems?

1. The 450–1100-cm^{-1} Region

Most vibrations having frequencies in the region from 450 to 1100 cm^{-1} are of complex origin (Table III), the skeletal coordinates and δ(BBH) being heavily mixed; therefore the corresponding band frequencies and their shifts should not be used by chemists.

The main characteristic feature in the Raman spectra of icosahedral boranes (and also of the α-rombohedral boron modification consisting of bonded boron icosahedra[40]) and carboranes is the most intense, strongly polarized line near 750 cm^{-1} which corresponds to the icosahedron "breathing" mode or, in other words, to the "pulsation" of the cage. In the IR spectra the intense ν(BB) band near 720 cm^{-1} is noticeable. In the case of *p*-carborane, this band corresponds to A_{2u} species motion, in which one half of the polyhedron is contracting while the second is expanding. The Raman line at ca. 760 cm^{-1} and the IR band near 720 cm^{-1} remain in the spectra of substituted carboranes and can be used in analytical practice.

2. CH Stretching and Bending Modes

Characteristic bands in carborane spectra are all features related to carbon–hydrogen bonds, these vibrations being well localized. Both stretching and bending CH modes are very useful for chemists. Their spectral manifestation is rather curious and important.

The situation is clear only for the *p*-carborane molecule. The polarized Raman band at 3060 cm^{-1}, which is shifted to 2289 cm^{-1} on C-deuteration, is obviously attributable to ν(CH) of the A_{1g} species. The assignment of the IR band at 3061 cm^{-1} (2286 cm^{-1} on deuteration) with a clear-cut P,Q,R structure in the gas-phase spectrum to the ν(CH) of A_{2u} species is also straightforward. The near coincidence of the frequencies of these modes indicates that two CH stretch oscillators do not interact; this is quite reasonable because they are spatially remote.

In *o*-carborane, the two CH bonds are adjacent, in *m*-carborane they are separated by one boron atom; both isomers belong to C_{2v} point symmetry group and should not obey the mutual exclusion rule. Hence, one should expect two CH stretchings in *o*- and *m*-carborane spectra: the symmetrical one of the A_1 species and the antisymmetrical one of the B_1 species, both being active in Raman and in IR. However, only one ν(CH) band is observed experimentally, its IR and Raman frequencies nearly coincide (see Figure 2 and Table V); this is just the same picture as that exhibited by the para isomer.

The reasons for such a puzzling ν(CH) behavior were thoroughly investigated.[41] It was shown that the two CH stretching coordinates in the *closo*-carboranes studied do not couple even if two carbon atoms are adjacent, as in the ortho isomer case, i.e. these two oscillators vibrate independently. This situation has a very important consequence: the carborane ν(CH) band behaves, in a sense, like a PMR signal. If two CH bonds in a molecule become nonequivalent, two ν(CH) bands with different frequencies and intensities may be expected in the spectrum. A spectacular example of *B*(9)-fluoro-*o*-carborane will be presented below.

Thus, if two ν(CH) bands are observed in the spectrum of a carborane molecule having two unsubstituted CH groups, an inference can be drawn that these two groups are nonequivalent. This statement is valid, of course, only for the spectra of liquids and gases. In the spectra of solids, the ν(CH) splitting may be due to crystal effects, such as those taking place, e.g., in deca-*B*-chloro-*o*-carborane (vide infra).

The CH stretching band is a powerful tool for spectrochemical investigation because all the parameters of this band, its frequency, intensity, half-width, and contour, are extremely sensitive to the molecular structure as well as to intra- and intermolecular effects. This statement is partially illustrated by the data of Table V, which shows that the ν(CH) frequencies are appreciably different for the three carborane isomers, increasing in the series para < meta < ortho and also depend on the phase state of the substance. The utility of the ν(CH) band will also be demonstrated in the following sections of this review, when dealing with phase transitions and hydrogen bonding phenomena.

The comparison of unsubstituted carborane spectra with those of C-deuterated and also of C-substituted and deca-*B*-chloro-substituted molecules shows that the modes with predominant CH deformation contribution are situated in the region 1100–1250 cm^{-1}. In the *p*-carborane molecule, both CH bonds lie on the C_5 axis,

hence the CH bending modes belong to degenerate E_{1g} and E_{1u} species and manifest themselves as spectral bands at 1120 cm^{-1} (Raman, dp) and 1169 cm^{-1} (IR, $\perp$), respectively.

In *o*- and *m*-carborane molecules, the CH deformation modes are subdivided into in-plane and out-of-plane bendings. Only the former can be identified in the spectra, the latter seem to be heavily mixed with other motions. In the spectrum of *m*-carborane only one δ(CH) mode is observed at 1160 cm^{-1} in both Raman and IR, whereas in the *o*-carborane molecule, two in-plane bending coordinates of adjacent CCH angles couple significantly and the frequencies of the A_1 and B_1 species diverge, giving rise to two δ(CH) bands at 1150 and 1215 cm^{-1} (Figure 2).

The presence of the latter band above 1200 cm^{-1} allows us to distinguish between *o*-carborane (and its B derivatives) and *p*- and *m*-carboranes, since the latter molecules do not exhibit bands above 1200 cm^{-1}.

3. BH Stretching Band

The last, but not least, important feature of carborane spectra is a broad band near 2600 cm^{-1}, very intense in both Raman and IR (Figure 2). This band is well-known to chemists as belonging to BH stretches and is frequently used in analytical practice as an evidence for the presence of a carborane cage.

In the spectra of solid carborane derivatives this broad feature is often split into several well-resolved peaks. This splitting is sometimes used by chemists to draw a conclusion about the BH bonds being nonequivalent, thus treating the IR bands like NMR signals.

However, such conclusions are rather doubtful because, generally speaking, there are at least three spectral reasons for the ν(BH) band splitting which have nothing to do with chemical nonequivalence. For instance, in the *p*-carborane molecule all 10 BH bonds are equivalent; however, at low temperature the corresponding Raman band is strikingly split (see Figure 6b).

The first possible reason for the ν(BH) band splitting is a partial resolution of the ν(BH) bands belonging to different symmetry species. Let us first consider, as usual, *p*-carborane with its 10 identical BH oscillators as the simplest case. The group theoretical treatment implies that the BH stretch coordinates may participate in Raman active A_{1g}, E_{1g}, and E_{2g} species and in IR active A_{2u} and E_{1u} species. The experimentally observed spectrum of solid *p*-carborane at room temperature (a plastic phase, vide infra) exhibits only one broad unresolved Raman feature and only one wide IR band, with the positions of their centers of gravity being nearly the same (Figure 2).

Polarization measurements, performed in CCl_4 solution,[9,30] allow us to distinguish two overlapping components in the broad Raman band (Figure 6a): one polarized (A_{1g} mode) and only one depolarized (superimposed E_{1g} and E_{2g} modes). Thus, it is seen that the *p*-carborane BH stretching bands, although belonging to different symmetry species, overlap, because they have similar frequencies (within a range of 50 cm^{-1}). This points to a weak coupling of the BH oscillators.

In the *o*- and *m*-carborane molecules, the 10 BH bonds are no longer identical, they form four sets of equivalent stretching coordinates. In the case of C_{2v} symmetry, these 10 stretches occur as $4A_1$, A_2, $4B_1$, and B_2 modes. Strictly speaking, we should observe 10 Raman lines in the ν(BH) region, nine of them having IR counterparts. However, the experimental spectra of solid *o*- and *m*-carboranes at room temperature exhibit the same type of pattern in the ν(BH) region as *p*-carborane (see Figure 2). Again, broad features in IR and Raman are observed in the same spectral region, but this time with more complicated contours. Polarization measurements in the Raman spectra[10] (Figure 7 presents an example of *m*-carborane) have revealed a polarized and a wide, depolarized components. Thus, it is obvious that all four symmetric ν(BH) modes have much the same frequencies and overlap to give only the one polarized component of the overall band. The frequencies of the six antisymmetric modes do not strictly coincide and give rise to a broad depolarized composite with a complicated pattern. The overlap of all the ν(BH) modes broadens the overall band, but in much the same manner as for *p*-carborane with its 10 equivalent BH bonds.

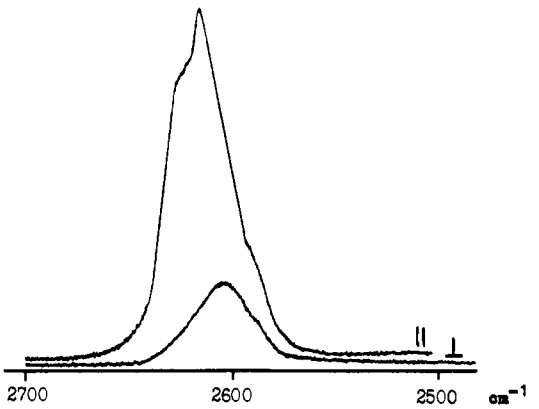

Figure 7. The ν(BH) region in the Raman spectrum of *m*-carborane (polarization measurements in CCl_4 solution).

Thus, the nonequivalence of *o*- and *m*-carborane BH bonds does not significantly affect their manifestation in vibrational spectrum at room temperature (as distinct from NMR spectra). Only in the crystal state at low temperature, when the spectral bands become narrow, may the broad ν(BH) feature be expected to split into well-resolved peaks due to the presence of different modes.

However, experience shows that the main factors, which bring about the ν(BH) splittings observed in borane and carborane spectra are crystal effects, namely, a site effect and a correlation field (or Davydov) splitting. The first effect comprises splitting of the bands, corresponding to the degenerate modes, because degeneracy is removed by the reduced symmetry of a crystal site. However, degenerate modes arise only when a molecule possesses a symmetry axis not lower than 3-fold; hence, the site effect is rather rare. The second effect is due to the resonance interaction of Z molecules ($Z \geq 2$) in a crystal unit cell and may lead to the splitting of each molecular fundamental into, generally speaking, Z components. Davydov splitting is widespread in carborane spectroscopy. It is evidently this effect together with the resolution of the different symmetry modes which causes the spectacular splitting of the *p*-carborane ν(BH) band at low temperature into at least seven components with 5–10-cm^{-1} spacing, as shown in Figure 6b.

For crystalline *o*- and *m*-carboranes such a splitting at 15 K was first reported by Freymann et al.[42] in 1974. The splitting is not compatible with the site effect because *o*- and *m*-carboranes have no degenerate modes and seems to be explained by the same two reasons as for *p*-carborane.

It was also noted[42] that the attachment of a substituent to the carborane cage (either via a carbon, or via a boron atom) brought about noticeable changes in the well-resolved pattern of the ν(BH) band at 15 K. The number, intensity, and position of the split peaks differ from those in the unsubstituted carborane spectra. The authors associated these changes with substitution effects (in other words, with emerging nonequivalence of BH bonds), but assuming, however, that their occurrence is due also to correlation field splitting and to isotopic effects.

A vast variety of substituted carboranes spectra was studied by Leites et al.,[10,15,30] who noticed that many carborane derivatives with bulky substituents (I, Br, SCN etc.) exhibited fine structure of the ν(BH) band already at room temperature. The authors argued that this structure was due to correlation field splitting, because analogous splitting in the same spectra was exhibited by the nondegenerate ν(CH) band even if the two CH bonds in the molecule were equivalent. Moreover, the splitting of both bands disappeared in the solution spectra.

Brint et al.[43] have also noted that, at low temperature, both IR and Raman spectra of a few *closo*-borate anions of the type $B_nH_n^{2-}$ show many more ν(BH) bands than group theory predicts but they regarded this fact as being due to multiple site effect operative in these cases and did not take into consideration the Davydov splitting mechanism.

As to the third possible reason for the ν(BH) band splitting, the isotopic effect (vide supra), the results of model normal coordinate analysis[30,31] on six main isotopomers of the $B_{12}H_{12}^{2-}$ anion (from $^{11}B_{12}$ to $^{11}B_7{}^{10}B_5$) show that the ν(BH) frequency spacing between the isotopomers is not more than 1 cm^{-1}; hence, this factor can lead only to the band broadening.

To conclude the discussion of this spectral region, it is not out of place to mention the report[43] that all peaks near 2600 cm^{-1} in both the IR and Raman spectra are due only to the ν(BH) stretches since no overtones or combinations of other modes are possible as a result of the lack of bands between 1200 and 2500 cm^{-1} and below 400 cm^{-1} in both spectra.

The above discussion shows that a decision whether BH bonds in a carborane molecule are identical or not on the basis of the ν(BH) band splitting is possible if, and only if, all the other reasons for such splitting, especially crystal effects, are excluded. Unfortunately, in some papers the splitting of the ν(BH) band in the spectra of crystalline carborane derivatives has been used for determination of the molecular structure (e.g. ref 44).

F. Icosahedral Deca-*B*-chlorocarboranes (DCC) $C_2H_2B_{10}Cl_{10}$ Spectra

After dealing with $C_2B_{10}H_{12}$ spectra, it is appropriate to consider the B-chlorinated derivatives, $C_2H_2B_{10}Cl_{10}$, since their molecules possess the same symmetry as the unsubstituted carboranes. As a starting point for DCC spectral interpretation, the analysis of the spectrum of the $B_{12}Cl_{12}^{2-}$ anion, which was given in refs 19 and 28 (vide supra) will be discussed.

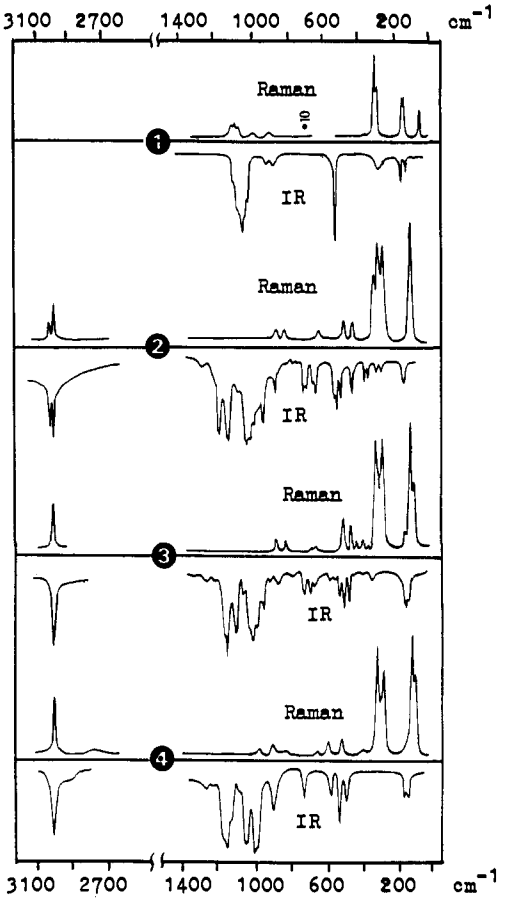

Figure 8. Vibrational spectra of solid $Cs_2B_{12}Cl_{12}$ and deca-*B*-chlorocarboranes $C_2H_2B_{10}Cl_{10}$ (DCC): 1, $Cs_2B_{12}Cl_{12}$; 2, *o*-DCC; 3, *m*-DCC; 4, *p*-DCC.

The IR spectra of deca-*B*-chlorocarboranes (DCC) in a limited region above 400 cm^{-1} were first reported in refs 3, 45, and 46. Their full IR and Raman spectra (see Figure 8) as well as the spectra of their C-deuterated analogues were presented and analyzed in refs 10, 30, and 47.

When comparing the spectra of the three isomers of DCC, the same conclusions as have been presented previously for the unsubstituted carboranes may be drawn:

(1) The spectra of the ortho, meta, and para isomers are very similar in spite of their different molecular symmetry.

(2) The spectra of *o*- and *m*-DCC nearly obey the mutual exclusion rule, which should be valid only for the spectrum of the centrosymmetric *p*-DCC.

(3) The number of DCC spectral features is significantly smaller than that predicted by group theory.

The reason for these peculiarities is the same as has been formulated before: vibrational modes which do not involve CH groups obey the higher effective symmetry.

Substitution of hydrogen atoms by chlorine atoms leads to an enhanced electron-accepting character of the carborane cage and to an increase in the CH acidity.[48] It is of interest that the latter effect manifests itself as a decrease in the ν(CH) band frequency by about 30 cm^{-1} with a simultaneous increase in its IR intensity by

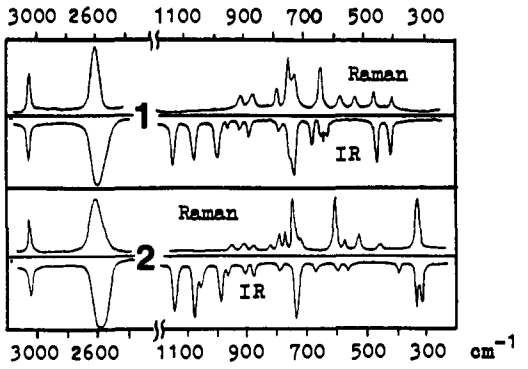

Figure 9. Vibrational spectra of 1,12-$CHB_{10}H_{10}El$: 1, El = P; 2, El = As.

a factor of about 10. The ability of the CH bonds of DCC to participate in strong hydrogen bonding with different bases will be discussed below.

The above discussion of the CH stretch vibrational behavior in the spectra of unsubstituted carboranes is also valid for the CH bands of DCC. The two CH stretch oscillators do not couple even in the *o*-DCC molecule and only one ν(CH) band is observed for all the DCC isomers. The splitting of the ν(CH) band in two components, observed in the spectrum of solid *o*-DCC, is the result of a correlation field effect because only one band is observed in solution.[46]

The CH in-plane deformation modes of DCC are not observed in the Raman spectrum due to their low intensity but manifest themselves as strong IR bands near 1150 cm^{-1}. These are the bands at 1145, 1154, and a pair at 1141 and 1186 cm^{-1} in the spectra of *p*-, *m*-, and *o*-DCC, respectively. The latter band is of analytical value and allows us to distinguish *o*-DCC from the meta and para isomers.

The interpretation of the remaining spectral features of DCC, as given in ref 30, is facilitated by the data obtained for the $B_{12}Cl_{12}^{2-}$ anion[19,28] (see Figure 8). We will confine ourselves only to mentioning the most intense polarized Raman line near 300 cm^{-1}, which originates from the analogous line of the totally symmetric ν_2 mode of $B_{12}Cl_{12}^{2-}$ at 300 cm^{-1}. It is assigned to a "breathing" motion in which BB and BCl stretches participate almost equally. The most intense broad IR band with a complicated pattern in the region 1000–1100 cm^{-1}, which is not observable in the Raman spectrum, is due to the overlap of asymmetric modes in which the ν(BB), ν(BCl), δ(BCH), and δ(BBCl) vibrational coordinates are heavily mixed.

For the most intense features in the spectra of $B_{12}Cl_{12}^{2-}$ and DCC much the same frequencies are observed (Figure 8), pointing to similar force fields in these species.

G. Icosahedral Boranes and Carboranes Containing Heteroatoms

The Raman and IR spectra of icosahedral carboranes, containing one carbon atom and also one phosphorus or arsenic atom in the cage, i.e. carbaphospha- and carbaarsaboranes of the general formula $B_{10}H_{10}CHEl$, El = P, As, are available.[49] All three 1,2- (ortho), 1,7- (meta) and 1,12- (para) isomers of both compounds were studied together with the CH-deuterated meta isomers.

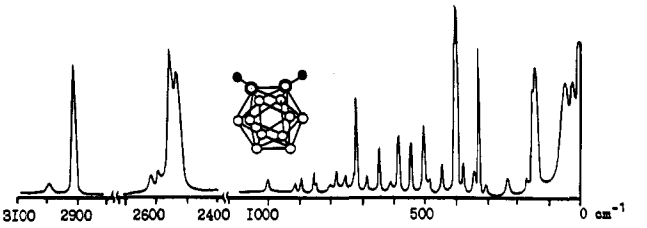

Figure 10. Molecular structure and the Raman spectrum of 1,2-dimethyl-1,2-disila-*closo*-dodecaborane: ○, silicon atom; and ●, methyl group.

The spectra of the most symmetrical para isomers are given in Figure 9. These molecules belong to the C_{5v} symmetry point group which does not obey the mutual exclusion rule; thus most of the spectral features are equally intense in Raman and IR, except for the strong IR bands in the region 1000–1150 cm^{-1}. The CH and BH stretching frequencies are somewhat (20–30 cm^{-1}) lower compared to those of *p*-carborane. The strong polarized Raman line, corresponding to the cage "breathing" mode, is also shifted toward low frequencies compared to the spectra of $C_2B_{10}H_{12}$ carboranes (from 770 to 740 cm^{-1}).

The most striking feature in the spectra of the heterocarboranes studied is the presence of very intense bands in the low-frequency region (635 and 450 cm^{-1} for all carbaphosphaboranes and 610 and 330 cm^{-1} for all carbaarsaboranes). The line at 330 cm^{-1} dominates in the Raman spectra of all carbaarsaboranes. It is obvious that these low-frequency bands are associated with the insertion of a heavy heteroatom into the carborane cage since their position depends on the mass of the heteroatom. The spectra of the three isomers are again very similar in spite of the different molecular symmetry. The IR spectra of C-deuterated meta isomers show that the intense IR bands near 1130 and 1000 cm^{-1} originate from the normal modes with a strong δ(CH) coordinate participation.

IR experiments[49] have demonstrated that these molecules, unlike triphenylphosphine, do not form H complexes with *p*-fluorophenol (in CCl_4 solution). This indicates that the lone electron pairs of the phosphorus and arsenic atoms in the molecules studied cannot serve as proton acceptors in hydrogen bonding.

Recently 1,2-dimethyl-1,2-disila-*closo*-dodecaborane, the first silicon analogue of *o*-carborane, was synthesized and studied by Seyferth et al.;[50] its structure (Figure 10) was proved by X-ray diffraction. For simplicity we will call this new compound simply dimethyl-*o*-silaborane.

It was of great interest to compare its vibrational spectrum with that of *o*-carborane. The Raman spectrum was obtained for a solid sample at different temperatures, polarization measurements were carried out for its solution in benzene, and the IR spectrum in the region 200–3700 cm^{-1} was recorded for a solid sample.[51] The Raman spectrum of solid dimethyl-*o*-silaborane is presented in Figure 10 and can be compared with that of *o*-carborane (Figure 2).

The most striking difference between the spectra of dimethyl-*o*-silaborane and *o*-carborane comprises the presence of several low-frequency bands, equally intense in Raman and IR, in the former spectrum. The most intense line in Raman is the strongly polarized line at 399 cm^{-1}. There is a temptation to assign it to the Si–Si

stretching mode because its frequency lies in just the same region as for Me_6Si_2.[52] However, the first argument against such an assignment is that the spectrum of carbaarsaboranes also contains a strong Raman line in this region and the second involves a general doubt about the existence of a localized Si–Si mode in this cluster-type molecule. This problem calls for further investigation.

The ν(BH) multiplet is centered near 2550 cm^{-1} and the icosahedron "breathing" mode at 715 cm^{-1}, both being markedly shifted to lower frequencies compared to those of *o*-carborane. However, the ν(BH) band is shifted to higher frequencies if compared to the average ν(BH) frequency 2480 cm^{-1} for the $B_{12}H_{12}^{2-}$ anion.

It seems reasonable to assign a polarized Raman band at 640 cm^{-1} to the symmetric stretch of exo-polyhedral Si–C bonds, its frequency lying in the usual range and being close in value to that of Me_3SiCl.[53] The frequencies of the internal vibrations of methyl groups attached to silicon atoms, 1265, 1395, 2915, and 2995 cm^{-1}, are also much the same as for methylchlorosilanes,[53] in particular $MeSiCl_3$; this is in accord with the well-known electron-deficient nature of the *closo*-borane cage.

Generalizing the spectral findings for the three molecules discussed above we can conclude that the substitution of icosahedral carborane CH groups by heavy heteroatoms (Si, P, As) leads to the appearance in the spectrum of intense low-frequency bands, associated with the heteroatom participation in the cage motions, and also to the decrease in the ν(BH) and cage breathing mode frequencies as compared to those of dicarba-*closo*-dodecaboranes, thus indicating a weakening of the molecular bonding.

III. Vibrational Spectra and Structure of Substituted Icosahedral closo-Carboranes. Carborane Cage as a Pseudoatom

Numerous IR spectra of substituted carboranes can be found in the literature. The spectra of most compounds, however, have been reported only in summaries of experimental procedures. Even so, there are a few purely IR spectroscopic papers,[15,42,54-57] which will be discussed when appropriate. Raman spectra of carborane derivatives have been studied only by Leites et al. Most vibrational studies are devoted to monosubstituted molecules, where a substituent X is attached to the carborane cage either via a carbon or via a boron atom.

To rationalize the peculiarities of these spectra, it is necessary to shed light on the spectral manifestations of the carborane cage as a substituent.

In section II we put the major emphasis on the absence of low-frequency modes (lower than 450 cm^{-1}) in the unsubstituted *closo*-borate and -carborane spectra, because this fact is indicative of the rigidity of the deltahedron. It is the cage rigidity, which clearly demonstrates itself in the spectra of carborane derivatives of the type Cb–X (Cb = $C_2B_{10}H_{11}$), causing their specificity. If the substituent X is heavy enough, the so-called "kinematic effect of the carborane nucleus" begins to work. This effect was first encountered and rationalized while studying the spectra of biscarboranyls[58] and we will discuss it, using this very spectacular example.

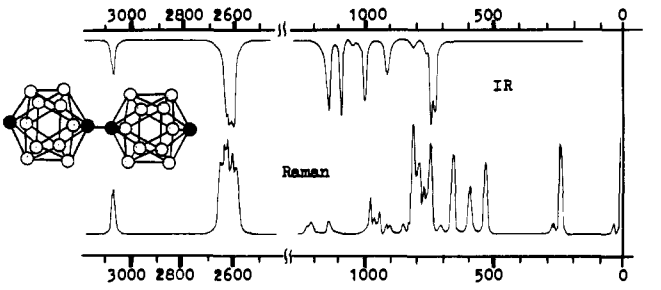

Figure 11. Vibrational spectrum and structure of bis(*C-p*-carboranyl) $(CHB_{10}H_{10}C)_2$.

A. Biscarboranyls $(C_2B_{10}H_{11})_2$

Two types of biscarboranyl molecules were studied by Raman and IR methods: those in which two carboranyl groups are linked either via C or via B(9) atoms. The spectrum of the most symmetrical bis(*C-p*-carboranyl) together with its molecular structure is presented in Figure 11.

In the molecules of all bis(*C*-carboranyl)s a new element arises, namely a C–C bond. Hence a new mode, C–C stretch or ν(CC), should appear in the spectrum. This mode must be active in the Raman, giving an intense polarized line, and forbidden by symmetry in the IR. By analogy with organic substances, this mode frequency could have been expected to lie near 1000 cm^{-1}. However, the only new strongly polarized line in the spectrum of bis(*C-p*-carboranyl), which has no IR counterpart, has a frequency of 250 cm^{-1}. Such a low value for ν(CC) could be explained by the weakness of the C–C bond in this molecule and hence by its small force constant. However, from the chemical reactivity data it is known that this C–C bond is as strong as that in ethane. Moreover, electron diffraction and X-ray data show the C–C bond in bis(*C*-carboranyl)s to have usual interatomic distance 1.52 Å.[59,60]

The low frequency of the new mode indicates that it belongs not to a C–C stretch, but to carborane–carborane bond stretching. The rigid carboranyl group participates in this normal mode, moving as a whole, as a point mass or a pseudoatom. From the point of view of this mode, a biscarboranyl molecule may be regarded as quasidiatomic and designated as Cb–Cb. Indeed, it has been possible to estimate this quasidiatomic molecule vibrational frequency by taking into account the total mass of the carboranyl group and using the K_{CC} force constant value taken from the ethane force field. Such a primitive model calculation gives a ν(CbCb) frequency value of ca. 300 cm^{-1} which is in rather good agreement with the experimentally observed value of 250 cm^{-1}.

If the two carboranyl groups are linked together via boron atoms in position 9, forming bis(*B*-carboranyl) molecules, the frequency of the new intense polarized Raman line, corresponding to carborane–carborane stretch, is even lower, 187 cm^{-1}.[58] Since the mass of the carboranyl group remains the same, it is obvious from this result that the exo-polyhedral B–B bond in bis(*B*-carboranyl)s is weaker than the respective C–C bond in bis(*C*-carboranyl)s; this is in accord with the reactivity data.

Treating the rigid icosahedral cage as a pseudoatom is very useful for rationalizing the spectral peculiarities of carborane derivatives of the type Cb–X, if X is

sufficiently heavy (see below). This approach proved to work well for monohalocarboranes with X = Cl, Br, I and also for carboranyl derivatives of non-transition metals.

B. Monohalocarboranes $C_2B_{10}H_{11}X$; X = Cl, Br, I

In the spectra of these molecules one should anticipate not the ν(CX) or ν(BX) bands in their traditional regions, but the Cb–X stretch. The frequency of the latter may be roughly estimated on the basis of the quasidiatomic Cb–X model calculation, treating carboranyl group as a pseudoatom with an atomic mass 143.2, in usual manner. If a halogen atom X is attached to the carborane cage via a carbon atom, the K_{CX} values for this primitive calculation can be taken from the force fields of alkyl halides as a first approximation. For *B*-carboranyl halides, the K_{BX} values employed by Cyvin et al.[28] for the $B_{12}X_{12}^{2-}$ ions can be used.

The following frequencies were predicted for the ν(CbX) modes of B(9)-carboranyl halides as a result of model calculation:[61]

$$\nu(\text{CbCl}) = 424\ \text{cm}^{-1} \qquad \nu(\text{CbBr}) = 305\ \text{cm}^{-1}$$

$$\nu(\text{CbI}) = 260\ \text{cm}^{-1}$$

Experimental data for B(9)-halogen derivatives of *o*- and *m*-carboranes are available.[30,61] In the Raman spectra of all the isomers of *B*-monochloro-substituted carboranes studied a new polarized strong line in the region of 350 cm^{-1} was observed, in good agreement with the model estimation. The same is true for the corresponding spectra of bromo- and iodocarboranes, the experimental ν(CbX) values for all bromides being near 250 cm^{-1} and for all iodides near 200 cm^{-1}. It is pertinent to remember here the similar values for the corresponding (B_{12})–X stretching frequencies of $B_{12}H_{11}X$,[29] which are equal to 331, 242, and 196 cm^{-1} in the series X = Cl, Br, I respectively. Figure 12, where the Raman spectra of *B*(9)-*m*-carboranyl halides are presented, demonstrates that the Raman line corresponding to the ν(CbX) vibration is very intense, and thus easily identified, and can be of great help in solving structural problems.

C. Carboranyl Derivatives of Non-Transition Metals

The kinematic effect of the carboranyl group was successfully used by Leites et al. in interpreting the spectra of carboranyl derivatives of non-transition metals of the type Cb_nM and Cb_mMX_{n-m}, where X is a halogen atom, M = a metal atom, and n = the metal valency. Carboranyl derivatives of mercury,[62] thallium,[63] tin,[64] arsenic, and antimony[30,65] have been investigated by Raman and IR spectroscopy.

It is well-known (see, e.g., ref 66) that the frequencies of non-transition metal–carbon (M–C) bond stretches are situated in the region 400–600 cm^{-1}. But now, with the kinematic effect in mind, it is not surprising that the authors[62-65] who studied the spectra of C-metalated carboranes did not find the bands of the carbon–metal stretches in their usual range. Instead, they observed Raman lines in the low-frequency region of 130–250 cm^{-1}. These lines have a high intensity and low values of depolarization ratio and are separated from other spectral features. This made their assignment to ν(CbM) vibrations straightforward.

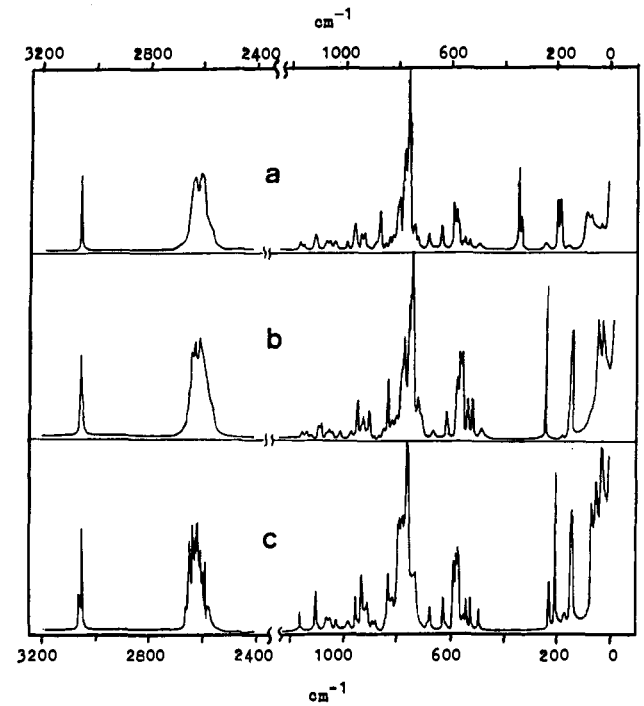

Figure 12. Raman spectra of solid B_9-halocarboranes: (a) 9-chloro-*m*-carborane; (b) 9-bromo-*m*-carborane; and (c) 9-iodo-*m*-carborane.

The value of the ν(CbM) frequency depends on the position in the carborane nucleus, to which the metal atom is attached. In the spectra of B-metalated carboranes, the ν(CbM) frequency is always lower than for corresponding C-derivatives by about 10–20 cm^{-1}, pointing to a weaker Cb–M linkage in the case of B-substitution.

If an organometallic molecule contains not only carboranyl but also alkyl groups attached to a metal atom (compounds of the type Cb_mMAlk_{n-m}), then both low-frequency ν(CbM) lines and the usual ν(CM) lines in the 400–600 cm^{-1} region are observed.

Identification of the ν(CbM) modes allows us to determine the selection rules, operating in a given spectrum and, thus, to elucidate the molecular structure.

The frequencies of the ν(CbM) modes for the derivatives of different metals are summarized in ref 65.

1. *Mercurated Carboranes*

The most detailed study has been performed on mercurated carboranes.[62] The full Raman and IR spectra of six symmetrical isomers of bis(carboranyl)-mercury have been obtained. The spectra have been found to obey the mutual exclusion rule. This means that all isomers of $(C_2B_{10}H_{11})_2Hg$ have a centrosymmetric structure. The spectrum of bis(*C*-*p*-carboranyl)mercury is given as an example in Figure 13. It is seen that the intense Raman line at 155 cm^{-1}, corresponding to the symmetric ν(CbHg) mode, is not active in IR, while the strong IR band at 216 cm^{-1}, corresponding to the antisymmetric ν(CbHg) mode, has no Raman counterpart.

The spectra of carboranylmercury halides of the type Cb–Hg–X (X = Cl, Br, I) were also studied. The only ν(CbHg) mode of these molecules is active in both the Raman and the IR spectra. The same is true of the Hg–X stretching mode.

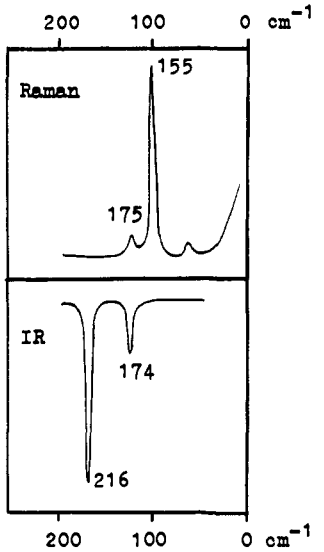

Figure 13. Raman and IR spectra of solid bis(*C-p*-carboranyl)mercury $(CHB_{10}H_{10}C)_2Hg$ in the region of skeletal vibrations.

TABLE VI. The Calculated PED Data[62] for Low-Frequency Skeletal Stretches of Quasitriatomic Models Cb–Hg–X (Cb = $C_2H_2B_{10}H_9$; X = Cl, Br, I)

		PED, %		
X	experimental frequency, cm^{-1}	Cb–Hg stretch	Hg–X stretch	assignment
Cl	300	7	93	τ_1
	175	91	9	τ_2
Br	220	44	56	τ_1
	155	52	48	τ_2
I	196	81	19	τ_1
	138	23	77	τ_2

The authors[62] produced normal coordinate analysis of triatomic models Cb–Hg–Cb and Cb–Hg–X, again treating the carboranyl group as a point mass of 143.2 au and assuming K_{Cb-Hg} and K_{Hg-X} force constants to be equal, in a first approximation, to K_{C-Hg} and K_{Hg-X} from the force fields of dialkylmercury and alkylmercury halides.[67] The calculated frequencies of the Cb–Hg–Cb and Cb–Hg–X skeletal vibrations were close to the experimental values, but somewhat higher, as in the cases of model calculations on biscarboranyls and carboranyl halides.

The frequencies and PED data obtained for Cb–Hg–X models are given in Table VI and demonstrate that the Cb–Hg and Hg–X stretching motions are heavily mixed, especially for X = Br, so the mode descriptions as ν(CbHg) and ν(HgX) are merely conventions. It is more correct in this case to speak about in-phase (τ_2) and out-of-phase (τ_1) combinations of Cb–Hg and Hg–X stretching coordinates. An analogous coupling of ν(PhHg) and ν(HgX) coordinates has been observed for phenylmercury halides.[68]

In the spectra of solid mercurated carboranes, the ν(CbHg) and ν(HgX) bands are often split in two or more components, the difference in resolved peak position being as much as 10–20 cm^{-1}. In the case of the soluble Cb_2Hg, the splitting is obviously caused by crystal effects, because it disappears in solution. An example is given in Figure 14, where the polymorphism of bis(*B*(9)-*m*-carboranyl)mercury is also demonstrated. At room temperature the latter substance can spontaneously form one of two possible crystal modifications

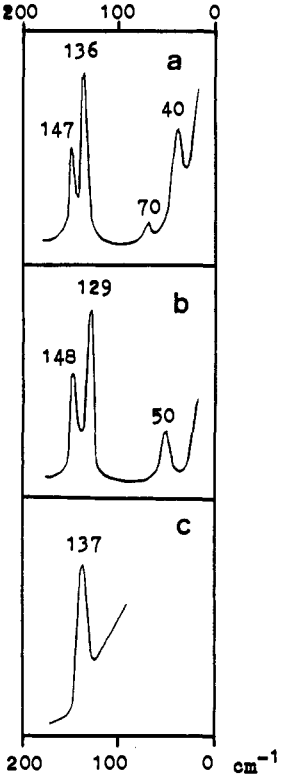

Figure 14. Raman spectrum of bis(9-*m*-carboranyl)mercury in the low-frequency region: (a) crystal modification I; (b) crystal modification II; and (c) solution of both modifications in benzene.

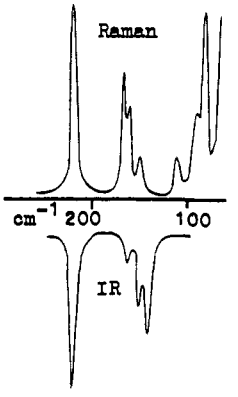

Figure 15. Crystal splittings in the low-frequency Raman and IR spectra of 9-*o*-carboranylmercury bromide.

which can be distinguished by means of the Raman spectrum, where the frequencies of the resolved ν(CbHg) split pairs and of the crystal lattice bands are different (Figure 14).

Analogous splittings in the spectra of insoluble carboranylmercury halides (an example of τ_2 splitting in the 150-cm^{-1} region of the spectrum of *B*(9)-*o*-carboranylmercury bromide is presented in Figure 15) may be explained either by the correlation field effect, or by the formation in the solid state of the following associates due to intermolecular coordination:

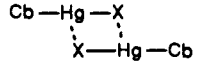

The spectra of alkyl- and phenylmercury halides exhibit similar splittings.[68,69]

2. Carboranyl Derivatives of Thallium

Vibrational spectra of the trivalent thallium compounds of the type Cb_2TlX and $CbTlX_2$ (X = Cl, Br),

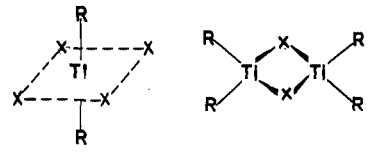

Figure 16. Possible structures of R_2TlX type molecules.

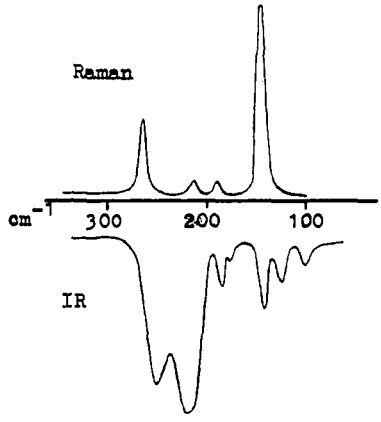

Figure 17. Low-frequency Raman and IR spectra of (1-*o*-$C_2HB_{10}H_{10})_2TlCl$.

in which the carboranyl group was attached to the thallium atom via the B(9) or via a C atom have been investigated.[63]

The structures of the Cb_2TlX type substances were not known. They can have either an ionic structure, the linear R_2Tl^+ cation being very stable, or a dimeric structure with bridged Tl–X bonds (Figure 16). A determination of the overall selection rules, operating in the region of skeletal modes (100–300 cm^{-1}), leaves no doubt that the solid compounds of Cb_2TlX type have the dimeric structure. Figure 17 presents as an example the low-frequency spectrum of $(o\text{-}B_{10}H_{10}C_2H)_2TlCl$. Indeed, the most intense Raman line of the symmetrical ν(TlCb) mode at 145 cm^{-1} does have an IR counterpart and the strong IR band, corresponding to the antisymmetrical ν(TlCb) mode at 220 cm^{-1}, also has a Raman counterpart. Thus, the mutual exclusion rule does not operate for the Cb_2Tl moiety. Furthermore, both IR and Raman spectra exhibit a band, corresponding to the Tl–X bond stretch (at 260 cm^{-1} with X = Cl). The same band is reported to be present in the spectra of analogous compounds with fluorinated alkyl groups, $(R_f)_2TlX$, which have dimeric structures,[70] but is absent from the spectra of Me_2TlX, having an ionic structure with the linear Me_2Tl^+ cation.[71]

It should be noted that, in the case of Tl compounds, the mode designations as "ν(TlCb)" and "ν(TlX)" are also only conventions, as in the case of Hg compounds, both vibrations being mixtures of Tl–Cb and Tl–X stretches.

The complicated spectral patterns of solid $CbTlX_2$ compounds give no possibility for unambiguous structure determination, but do provide some evidence to suggest intermolecular association.[63]

3. Carboranyl Derivatives of Tin

Two sets of compounds have been studied by Leites et al.:[64] $CbSnCl_3$ and Cb_2SnCl_2. In most of these compounds, the tin atom is attached to the carboranyl group via the boron atom in position 9, and only in the case of two molecules is it attached via a carbon atom. These different types of substitution lead to markedly

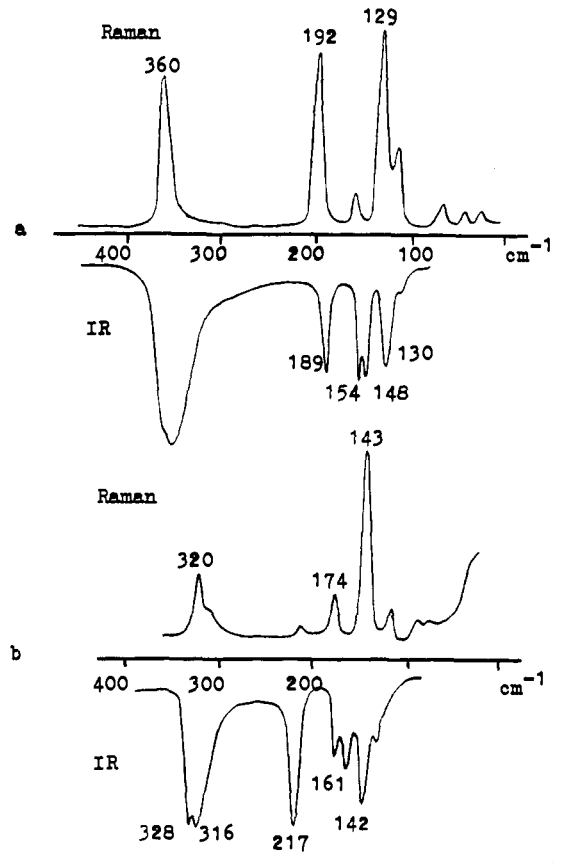

Figure 18. Low-frequency Raman and IR spectra of (a) (9-*o*-$C_2H_2B_{10}H_9)SnCl_3$ and (b) $(9\text{-}o\text{-}C_2H_2B_{10}H_9)_2SnCl_2$.

different chemical properties of the respective substances[72] and to different frequencies of the skeletal modes in their vibrational spectra.

The frequencies of the skeletal vibrations are situated in the region 100–360 cm^{-1}. As can be seen from Figure 18, the spectral pattern observed in this region is complicated and cannot be assigned easily.

A normal coordinate analysis on $CbSnCl_3$ and Cb_2SnCl_2 was accomplished[64] using the same approximation as described above and treating these molecules as quasi-pentaatomic models with the carboranyl groups as point masses. The force fields employed were set up on the basis of the corresponding data for alkyltin chlorides.[73] The model adopted permitted calculations of skeletal frequencies in sufficiently good agreement with the experimental values.

The calculated PED data along with the experimental data on the IR and Raman intensities and the polarization of the Raman lines made the interpretation of the skeletal vibrations possible.

The model for the $CbSnCl_3$ molecule belongs to the C_{3v} symmetry point group, its nine fundamentals occur as three totally symmetric modes of A_1 species and three degenerate modes of E species. Fundamentals of A_1 species may involve Sn–Cl and Cb–Sn stretching as well as ClSnCl deformation coordinates. Three polarized intense lines observed in the Raman spectra of *B*(9)-$CbSnCl_3$ type molecules near 360, 190, and 125 cm^{-1} are assigned to A_1 modes, the latter line being the strongest (the spectrum of *B*(9)-*o*-$CbSnCl_3$ is given in Figure 18a as a typical example). The PED data presented in Table VII show that the band at 360 cm^{-1} belongs to the ν(SnCl) mode, mixed to some extent with the ν(CbSn). Both the 190 and the 125 cm^{-1} lines are

TABLE VII. The Frequencies and PED Data[64] Data for $CbSnCl_3$ and Cb_2SnCl_2 Models (Cb = $C_2B_{10}H_{11}$)

symmetry species	ν, cm^{-1} average exptl	ν, cm^{-1} calculated	PED,[a] %
		$CbSnCl_3$	
A_1	125	140	27Q + 31α + 41β
	190	210	38Q + 37q + 18β
	350	359	36Q + 60q
E	110	125	97α
	135	142	38β
	350	362	98q
		Cb_2SnCl_2	
A_1	120	96	78γ + 27α
	140	141	10Q + 75β
	175	180	88Q + 12β
	330	328	93q
B_1	120	120	21Q + 79α
	220	225	79Q + 21α
B_2	120	119	95α
	330	322	95q

[a] The terms less than 10% are omitted. The symbols are as follows: Q, ν(SnCb); q, ν(SnCl); α, δ(CbSnCl); β, δ(ClSnCl); γ, δ(CbSnCb).

of heavily mixed origin, the stretching Cb–Sn and Sn–Cl motions dominating in the former, while the angle deformations dominate in the latter. Degenerate modes near 350, 135, and 110 cm^{-1} are well localized, corresponding to the ν(SnCl) and to two bending vibrations, respectively. Much the same frequency values for the ν(SnCl) modes of A_1 and E species as observed experimentally automatically follow from the results of the normal coordinate analysis.

The Cb_2SnCl_2 model belongs to the C_{2v} symmetry point group. The reduced representation of its nine fundamentals is as follows:

$$\Gamma_{vib} = 4A_1 + A_2 + 2B_1 + 2B_2$$

The calculated and experimental frequencies (the latter are given as averaged values of all isomeric (*B*-(9)-Cb)$_2SnCl_2$ molecules studied) along with PED data are listed in Table VII, while Figure 18b illustrates the spectrum of (*B*(9)-*o*-Cb)$_2SnCl_2$. It is seen that both bands near 330 cm^{-1} are pure ν(SnCl) modes. Both polarized Raman lines at ca. 175 and 140 cm^{-1} belong to ν(CbSn) and δ(ClSnCl) coordinate mixtures, the former line, however, being more ν(CbSn) stretch in character in spite of its lesser Raman intensity, while the latter has more δ(ClSnCl) character. In the antisymmetric mode, which shows itself as the strong IR band near 220 cm^{-1}, the ν(CbSn) stretching motion is predominant.

Thus, the mode eigenvectors for $CbSnCl_3$ and Cb_2SnCl_2 type molecules differ significantly. For the former, the contribution from Cb–Sn stretch coordinate is distributed almost equally among three totally symmetrical modes, while for the latter this coordinate participates actually in only one A_1 mode.

It seems interesting to compare the spectra of the corresponding B(9)- and C-substituted molecules because they strongly differ in reactivity. Experimental data[64] are available for a comparison of the spectra of a pair of (*C*-*m*-Cb)$_2SnCl_2$ and (*B*(9)-*m*-Cb)$_2SnCl_2$ isomers. It is seen that in the spectrum of C-derivative the frequencies of the ν(SnCl) and ν(CbSn) modes are higher by about 50 and 15 cm^{-1}, respectively, compared with B-substituted isomer.

Spectral studies of alkylchlorostannanes[73] have shown that the ν(SnCl) frequencies depend on the number and nature of the alkyl groups, attached to the tin atom. Comparison of the ν(SnCl) frequencies of carboranylchlorostannanes with those of corresponding alkylchlorostannanes confirms the electron-donating effect of the B(9)-carboranyl group and the electron-accepting effect of the C-carboranyl group, which have been established by reactivity studies (see, e.g., ref 72).

D. Limitations of the "Carborane Cage as a Pseudoatom" Model Treatment

All the foregoing results have demonstrated that the treatment of rigid deltahedral carborane cage as a pseudoatom allowed us to rationalize the low frequencies of the skeletal vibrations of substituted carboranes and even to roughly estimate the frequencies of Cb–X stretching modes.

However, this treatment is useful only when X is a sufficiently heavy atom. Then the Cb–X stretch mode is almost pure in respect to PED with its frequency lying below 400 cm^{-1}, i.e. below the region where internal carborane vibrations are situated. In this case the intense polarized Raman line, corresponding to the ν(CbX) mode, is characteristic for a given X and for its position in the carborane nucleus and thus can be used in analytical practice.

However, if a substituent X is light (e.g., Me, NH_2, OH, F, etc.), then the approach developed above does not work any more. In the latter cases, the Cb–X stretching frequency of a quasidiatomic model occurs just in the 700–800-cm^{-1} region, where the stretching vibrations of the carborane cage are situated, and begins to couple with them. It is well-known that the interaction of two vibrational energy levels of the same symmetry species in a molecule gives rise to a change in their energies and to a mixing of the vibrational wave functions (see, e.g., ref 74).

In other words, in the case of a light X substituent, the Cb–X stretching coordinate participates in several normal vibrations of the same symmetry, where it is heavily mixed with carborane skeletal stretching coordinates. This implies, that the Cb–X stretching vibration is no longer localized, i.e., it does not make an overwhelming contribution to the PED of any fundamental. There is, in fact, no band that can be assigned simply as the ν(CbX) stretch. That is why we can no longer find a single Raman line in the spectra of Cb–X type compounds with light substituents X, which can be confidently assigned to the ν(CbX). This situation is graphically depicted in Figure 19.

1. *Fluoro- and Aminocarboranes*

The spectra of monofluorocarboranes[75] present a spectacular example of the above-mentioned phenomena.

The introduction of a fluorine atom to a boron atom of the *o*-carborane cage (in either the 3 or 9 position) should lead to the occurrence of a new B–F stretching mode. By analogy with the spectra of the monohalocarboranes, discussed above, the emergence of a strong polarized Raman line, corresponding to the ν(CbF) stretch, might be expected.

However, in the spectra of both 3- and 9-fluoro-*o*-carboranes two new features appear in fact: a polarized

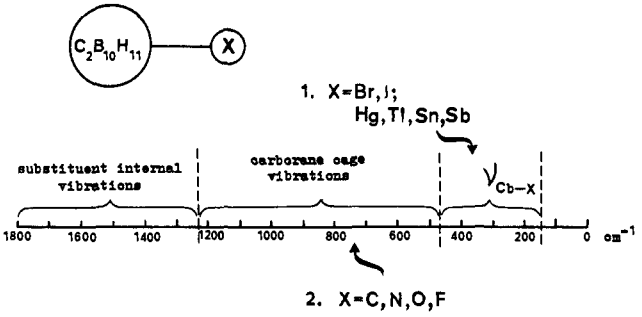

Figure 19. Schematic representation of the Cb–X stretching frequency position relative to the internal spectrum of carborane.

Raman line of medium intensity near 430 cm^{-1} and a very strong IR band near 1250 cm^{-1}. It is noticeable that both their frequencies lie outside the range of the vibrations of *o*-carborane (see Figure 19). What happens is that the frequency of the Cb–F stretch, as estimated for the quasidiatomic model Cb–F using Cyvin's K_{B-F} force constant,[28] is equal to 797 cm^{-1}, which is very close to the frequency of the carborane cage "breathing" vibration.[61,75] It is the coupling of these two modes (a kind of intramolecular mode resonance) which leads to the frequency divergence of up to 430 and 1250 cm^{-1} observed in the fluorocarborane spectra.

The same situation has been observed for *B*(9)-amino-*m*-carborane,[61] although in this case it is complicated by the presence in the spectrum of amino group internal modes. The new bands, which may be associated with the appearance of a new Cb–N stretch coordinate, lie at 290 and 1230 cm^{-1}.

2. "Dicarboranyl Ether" $(C_2H_2B_{10}H_9)_2O$

An interesting case presents the molecule of "dicarboranyl ether", [*B*(9)-*m*-$C_2H_2B_{10}H_9$]$_2$O which we will for the sake of brevity denote as [*B*(9)-*m*-Cb]$_2$O. Its structure has been resolved by X-ray analysis in ref 76, where also the vibrational spectrum has been discussed.

From the chemistry of *B*(9)-carborane derivatives it is known that the properties of the B(9)–X bond are much the same as those of the C–X bond in the corresponding aliphatic and aromatic compounds.[72] Hence, it is possible that the force field for dialkyl ethers would be suitable for a model description of the [*B*(9)-*m*-Cb]$_2$O skeletal modes. With this in mind, the authors[76] produced a normal coordinate analysis of the Cb–O–Cb triatomic model, while varying the force constants from the values for dialkyl ethers (K_q = 8.0, K_α = 2.0 in 10^6 cm^{-2} units) to the values for boron oxide (K_q = 6.2, K_α = 1.0). The main results show only a minor dependence on force constants variation and predict two symmetrical modes for this model at ca. 200 and 650 cm^{-1} and the antisymmetric Cb–O stretch near 900 cm^{-1}. In the two symmetrical vibrations, Cb–O stretch and Cb–O–Cb deformation coordinates appear to be heavily mixed.

In the experimental spectrum of the molecule discussed, the following new features arise (apart from the usual bands of *m*-carborane): a very strong polarized Raman line at 194 cm^{-1}, a medium IR band at 301 cm^{-1}, and a very intense IR band at 1290 cm^{-1}. It is obvious that Raman line at 194 cm^{-1} corresponds to calculated symmetrical mode at 200 cm^{-1}, assigned as a mixture of the ν(CbO) and δ(CbOCb) coordinates. The presence of the bands at 300 and 1280 cm^{-1} in the observed spectrum and the absence of the predicted modes near 650 and 900 cm^{-1} are explained by the authors[76] in the same manner, as for the case of the spectra of fluoro- and aminocarboranes,[61,75] by some intramolecular mode resonances, leading to the frequency divergence.

In this section we have discussed only skeletal vibrations of substituted carboranes, while ignoring the problem of a substituent influence on the carborane modes. This influence can be detected only by the pure, well-localized ν(BH) and ν(CH) modes. The behavior of the BH stretching band at 2600 cm^{-1}, which is of complicated origin, being a superposition of different symmetry species, and thus not useful for the analytical purposes, was discussed in section II. We will now discuss the CH stretching band.

E. The Effect of Substituents on the Carborane ν(CH) Band Parameters

As already mentioned, the carborane ν(CH) band has turned out to be extremely sensitive to all inter- and intramolecular interactions. In the discussion on phase transitions and molecular mobility in section V, we shall demonstrate the sensibility of the ν(CH) band frequency, intensity and half-width to the slightest changes in the molecular environment. The ν(CH) band is sensitive to intramolecular changes to a similar degree. When a substituent is attached to either a carbon or a boron atom of the carborane cage, the ν(CH) band immediately "feels" its influence, reacting by a frequency shift and an alteration in the IR integrated intensity.

We will consider the effects of a substituent on the ν(CH) band of C- and B-substituted carboranes separately.

In mono-C-substituted carborane molecules only one CH bond remains and consequently only one ν(CH) mode exists. The frequency and the integrated intensity (*A*) of the ν(CH) band have been measured[30,77] in the IR spectra of CCl_4 solutions for a vast number of C-substituted *o*- and *m*-carboranes with substituents of different nature. It was found that the ν(CH) frequency varies within small limits, 10 cm^{-1}, and without any regularity. In contrast, the IR-integrated intensity alters significantly, its value being correlated to the nature of the substituent (the data for *o*-carborane derivatives are presented in Table VIII). Electron-donating substituents proved to decrease *A* values, while electron-accepting ones serve to increase them; a linear correlation between the *A* values and the substituent inductive constants σ was found. It is obvious that introduction of a substituent to a carbon atom of the carborane cage influences the remaining CH bond polarity and thereby the $(\delta\mu/\delta q)_0^2$ value, which determines the IR band integrated intensity.

The large A_{CH} values for the $NHCOCH_3$ group does not comply with the correlation[77] and is evidently due to intramolecular hydrogen bond formation:

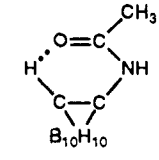

The ability of carborane CH bonds to participate in hydrogen bonding will be discussed later in section VII.

TABLE VIII. Integrated Intensity A of the CH Stretching Band[30,77] in the IR Spectra of C- and B-Substituted o-Carboranes $C_2B_{10}H_{11}X$ (in CCl_4 Solution)

substituent X	$A \times 10^{-3}$, l mol^{-1} cm^{-2}: substituent position		
	C	B(3)	B(9)
H	1.6	1.6	1.6
CH_3	1.2	1.2	1.8
C_2H_5	1.3		
i-C_3H_7	1.1		
CH_2Cl	2.3	1.9	
CH_2Br	2.1		
CH_2OH	2.3	2.0	
$CH{=}CH_2$	1.7	1.7	
$COCH_3$	2.8	2.4	
$COOCH_3$	2.9	2.1	
CHO	3.0		
OCH_3	1.7	1.4	
NH_2	1.6	1.1	
F		1.8	2.1
Cl		2.0	2.5
Br			2.3
$HgCH_3$	0.8		
$Si(CH_3)_3$	0.9		
$NHCOCH_3$	4.3	3.1	

Before we comment on the data for B-substituted carboranes, it must be emphasized that these molecules preserve both CH bonds; thus, all the previous remarks (in section II) about the CH stretches for unsubstituted carboranes are valid for their B-derivatives.

When a substituent is attached to a boron atom adjacent to a carbon atom (position 3 in o-carboranes or 2 in m-carboranes), both CH bonds remain equivalent and only one CH stretching band is observed in the spectrum. However, to make the data on IR integrated intensity measured for B(3)-ortho- or B(2)-meta-substituted carboranes comparable with those for the corresponding C-derivatives, one has to divide the A value obtained for a B(3) or a B(2) derivative by two, because the ν(CH) band in the case of these B derivatives originates from two independent CH oscillators.

The data obtained[30,77] for B(3)-o-carborane and B-(2)-m-carborane derivatives show that the ν(CH) band frequencies again alter within a narrow interval 10 cm^{-1}, while the A values undergo substantial changes (see Table VIII). However, they no longer exhibit a dependence on the inductive σ constants; the mechanism of a substituent interaction with the carborane cage via the boron atom is more complex. The same seems to be true for B(9)-derivatives, although the experimental data are scanty.

It should be taken into account that the introduction of a substituent in position 9 of the o-carborane nucleus makes the two CH bonds nonequivalent. If a substituent is "strong" enough, its different influence on the near and remote CH bonds will make their stretching frequencies shift differently, which could lead to ν(CH) band splitting or, at least, to a complicated contour for this band. The latter was observed in the IR spectrum of B(9)-fluoro-o-carborane in CCl_4 solution,[75] where the ν(CH) band exhibited a pronounced shoulder (see Figure 20).

Indeed, the two nonequivalent independent ν(CH) bands of B(9)-o-carborane derivatives will have different IR intensities even if the difference in their frequencies is small, the intensity being more sensitive. In this case, the measured A value of the overall ν(CH) band will, in fact, consist of two different values. In Table VIII

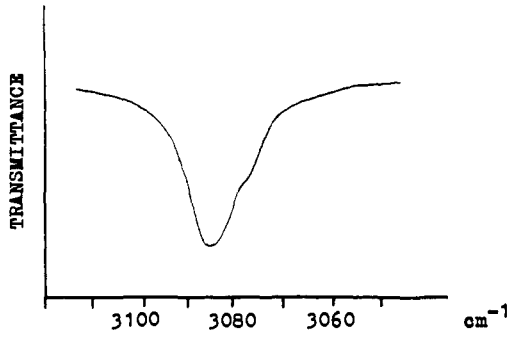

Figure 20. The ν(CH) band contour in the IR spectrum of 9-fluoro-o-carborane.

the "average" A_{CH} values (divided by 2) are presented to enable an approximate comparison of the data for the B(9)-derivatives with those for the corresponding C- and B(3)-derivatives.

Thus, IR spectra have shown that, in C-substituted carboranes, the effect of the substituent on the CH bond is transferred via an inductive mechanism, while, in the B-derivatives, the interaction is more complicated.

However, in spite of all complications, it is clear from the experimental results that the substituent attached to the boron atom in the remote position 9 affects the CH bonds more significantly than that attached to the nearer position 3. This is seen from the comparison of the A_{CH} values for 9- and 3-fluoro-o-carboranes, which are equal to 2.1 and 1.8 intensity units, respectively. The corresponding values for the 9- and 3-chloro-o-carboranes are 2.5 and 2.0. The more pronounced substituent effect on the ν(CH) IR band parameters from the remote position 9 was also noted for hydroxy-[55] and halocarboranes.[56]

It is important to note that carborane 3- (or 2-) and 9-halogen derivatives can be distinguished by their ν-(CH) frequencies; a halogen atom in the near position 3 (or 2) decreases the ν(CH) frequency and in the remote position 9 increases it. For instance, the ν(CH) frequencies of 3- and 9-fluoro-o-carboranes are equal to 3070 and 3084 cm^{-1}, respectively. This difference can be used in analytical practice.

Parameters of the ν(CH) band in the IR spectra of polyhalogen-substituted carboranes have been also measured.[30,56,77] An accumulation of halogen atoms in the carborane molecule was shown to lead to a gradual increase in the ν(CH) band IR intensity, its value reaching as much as 10.0 units per CH bond for B-decachloro-o-carborane. The frequency behavior is more complicated and depends on the positions of the substituents. The introduction of halogen atoms in the remote 9,12-positions obviously increases the ν(CH) frequency, whereas subsequent halogenation of the nearer positions leads to its decrease. It is only due to the interplay of these two factors that an overall decrease in the ν(CH) frequency down to 3040 cm^{-1} is observed for deca-B-chlorocarboranes.

F. The Effect of a Carboranyl Group on the Internal Vibrations of a Substituent

It is interesting to follow the inverse influence of a carboranyl group on a substituent by means of vibrational spectroscopy.

TABLE IX. Vibrational Frequencies (cm^{-1}) of Methyl Groups in the Spectra of Methylcarboranes[78]

vibration	local symmetry species	compound: 1-CH_3-o-$C_2B_{10}H_{11}$	1,2-$(CH_3)_2$-o-$C_2B_{10}Cl_{10}$	9-CH_3-o-$C_2B_{10}H_{11}$	9-CH_3-m-$C_2B_{10}H_{11}$	11-CH_3-2,7-$C_2B_9H_{12}$	monomethyldiborane (ref 79)
ν(CH)	E	3004	3004	2957	2963	2960	2944
ν(CH)	A_1	2947	2945	2911	2915	2915	2911
δ(CH)	E	1450	1442	1435	1440	1430	1424
δ(CH)	A_1	1391	1385/1398	1314	1316	1325	1319
$\tau(CH_3)$		273		218	218	239/219	

TABLE X. Vibrational Frequencies (cm^{-1}) of Vinyl Group in the Spectra of Vinylcarboranes[78]

vibration	compound: CH_2=CH—CH_3	1-(CH_2=CH)-o-$C_2B_{10}H_{11}$	3-(CH_2=CH)-o-$C_2B_{10}H_{11}$	9-(CH_2=CH)-o-$C_2B_{10}H_{11}$	(CH_2=CH)$_3$B
ν(C=C)	1648	1644	1619	1608	1604
$\delta(CH_2)$	1415	1414	1419	1411	1423
δ(CH)	1297	1308	1289	1285	1301

The authors[78] have compared the effect of *C*-, *B*(9)-, and *B*(3)-*o*- and *m*-carboranyl groups on the frequencies of Me, Vin, and ethynyl groups in the spectra of different isomers of methyl-, vinyl-, and ethynylcarboranes, respectively. The effect of carboranyl groups on the frequencies of the carbonyl group in different types of carbonyl derivatives (carbonyl chlorides, carboxylic acids, aliphatic and aromatic ketones, and aldehydes) has been also followed.[30]

The data on different methyl- and vinylcarboranes are given in Tables IX and X. It is seen that the methyl group frequencies in the spectra of C-derivatives are close to those of the corresponding methyl halides, which is to be expected when taking into account the electron-accepting properties of the C-carboranyl groups. If the methyl group is attached to the carborane cage via the B(9) atom, its frequencies are significantly lower as compared to C-substitution and close to corresponding values in the spectra of methylboranes.[79] The presence of the methyl group torsional mode in the spectra of methylcarboranes (at 270 cm^{-1} for *C*-methyl-*o*-carborane and at 218 cm^{-1} for *B*(9)-methyl-*o*- and *m*-carboranes) is indicative of the restricted methyl group rotation in the molecules discussed. The lesser degree of restriction (the lower frequency value) in the case where the methyl group is attached to a boron atom is reasonable when the free rotation of methyl groups in trimethylboron[32] or the low barrier to internal rotation (about 1 kcal/mol) in tetramethyldiborane[80] are taken into account.

The same is true of the vinyl and ethynyl group frequencies. The positions of these groups, attached to boron atoms of different nature [B(9)-carboranyl group is an electron donor, while B(3)-carboranyl group is an electron acceptor[72]] can also be recognized by using the ν(C=C) and ν(C≡C) mode frequencies, respectively, although the difference in this case is less than that between C- and B-derivatives. For instance, the ν(C≡C) frequencies for *C*-, *B*(3)-, and *B*(9)-ethynyl-*o*-carboranes are equal to 2140, 2095, and 2085 cm^{-1}, respectively (in the spectra of CCl_4 solutions).

Analogous results were obtained for other functional group frequencies, which are not superimposed with the carborane nucleus internal modes.

Summing up all the experimental data, we may conclude that, as a rule, the frequency values of all groups attached to a carbon atom of the carborane cage are higher when compared to those for B-substitution, which allows us to distinguish between C- and B-substitution by means of vibrational spectroscopy.

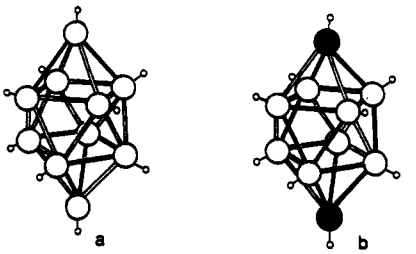

Figure 21. "Archimedian antiprisms": (a) *closo*-decaborate anion $B_{10}X_{10}^{2-}$; and (b) 1,10-dicarba-*closo*-decaborane (*p*-$C_2B_8H_{10}$).

IV. Vibrational Spectra of "Medium" and "Small" closo-Carboranes and Parent closo-Borate Anions

A. Medium-Sized Polyhedra

Among the "medium" boron polyhedra, only the family of the "Archimedian antiprisms" (see Figure 21) belonging to the D_{4d} symmetry point group has been widely studied. These are the $B_{10}X_{10}^{2-}$ *closo*-decaborate anions and 1,10-dicarba-*closo*-decaborane (*p*-$C_2B_8H_{10}$). All these moieties have 54 fundamentals which are distributed among symmetry species as follows:

$$\Gamma_{vib} = 6A_1 + A_2 + 2B_1 + 5B_2 + 7E_1 + 6E_2 + 7E_3$$

A_1, E_2, and E_3 modes are Raman active; A_1 modes give polarized lines, while E_2 and E_3 modes give depolarized lines; B_2 and E_1 modes are IR active, giving parallel and perpendicular bands, respectively. Thus, the assignment to symmetry species in these spectra is straightforward.

1. $B_{10}X_{10}^{2-}$ Anions (X = H, D, Cl, Br, I)

These polyhedra contain two types of boron atoms: apical and equatorial, the former being more negatively charged than the latter.[81] In contrast to icosahedral $B_{12}X_{12}^{2-}$ anions, here all the ν(BX), ν(BB), and δ(BBX) coordinates are not equivalent, each set being subdivided into subsets.

IR spectra of solid salts containing $B_{10}X_{10}^{2-}$ anions (X = H, Cl, Br, I) in the limited region 400–3700 cm^{-1} with some assignments can be found in refs 20, 22, 82,

TABLE XI. Comparison of Some Related Mode Frequencies (cm^{-1}) of the Polyhedra $B_{12}X_{12}^{2-}$ and $B_{10}X_{10}^{2-}$ in the Series X = H, D, Cl, Br, I[a]

anion	symmetry species	activity	assignment (refs 19 and 84)	X				
				H	D	Cl	Br	I
$B_{12}X_{12}^{2-}$	A_{1g}	R, p	ν_1 (out-of-phase pulsation of coaxial polyhedra)	2517 s	1899 m	1075 w	984 vw	
$B_{10}X_{10}^{2-}$	A_1			2483 m	1862 m	1154 m	1120 w	1066 w
$B_{12}X_{12}^{2-}$	A_{1g}	R, p	ν_2 (in-phase pulsation of coaxial polyhedra)	745 s	713 s	300 vs	193.5 vs	145 vs
$B_{10}H_{10}^{2-}$	A_1			836 vs	756 vs	303 vs	193 vs	146 vs
$B_{12}H_{12}^{2-}$	H_g	R, p	ν_5 (analogue of ν_2)	770 m	616 s	295 m	192 m	143.5 m
$B_{10}H_{10}^{2-}$	E_2, E_3			755 w	658 w	217 m	182 m	138 m
$B_{12}H_{12}^{2-}$	F_{1u}	R, p	ν_7 (analogue of ν_1)	2485 s	1872 s	1040 vs	983 s	926 s
$B_{10}H_{10}^{2-}$	B_2, E_1			2467 m	1652 s	1008 s	974 s	935 s
$B_{12}H_{12}^{2-}$	F_{1u}	R, p	ν_8 (mixed)	1071 m	928 w	540 s	442 s	379 s
$B_{10}H_{10}^{2-}$	B_2, E_1			1030 s		525 s	433 s	373 m

[a] Abbreviations are as follows: R, Raman; IR, infrared; s, strong; m, medium; w, weak; p, polarized; dp, depolarized.

and 83. A few Raman findings were mentioned in refs 17 and 82. In 1983 a paper of Leites, Kurbakova, et al.[84] appeared where vibrational spectra of these anions were presented in full for the first time. These authors reported the Raman and IR spectra of $M_2[B_{10}X_{10}]$ salts (X = H, Cl, Br, I; M = K, Cs) in aqueous solution and in the solid state and also of the acid $(D_3O)_2[B_{10}D_{10}]$ in D_2O solution. The objective of the paper was a comparison of the spectra of $B_{12}X_{12}^{2-}$ and $B_{10}X_{10}^{2-}$ anions.

The assignment of $B_{10}H_{10}^{2-}$ spectrum was made on the basis of Raman and IR activities, depolarization ratio measurements, and comparison with the spectra of $B_{10}D_{10}^{2-}$ and *p*-$C_2B_8H_{10}$.

Polarized Raman lines at 2515 and 2483 cm^{-1} were assigned to apical and equatorial BH stretching modes, respectively (in line with the assignments[17,20]), on the basis of partial deuteration experiments. Apical B–H bonds are more polar, and they are deuterated first, hence the BH stretching bands associated with them disappear from the spectrum first. Three intense polarized Raman lines at 1002, 836, and 741 cm^{-1} were shown to be skeletal stretches with predominant contribution from ν(BB) coordinates of different types. However, their significant shift on deuteration is indicative of their mixed origin with a certain participation of BH coordinates. The very high intensity of the Raman line at 836 cm^{-1} shows that it is due to the totally symmetric in-phase pulsation of coaxial polyhedra (by analogy with 745 cm^{-1} line of the $B_{12}H_{12}^{2-}$ anion).

Only seven depolarized lines are observed in the Raman spectrum of $B_{10}H_{10}^{2-}$ instead of the theoretical 13 (as for *p*-carborane). To explain this fact, an analogous assumption was made that the frequencies of related E_2 and E_3 modes with similar eigenvectors coincide. The same was assumed about related B_2 and E_1 IR-active modes because the number of observed IR bands was also less than theory predicted.

It is notable that all vibrational frequencies in the spectrum of the $B_{10}H_{10}^{2-}$ anion associated with apical B–H bonds are higher than those of equatorial ones.

The main frequencies of $B_{10}X_{10}^{2-}$ spectra are presented in Table XI, where they are compared with the corresponding data for $B_{12}X_{12}^{2-}$ anions. The point symmetry group D_{4d} of the Archimedian antiprism is not a subgroup of the icosahedral I_h group; hence, direct correlations between them are not possible. However, the comparison reveals much the same frequencies for related modes, which are similar in symmetry and character; this is striking and points to similar force fields of these anions.

Full Raman and IR spectra of solid cesium salts of $B_{10}H_{10}^{2-}$ and its 2-halogenated derivatives of the type 2-$XB_{10}H_9^{2-}$, X = Cl, Br, I have been presented by Preetz et al.[85] The authors have noted complex multiplets in the ν(BH) Raman region; the pattern observed is not much influenced by the introduction of different halogen atoms. These observations agree well with the above discussion (section II) about the reasons for the ν(BH) band splitting. On going from $B_{10}H_{10}^{2-}$ anion to its monohalo derivatives, the symmetry lowering leads to the occurrence of new bands in the skeletal mode region 500–1100 cm^{-1}. Introduction of the halogen atom into equatorial position results in the appearance of a strong IR band between 930 and 950 cm^{-1} which is absent from the spectra of axially halogenated anions and thus allows spectral differentiation between the two isomers. In the low-frequency region of halogenated species a pronounced feature appears, corresponding to (B_{10})–X stretch, its frequency being 335, 249, and 215 cm^{-1} in the series Cl, Br, I, respectively. These frequencies are much the same as those of the "cage–X" stretch for the other cage systems studied.[19,29,61,84]

The findings[19,84] on $B_nX_n^{2-}$ (n = 10, 12; X = Cl, Br) vibrational spectra appeared to be useful for Zakharova et al.[86,87] in elucidating the structures of new types of Ni and Pd complexes, containing *closo*-borate anions.

2. 1,10-Dicarba-closo-decaborane (*p*-$C_2B_8H_{10}$)

This molecule also belongs to the Archimedian antiprism family (Figure 21). The IR spectrum of this compound in the limited region 600–3700 cm^{-1} was first published by Hawthorne et al.[88,89] Leites, Vinogradova, et al.[90] presented its Raman and full IR spectrum and also the spectra of its *C,C*-dideutero analogue, *p*-$C_2D_2B_8H_8$. An assignment was proposed on the basis of Raman and IR activities, depolarization ratio measurements, band envelopes in the IR gas-phase spec-

trum, and also on comparisons with the spectra of the deuterated molecule and the $B_{10}H_{10}^{2-}$ anion.

The frequency of the totally symmetric BH stretching mode of p-$C_2B_8H_{10}$ is 2615 cm^{-1}, i.e., ca. 100 cm^{-1} higher than that of the $B_{10}H_{10}^{2-}$ anion. Considering that this mode is well-localized, this fact reflects a real strengthening of B–H bonds in a carborane as compared to a parent borane.

The CH stretching frequency of p-$C_2B_8H_{10}$ (3106 cm^{-1}) is about 50 cm^{-1} higher than that of p-$C_2B_{10}H_{12}$, which is also chemically significant and will be discussed later.

The most intense features in Raman are the strongly polarized lines at 737 and 871 cm^{-1}, which shift only slightly on C-deuteration. They are analogous to the 741 and 836 cm^{-1} modes of $B_{10}H_{10}^{2-}$ anion and are assigned to totally symmetric polyhedron vibrations. The polarized Raman line at 1120 cm^{-1} is predominantly a BC stretch.

The depolarized Raman line at 850 cm^{-1} which shifts to 720 cm^{-1} on C-deuteration is an E_3 mode with an overwhelming contribution from CH deformation. Its frequency is significantly lowered compared to that of the icosahedral p-carborane (1120 cm^{-1}). However, this comparison is not meaningful because both vibrations, as well as other vibrations situated in this spectral region, are of heavily mixed origin.

The number of spectral features attributable to degenerate modes in the spectrum of this molecule is also less than theoretical, as in the spectra of p-carborane-(12) and $B_{10}H_{10}^{2-}$, again suggesting similar frequencies of related E_2 and E_3 modes with close eigenvectors.

The vibrational data[90] were used by Atavin, Mastryukov, et al.[91] who carried out a normal coordinate analysis of p-$C_2B_8H_{10}$ for the purpose of obtaining a mean amplitude estimation which was needed for the refinement of gas electronography data.

3. Other $B_nH_n^{2-}$ Anions

Recently, a paper by Brint et al. devoted to the nature of BH groups in *closo*-borate anions appeared.[43] The IR spectra of the solid salts $Cs_2[B_nH_n]$, (n = 6, 8, 9, 10, 11, 12) in the region 600–3000 cm^{-1} at liquid nitrogen temperature along with the room temperature Raman spectra of the solids $Cs_2[B_{10}H_{10}]$ and $Cs_2[B_9H_9]$ were reported, the latter for the first time. The analysis of normal modes of the $B_9H_9^{2-}$ anion is given in terms of the D_{3h} symmetry point group. However, the assignment is restricted to the BH stretching modes as an indirect measure of the electronic properties of the B–H bonds. The authors came to the conclusions that the BH stretching frequencies have much the same energy (independent of cluster site or size) and that the hybridization of the B–H bonds in the whole series of *closo*-borate anions studied is sp^2.

B. "Small" *closo*-Borates and *closo*-Carboranes

The most comprehensive spectral studies have been produced for octahedral entities: the anionic *closo*-hexaborates $B_6X_6^{2-}$ (X = H, Cl, Br, I) and 1,6-dicarba-*closo*-hexaborane, p-$C_2B_4H_6$ (Figure 22).

1. Octahedral closo-Hexaborate Anions $B_6X_6^{2-}$ (X = H, Cl, Br, I)

The $B_6X_6^{2-}$ anion belongs to the O_h symmetry point

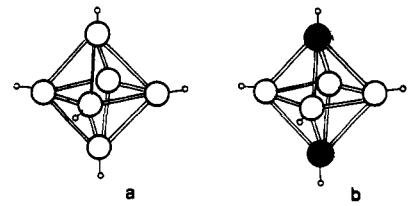

Figure 22. Octahedral clusters: (a) *closo*-hexaborate anion $B_6X_6^{2-}$; and (b) 1,6-dicarba-*closo*-hexaborane (p-$C_2B_4H_6$).

group. Its 30 fundamentals are distributed among symmetry species as follows:

$$\Gamma_{vib} = 2A_{1g} + 2E_g + F_{1g} + 2F_{2g} + 3F_{1u} + 2F_{2u}$$

The A_{1g}, E_g, and F_{2g} modes are Raman-active. The totally symmetric A_{1g} modes must exhibit polarized lines while degenerate E_g and F_{2g} modes must show depolarized lines. Only the F_{1u} modes are IR-active.

Full Raman and IR spectra of $B_6H_6^{2-}$ anion were first reported in 1982 by Bragin, Urevig, and Diem,[38] who presented Raman spectra of the solid $(Me_4N)_2B_6H_6$ and $Cs_2B_6H_6$ salts and also of tetramethylammonium salt in aqueous solution as well as the IR spectrum of a solid cesium salt.

An assignment of the experimental bands to symmetry species on the basis of Raman and IR activities, polarization measurements in the Raman spectrum of the aqueous solution, and also by analogy with the spectrum of $B_{12}H_{12}^{2-}$ was proposed.

Using these data, the authors carried out a normal coordinate analysis on the $B_6H_6^{2-}$ anion as well as on the isoelectronic p-$C_2B_4H_6$ molecule (see below) and estimated the eigenvectors of normal modes and principal force constants.

In 1984 a paper of Preetz and Fritze appeared,[92] where full spectra of a set of the anions $B_6X_6^{2-}$ (X = H, Cl, Br, I) were reported. The authors obtained the Raman and IR spectra of solid $Cs_2[B_6X_6]$ salts and also the Raman spectra of $Na_2[B_6X_6]$ in aqueous solution and proposed an assignment. These data are listed in Table XII, however, with exchanged ν_1 and ν_2 modes for $B_6H_6^{2-}$ (this transposition is necessary in order not to contravene the Rayleigh theorem and the "noncrossing rule"[93]).

The assignment[92] of $B_6H_6^{2-}$ bands to symmetry species substantially differs from that proposed by Bragin et al.[38] Preetz and Fritze presented experimental data, which clearly demonstrated that the Raman lines at 2452 and 820 cm^{-1} were depolarized while that at 993 cm^{-1} was polarized, in contrast to the earlier data.[38]

By following the frequency changes of $B_6X_6^{2-}$ in the series X = H, Cl, Br, I (Table XII), one can see excellent correspondence between these data and those found previously[19,84] for the $B_{12}X_{12}^{2-}$ and $B_{10}X_{10}^{2-}$ anions (Table XI). Thus, the analogy in $B_nX_n^{2-}$ deltahedra spectral behavior is obvious.

On analyzing the $B_6X_6^{2-}$ spectra, Preetz and Fritze came to the conclusion that, due to weak coupling, all fundamentals can be divided in two groups. The first group involves the internal modes of the B_6 rigid cage, observed in the range 750–1250 cm^{-1} at nearly unchanged positions for all X. The corresponding bands show multiplet substructures consistent with boron isotope effects. The second group consists of the modes

TABLE XII. Fundamental Frequencies (cm^{-1}) of $B_6X_6^{2-}$ Anions,[92] X = H, Cl, Br, I[a]

symmetry species	activity	vibration	X			
			H	Cl	Br	I
A_{1g}	R, p	ν_1	2500	1231	1216	1178
		ν_2	994	328	207	151
E_g	R, dp	ν_3	2451	991	(947)	(902)
		ν_4	938?	328	208	155
F_{2g}	R, dp	ν_5	767	749	753	758
		ν_6	824		38	32
F_{1u}	IR	ν_7	(2432)	(1122)	(1091)	(1057)
		ν_8	(1051)	(527)	(418/438)	(380)
		ν_9	(731)	(143)	(95)	(70)

[a] The frequencies are taken from the spectra of aqueous solutions, those in brackets, from the spectra of solid cesium salts. The Raman band at 938 cm^{-1} is assigned[92] to ν_4 in spite of being polarized.

originating from the motions of the substituent shell, their frequencies depending on the mass of X. They can be considered as the vibrations of a regular MX_6 octahedron, the rigid B_6-cluster playing the role of the central atom M. This point of view was corroborated in the subsequent paper by the same authors,[94] dealing with the spectra of 20 different halohydrohexaborates in the series $B_6X_nH_{6-n}^{2-}$ (X = Cl, Br, I; n = 1–5).

It is noteworthy that this approach is very similar to the "carborane cage as a pseudoatom" model, developed for the icosahedral carboranes[58,61-64] (see section III).

The IR spectrum of $Cs_2[B_6H_6]$ at liquid nitrogen temperature has been published recently.[43]

2. 1,6-Dicarba-closo-hexaborane (p-$C_2B_4H_6$)

This molecule (Figure 22) belongs to the D_{4d} symmetry point group. Its 30 fundamentals are distributed among symmetry species as follows:

$$\Gamma_{vib} = 4A_{1g} + A_{2g} + 2B_{1g} + 2B_{2g} + 3E_g + 3A_{2u} + 2B_{2u} + 5E_u$$

The spectrum must obey the mutual exclusion rule. The A_{1g}, B_{1g}, B_{2g}, and E_g modes are Raman active, A_{1g} exhibiting polarized lines while all the other species showing depolarized lines. The A_{2u} and E_u modes are IR active, the former giving parallel bands while the latter give perpendicular bands.

The IR spectrum of gaseous p-$C_2B_4H_6$ along with the salient features of the IR spectra of its main isotopic variants have been reported by Shapiro et al.[95] Full Raman and IR spectra have been presented by Jotham and Reynolds.[96] These authors proposed an assignment, based on band intensities, Raman polarization data, and IR band contours. Bragin, Urevig, and Diem[38] carried out a correlation of the vibrational modes of the isoelectronic $B_6H_6^{2-}$ anion and the p-$C_2B_4H_6$ molecule. Their assignment of p-$C_2B_4H_6$ is essentially that of ref 96 with the exception of the B_{1g} and B_{2g} skeletal motions. The reassignment was prompted by the revised Raman data on gaseous and liquid p-$C_2B_4H_6$ obtained by Urevig.[97] The authors[38] also produced a normal coordinate analysis for both octahedral entities and estimated principal force constants. Their results show that, except for the high-frequency ν(CH) and ν(BH) vibrations, both BH deformation and skeletal motions contribute significantly to the other normal modes. Thus, the description of the mixed modes, given in ref 38, is approximate, being based on the predominant contribution to the potential energy or displacement eigenvector.

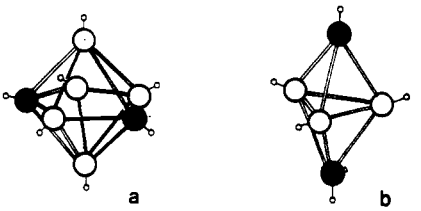

Figure 23. "Small" carboranes: (a) 2,4-dicarba-*closo*-heptaborane 2,4-$C_2B_5H_7$; and (b) 1,5-dicarba-*closo*-pentaborane (p-$C_2B_3H_5$).

The comparison of the totally symmetric frequencies and the force constants of the two octahedral clusters reveals that substitution of CH for BH^- results in bonding strengthening. An analogous conclusion based on vibrational data has been drawn for icosahedral and medium-sized boron clusters (see above).

3. Other Small closo-Carboranes (1,5-$C_2B_3H_5$ and 2,4-$C_2B_5H_7$)

Jotham and Reynolds[96] have also presented an analogous comprehensive Raman and IR study on two other small carboranes, namely, 1,5-dicarba-*closo*-pentaborane and 2,4-dicarba-*closo*-heptaborane, belonging to the D_{3h} and C_{2v} symmetry point groups, respectively (see Figure 23). Previously, only IR data were available for these molecules,[98-100] including the spectra of various isotopic species of 1,5-$C_2B_3H_5$.[98]

For the 24 fundamentals of p-$C_2B_3H_5$ the reduced representation is

$$\Gamma_{vib} = 4A_1' + A_2' + 5E' + 3A_2'' + 3E''$$

The modes of A_1', E', and E'' species are Raman-active. Of these, the A_1' modes should give rise to polarized lines. The modes of the A_2'' and E' species are IR-active. Thus, one should observe Raman and IR coincidences only for the E' modes. The spectrum of this molecule has been assigned, using Raman and IR relative intensities, Raman polarization data, IR band contours,[96] and the data on the IR spectra of deuterated species.[98]

The case of 2,4-$C_2B_5H_7$ proved considerably more difficult because of the much lower molecular symmetry. Thus, all 36 fundamentals should be Raman-active (13 polarized lines) and all but five should also be IR-active. However, it is seen from the experimental data[96] that the number of spectral features observed is less than the theoretical prediction and that the Raman counterparts of some IR bands are not observed and vice versa. This situation resembles that of icosahedral *o*- and *m*-carboranes, also belonging to the C_{2v} sym-

metry group but obeying the selection rules of higher effective symmetry. It would seem reasonable to analyze some of the $C_2B_5H_7$ spectral features by using effective D_{5h} symmetry.

Many of the assignments given for such a complex molecule are necessarily very tentative because of the insufficient information available.

The spectra of the three small carboranes (their main features will be presented in section VIII) have enabled the authors[96] to compare the related vibrations in the series $C_2B_nH_{n+2}$ (n = 3–5) in accord with the increase in polyhedron size.

A striking feature of these spectra is again the absence of any band below 450 cm^{-1}, which points to the marked rigidity within the cage systems.

The CH stretching vibrations of all three molecules occur at a very high frequency, which reflects, in the author's opinion, the high electron-withdrawing power of the whole carborane framework. Only one ν(CH) mode is observed for each molecule as a Raman line of medium intensity, its frequency decreasing in the series discussed as follows: 3158, 3118, and 3096 cm^{-} The IR-active ν(CH) modes were barely detectable in all cases, suggesting almost homopolar C–H bonds. It is only in 1,5-$C_2B_3H_5$ that the carbon atoms are present in four-coordinate sites, and this is manifested by the highest CH stretching frequency of any carborane.

The average BH stretching frequencies of the molecules discussed vary within small limits, being equal to 2622, 2660, and 2633 cm^{-1}, respectively, and thus showing no correlation with polyhedron size. The authors[96] have presented a linear correlation between BH stretching frequencies and NMR coupling constants for various boranes and carboranes, where the general trend is well established. However, they have concluded that evidently the carborane BH stretching frequencies are remarkably constant.

All the Raman and IR bands attributed to CH deformation modes are of low intensity. The characteristic region for these vibrations appears to be ca. 1200 cm^{-1}.

The assignment of the bands in the region 500–1100 cm^{-1} is not without ambiguity. Moreover, the calculations[38] show these modes to be of heavily mixed origin. Only the most intense, strongly polarized Raman lines can be confidently assigned to the cage stretches. These are 1125 and 842 cm^{-1} for 1,5-$C_2B_3H_5$, 1096 and 986 cm^{-1} for 1,6-$C_2B_4H_6$ and, probably, several lines in the interval 1000–800 cm^{-1} for the less symmetrical $C_2B_5H_7$. The higher frequencies are evidently more ν(BC) while the lower are more ν(BB).

Köster and Rotermund[101] reported some Raman data on 1,5-dimethyl-2,3,4-triethyl-1,5-dicarba-*closo*-pentaborane. They ascribed D_{3h} symmetry to the molecule studied on the basis of the non-coincidence of Raman and IR frequencies in the region 450–1050 cm^{-1}.

V. Spectral Investigation of closo-Carborane Phase Transitions and Reorientational Molecular Motion in the Solid State

A. Introduction

Modern vibrational spectroscopy, which considers not only band frequency, but also intensity, half-width, and contour, is diagnostic for phase-state identification.[102] An experienced spectroscopist can determine at a glance if a given spectrum belongs to a gaseous, liquid, or solid sample.

It is well-known that vibrational bands in a gas-phase spectrum exhibit specific rotational envelopes; in the spectrum of a crystalline substance the bands become narrow and band splittings due to crystal (site and correlation field) effects are observed; in the spectrum of a liquid the bands are rather broad without fine structure.

However, if we look at the spectra of solid $C_2B_{10}H_{12}$ carboranes, obtained at room temperature and presented in Figure 2, we will see broad bands with no sign of crystal splittings. In other words, the spectra of solids look like those of liquids. Moreover, the authors[11,14] have compared the spectra of solutions of *p*-carborane in CCl_4 and CS_2 with that of a crystalline sample (all at room temperature) and found that the half-widths of the same bands remained practically equal in both phases.

This modest fact is actually of great importance. After considering the relevant literature,[103–106] one can conclude from this fact that carboranes form so-called "plastic crystals" at room temperature.

The term "plastic crystal" was introduced by J. Timmermans[107] as far back as in 1938 and means a state of a solid substance in which the centers of mass of "globular" (another Timmermans's term) molecules are fixed in crystal sites while the molecules undergo reorientational motion. Plastic crystals are also more correctly called "plastic mesophases" or "rotatory phases" or, according to Kitaigorodsky, "rotationally-crystalline state". A necessary condition for rotatory phase formation is a weak van der Waals interaction between globular molecules.

It is natural that, on lowering the temperature, sooner or later a phase transition should occur and the plastic crystal will turn into a normal ordered crystal. Phase transitions may be detected by means of calorimetry, NMR spin–lattice relaxation measurements, and of course vibrational spectroscopy.

Much attention is paid to the mechanism of molecular reorientational motion in plastic mesophases and its "turning-off", as well as to the nature of the corresponding phase transitions.[104–106] However, many problems are still awaiting solution.

All *closo*-carboranes can be regarded as ideal models for plastic phase investigations since they are "the most globular" among all molecules, and also rigid and weakly interacting. A more extensive study on the phase transitions of large, medium, and small carboranes was published by Bukalov and Leites. They also established a correlation of molecular shape with the mechanism of reorientational mobility in a plastic phase.[108–109]

B. Icosahedral Carboranes $C_2B_{10}H_{12}$

We will demonstrate the logic of these authors' work, taking as an example, as usual, 1,12-dicarba-*closo*-dodecaborane which will be hereafter again referred to as simply *p*-carborane.

1. p-Carborane

The temperature dependence of the Raman spectrum of *p*-carborane in the region 5–3200 cm^{-1} over the temperature interval 12–550 K and of its IR spectrum in

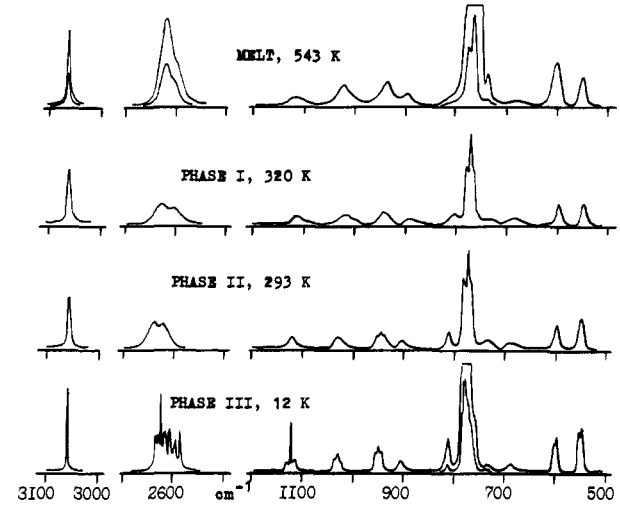

Figure 24. Raman spectra of *p*-carborane in different phase states.

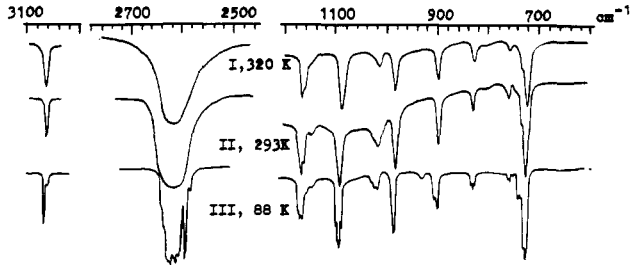

Figure 25. IR spectra of *p*-carborane in different phase states.

the region 400–3200 cm^{-1} over the temperature interval 12–400 K was studied in detail.[11,14,110] NMR, X-ray, and calorimetry methods were also used, when needed.[11,14,111,112]

The results show that solid *p*-carborane exists in three crystalline modifications, successively, designated as phase I (in the interval 543–303 K), phase II (303–240 K), and phase III (below 240 K). Thus, *p*-carborane exhibits two phase transitions at 303 and 240 K. The substance melts at 543 K in a sealed ampule.

The Raman spectra of phases I–III are presented in Figure 24 and the IR spectra in Figure 25. In the Raman spectrum of phase I above 303 K the frequencies and widths of the lines do not differ from those in the solution spectra. Neither band narrowing nor crystal splitting is observed. In the low-frequency region, the Rayleigh line shows a wide wing, which is usually characteristic of liquids, where it is due to molecular rotational motion. These facts point to the plastic character of phase I. The phase transition I–II does not markedly alter the intramolecular Raman spectrum, only slight changes in several line shapes being observed (e.g., in the ν(BH) contour in the region 2600 cm^{-1}). The same can be said about the IR spectra. Thus, the spectrum of the internal vibrations proved to be of no use for the detection of the phase transition I–II. However, this transition is clearly manifested in the low-frequency region of the Raman spectrum (Figure 26), where the Rayleigh line wing disappears abruptly and two broad, weak bands appear instead.

The second *p*-carborane phase transition II–III has been found to occur at 240 K. Below this point pronounced narrowing of Raman lines and IR bands as well as crystal field splittings of bands are observed (Figures

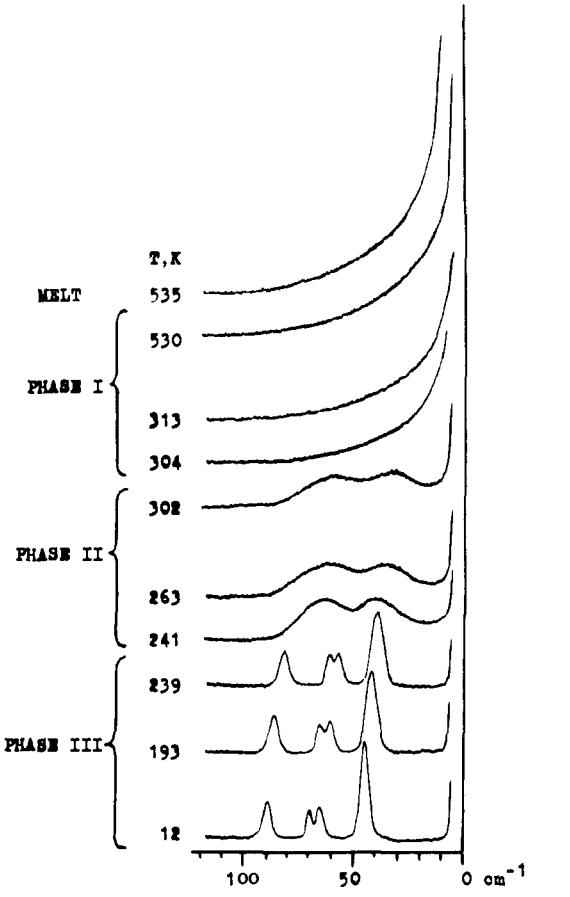

Figure 26. Low-frequency region of the Raman spectrum of *p*-carborane at different temperatures.

24 and 25). In the low-frequency Raman region a clear-cut spectrum of lattice vibrations appears, its frequencies increasing, as usual, on lowering the temperature (see Figure 26). These two phase transitions of *p*-carborane at the given temperatures have been confirmed by calorimetric and NMR studies.[14,111]

The vibrational results obtained allowed the authors to conclude that the *p*-carborane phases I and II are plastic, while the phase III is an ordered crystal. The plastic character of the phases I and II is indicated not only by vibrational spectral patterns, but also by the typical appearance of the substance in this temperature interval (semitransparent waxy soft crystals, extremely volatile) and also by NMR and X-ray data.

The existence of two successive plastic modifications for one compound has been observed previously, e.g. for cyclopentane,[113] *tert*-butyl bromide,[114] etc., but the difference between the two plastic phases has not been clarified.

X-ray investigations performed on *p*-carborane[11,112] have demonstrated that both plastic phases are cubic and face-centered, with four molecules per unit cell. The symmetry of the unit cell does not change upon the I–II phase transition.

The nature of the difference between the two *p*-carborane plastic modifications, as seen in the low-frequency Raman spectrum,[11,110] thus drew attention.

A wide Rayleigh wing in this range, observed for plastic phase I, is typical for liquids where molecular rotational motion is isotropic. This suggests by analogy that the rotational motion of *p*-carborane molecules in plastic phase I is also isotropic.

The low-frequency Raman region of plastic phase II with its weak, broad features (see Figure 26) resembles that of an ordered crystal just before melting, when the reorientations about the axes with the least moment of inertia become "unfrozen".[115,116] Hence the authors[11] assumed, also by analogy, that rotational motion in the *p*-carborane plastic phase II was also anisotropic, viz. reorientations about the preferred molecular axes occurred.

These assumptions were borne out in full by NMR, X-ray, and calorimetric experiments and also by the temperature study of the ν(CH) IR band contour, reported in ref 14. Calorimetric data showed that both *p*-carborane phase transitions were of the first order and of the partial ordering type, with rather large entropy increments.

Thus, vibrational spectroscopy has been able to prove that solid *p*-carborane forms three crystal modifications in succession, two of them being plastic and the low-temperature one being an ordered crystal. In both plastic phases dynamic orientational disorder takes place, but they differ in the rate and character of the reorientational motion. These conclusions[11,110,111] were confirmed later by a spin–lattice relaxation NMR study.[117]

2. *m*-Carborane

Phase transitions of *m*-carborane have been studied by IR,[118] Raman,[13] and NMR[13,119,120] methods. In contrast to refs 119 and 120, two phase transitions were found in refs 13 and 118. The results[13] are quite similar to those obtained for *p*-carborane but with somewhat differing phase transition temperatures: 277 and 165 K, which are in good agreement with adiabatic calorimetric data reported for *m*-carborane by Westrum and Henriquez.[121] It is of interest that *m*-carborane, unlike *p*-carborane, exhibits its II–III phase transition point in dependence on the thermal prehistory of the sample, the temperature interval of this phase transition being "stretched out".[13]

3. *o*-Carborane

While carrying out Raman investigations of phase transitions of the most wide-spread isomer, the *o*-carborane, Bukalov and Leites encountered unexpected difficulties.[12,112]

As distinct from the para and meta isomers, a rather voluminous literature was devoted to *o*-carborane plasticity and phase transitions. There were detailed ^{1}H and ^{11}B NMR studies,[117,119,122,123] X-ray,[119,124] DSC,[119] and adiabatic calorimetric data,[121] and also one vibrational study where an attempt was made to elucidate the molecular dynamics of *o*-carborane by exploring the temperature dependence of band shapes in the Raman spectrum.[125]

However, the results of all these works were inconsistent and even contradictory. All the authors agreed that solid *o*-carborane underwent a phase transition near 273 K. Above this point molecular rotational motion was shown to be isotropic and below, anisotropic.

In one group of papers it was stated that this phase transition was the only one in the temperature interval studied, from 473 to 143 K. It was assumed that either an order–disorder phase transition would occur at a lower temperature, or the ordered state would not be attained by *o*-carborane at all for kinetic reasons,[119] or the process of ordering would be gradual.[122]

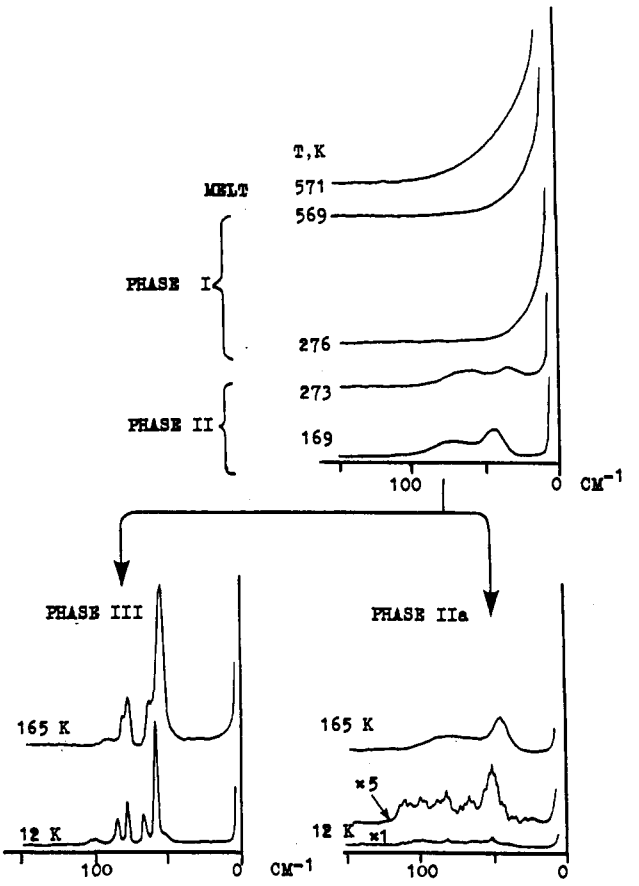

Figure 27. Phase transformations of *o*-carborane according to the temperature evolution of its low-frequency Raman spectrum.

Another group of publications contained information about the second low-temperature phase transition. For instance, in the excellent adiabatic calorimetric study produced by Westrum and Henriquez[121] the second phase transition was determined precisely to be at 158.2 K. NMR investigation presented by Reynhardt et al.[123] reported the second phase transition at 200 K.

Thus, the vibrational study of Bukalov and Leites[12,112] was aimed to solve the *o*-carborane problem. Bearing in mind that the three $C_2B_{10}H_{12}$ isomers were very similar in their dimensions, nature, and properties, it was difficult to understand on physical grounds why ortho isomer should behave distinctly from the para and meta isomers.

Temperature investigation of the Raman spectrum of *o*-carborane[12] in the interval 550–12 K shows that, after solidification at 550 K (in a sealed ampule) and down to 274 K, *o*-carborane exists as a plastic phase I, exhibiting rather wide lines for intramolecular vibrations and a broad Rayleigh wing in the low-frequency region (Figure 27). This plastic phase I is very much the same as those of *p*- and *m*-carboranes and corresponds, according to NMR data,[117,119,122] to isotropic molecular motion.

At 274 K phase I inevitably transforms into the plastic phase II with its two broad features in the low frequency Raman region (see Figure 27). This phase II with anisotropic molecular reorientations, evidenced by the NMR data,[122] is also quite similar to phases II

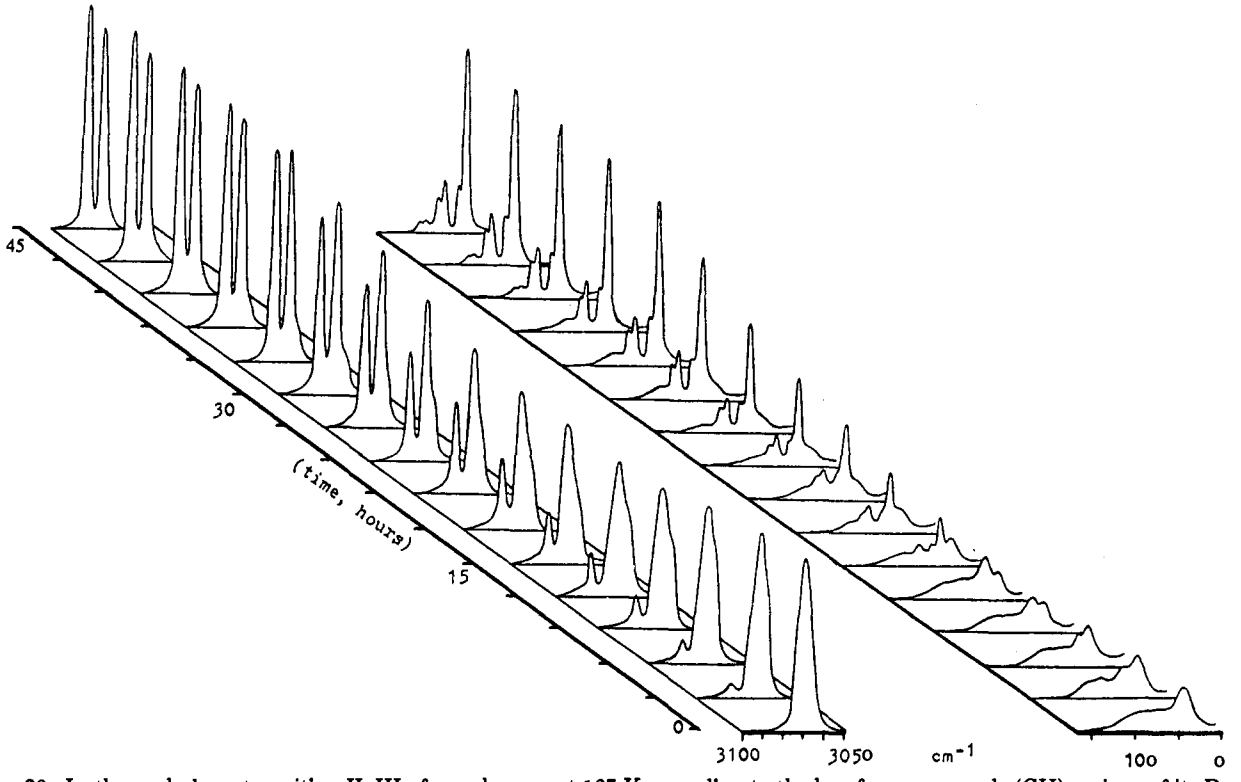

Figure 28. Isothermal phase transition II–III of *o*-carborane at 167 K according to the low-frequency and ν(CH) regions of its Raman spectrum.

of the para and meta isomers. On lowering the temperature, it continued to exist down to 167 K.

However, the subsequent course of events depends on uncontrolled experimental conditions and on the rate of cooling.

If the sample of *o*-carborane is cooled comparatively rapidly (10 K per hour) then phase II transforms near 166 K into a new phase. However, according to its Raman pattern, this new phase does not correspond to the ordered crystal phases III of *p*- and *m*-carboranes. Bukalov[112] designated this new phase as IIa. It is noteworthy, that the difference between phases II and IIa of *o*-carborane, as observed in the Raman spectrum, is not pronounced and can be revealed only by precise measurements. The II–IIa phase transition manifests itself only by a slight shift of the ν(CH) line from 3069 to 3067 cm^{-1} (this line also acquires a shoulder) and by a slight but noticeable alteration of the low-frequency broad feature. It is pertinent to remember here that Baughman,[119] who was the first to investigate phase transformations of solid *o*-carborane, reported a small jump ("anomaly") in the heat capacity curve (with $\Delta S < 0.15$ eu) in his DSC experiment at just the same temperature, namely ca. 166 K. It is of interest to note that the II–IIa phase transition has not been detected by NMR.

However, if the temperature of the sample in phase II is maintained at 169 K for 12 h and then lowered to 167 K extremely slowly, under equilibrium conditions, then an isothermal transition from phase II to the ordered phase III does occur. This slow phase transition is completed within 45 h; its spectral pattern is given in Figure 28.

Phase III manifests itself as an ordered crystal by its clear-cut phonon spectrum in the low-frequency Raman region and by the correlation field splitting of several lines, in particular, the ν(CH) band (see Figures 27 and 28), i.e. just like phases III of the para and meta isomers.

Phase IIa, when subsequently cooled, can either spontaneously change to phase III or remain down to 12 K, depending on the experimental factors which still require elucidation. Heating of the *o*-carborane ordered crystal phase III led in all experiments to the phase transition III–II (with a large hysteresis), but never to III–IIa. Hence, phase IIa is metastable while the phase transition IIa–III is monotropic.

Thus, Raman spectroscopy experiments have shown that the phase state of *o*-carborane is not a single-valued function of the temperature, but also depends on the thermal prehistory of the sample. If the sample is cooled adiabatically, the substance being able to "follow" the external effect, then an equilibrium ordered crystal is formed. However, if the substance is cooled rapidly, under nonequilibrium conditions, then a metastable modification arises, which can exist for a long time for kinetic reasons.

o-Carborane metastable phase IIa seems to be much the same as that named "glassy crystal" by Adachi, Suga, and Seki,[126] who studied the phase transitions of plastic cyclohexanol in 1968. The authors used this term to describe a state of matter which arose when the dynamic orientational disorder in a plastic phase was suddenly "frozen-out". The transition to this "glassy" modification resembles the glassification point T_g. However, subsequent investigations have demonstrated that this point of view was to some extent a simplification.[127–129]

The *o*-carborane "glassy crystal" phase IIa, when cooled to 12 K, exhibits an unusual and peculiar spectral pattern: all the lines in the Raman, including the low-frequency feature, are split into a lot of sharp, extremely narrow peaks, their half-width seems to be

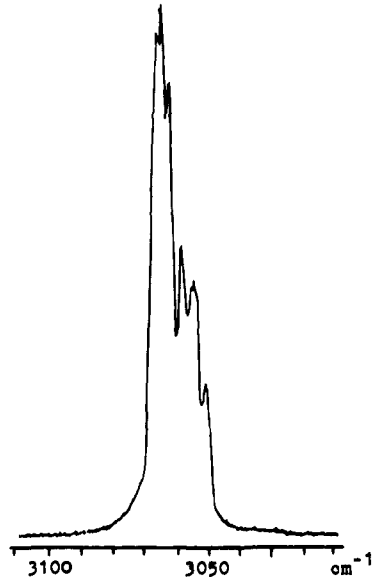

Figure 29. The ν(CH) Raman band of *o*-carborane in phase IIa at 12 K (spectral slit width 0.5 cm^{-1}).

limited only by the spectrometer resolution.

This is exemplified in Figure 29 by the ν(CH) Raman band, recorded at 12 K with a spectral slit width of 0.5 cm^{-1}. The band is split into at least seven peaks. This superfine structure is unique and suggests a domain structure of the nonequilibrium "glassy" phase (in accordance with ref 129), but this problem calls for further investigation and is outside the scope of this review.

The above results enabled Bukalov and Leites to propose the following scheme for *o*-carborane phase transformations:

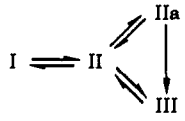

which is illustrated by the Raman spectrum evolution, shown in Figure 27. Thus, the discrepancies encountered in the literature concerning the *o*-carborane phase diagram are explained merely by the fact that one group of investigators, including Baughman[119] and Leffler et al.,[117,122] dealt with the metastable phase IIa formed on rather rapid cooling, while Westrum and Henriquez[121] succeeded in obtaining the equilibrium ordered crystal phase III.

4. Conclusions

The results obtained for phase transformations of the three carborane isomers are summarized in Figure 30 and can be formulated as follows:

1. All the three isomers form in the solid state three crystal modifications in succession, two of them (I and II) being plastic and the low-temperature one being an ordered crystal (III).

2. The two plastic phases of a carborane differ in the low frequency part of the Raman spectrum. Phase I exhibits a broad Rayleigh wing, which is indicative of isotropic molecular rotational motion; for phase II weak broad features are typical, which correspond to anisotropic molecular reorientations about preferred axes.

3. Icosahedral carboranes have proved to be ideal models for the study of the phase transition I–II between two plastic phases. This phase transition was found to be of the first order and of the partial ordering type in which the rate and the mechanism of molecular reorientational motion change abruptly.

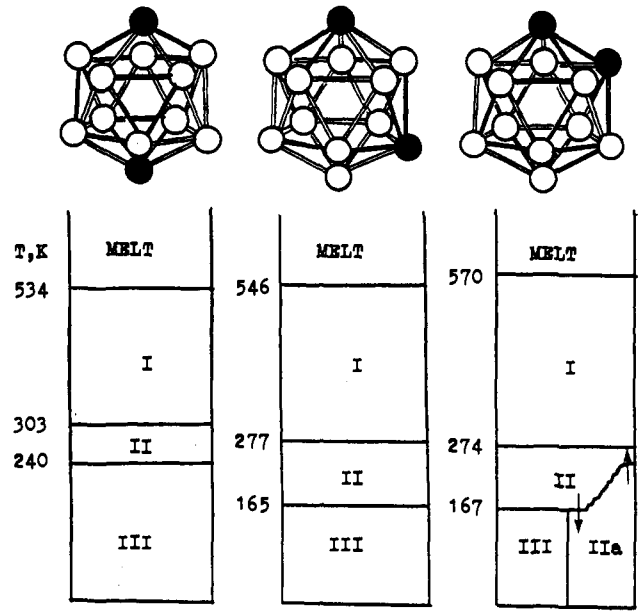

Figure 30. Phase diagrams of the three isomers of dicarba-*closo*-dodecaborane: I, plastic phase I; II, plastic phase II; IIa, metastable "glassy-crystalline" phase; and III, ordered crystal.

4. In contrast to the para and meta isomers, the phase transition II–III in *o*-carborane occurs with difficulty and a metastable phase IIa can emerge instead. To make *o*-carborane molecules form an ordered crystal, it is necessary to create equilibrium conditions by lowering the temperature very slowly.

5. The metastable *o*-carborane phase IIa seems to be a "glassy crystal", its nature being not yet clear. Peculiar superfine structure of its Raman bands at helium temperatures suggests a kind of domain structure.

For solid *o*-carborane, the temperature range for existence in orientationally disordered state (both plastic phases) is 403 K, for *m*-carborane 381 K, and for *p*-carborane 294 K. Taking into account the fact that para isomer has no electric dipole moment, while the values of the latter are 2.8 D for the meta isomer and 4.3 D for the ortho isomer, an inference can be drawn that dipole–dipole interactions do not play a prominent role in the process of orientational ordering in molecular crystals, which is in keeping with Kitaigorodsky's conclusion, presented in his well-known monograph *Molecular Crystals and Molecules*.[103]

Comparing the data obtained for carboranes with the data on the temperature duration of orientationally disordered plastic phases for organic molecules,[130,131] it can be said that *o*-carborane is an absolute champion in this respect, because it manages to keep its rotational freedom in the temperature range 403 K. In other words, the *o*-carborane molecule is the most freedom-loving among all globular molecules.

It is noticeable that plastic phases are formed not only by unsubstituted carboranes, but also by those carborane derivatives in which small substituents are attached to the carborane nucleus, e.g. CH_3, F,[75] etc.

C. "Medium" and "Small" Carboranes

Bukalov and Leites have also studied in the same manner (measuring above all the temperature depen-

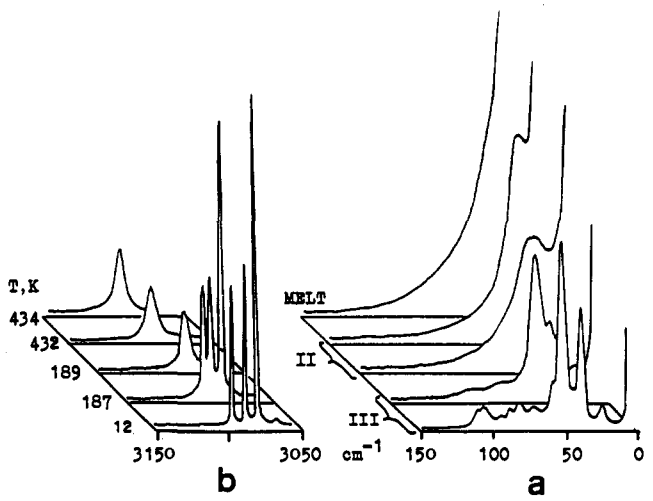

Figure 31. Temperature evolution of the Raman spectrum of dicarba-*closo*-decaborane: (a) low-frequency region and (b) CH stretching band. The symbols are as follows: M, melt; II, plastic phase; and III, ordered crystal.

dence of the Raman spectra but also using, when needed, IR, NMR, and X-ray methods) the phase transformations of a medium carborane *p*-$C_2B_8H_{10}$[132] and also of the small carboranes *p*-$C_2B_4H_6$ and *p*-$C_2B_3H_5$.[112,133,134]

1. 1,10-Dicarba-closo-decaborane

As mentioned above, the *p*-$C_2B_8H_{10}$ molecule has the form of an Archimedian antiprism (see Figure 21). In contrast to the nearly spherical $C_2B_{10}H_{12}$, it is stretched along the S_8 axis.

At room temperature the sample is a soft, volatile, semitransparent polycrystalline colorless solid, i.e. a typical representative of plastic crystals. Its plasticity is confirmed by the vibrational spectrum.[90,132] Indeed, at room temperature the width and shape of Raman lines, originating from intramolecular modes, do not differ from those obtained in solution spectra. However, the spectral pattern in the low-frequency Raman region (Figure 31), where a weak broad feature is observed, indicates that this plastic phase corresponds not to phase I, but to phase II of icosahedral carboranes. This fact suggests that at room temperature *p*-$C_2B_8H_{10}$ forms a plastic phase with anisotropic molecular reorientations. It was possible that on increasing the temperature a phase transition might occur to plastic phase I with its isotropic molecular motion. This phase I should have a broad Rayleigh wing in the low-frequency Raman region. Therefore the sample was heated to 470 K, but no phase transition in the solid state was observed, and at 433 K the sample melted (in a sealed ampule).

On cooling the sample from ambient temperature to 188 K, the single plastic phase turns into an ordered crystal, which exhibits a clear-cut phonon spectrum in the low-frequency Raman region and correlation field splittings of the intramolecular bands. The temperature evolution of the two most informative parts of the Raman spectra (low frequency and the ν(CH) regions) are shown in Figure 31.

NMR data confirmed the phase transition at 187 K for this substance and the anisotropic reorientations in its plastic phase. Reorientational disorder in the sample

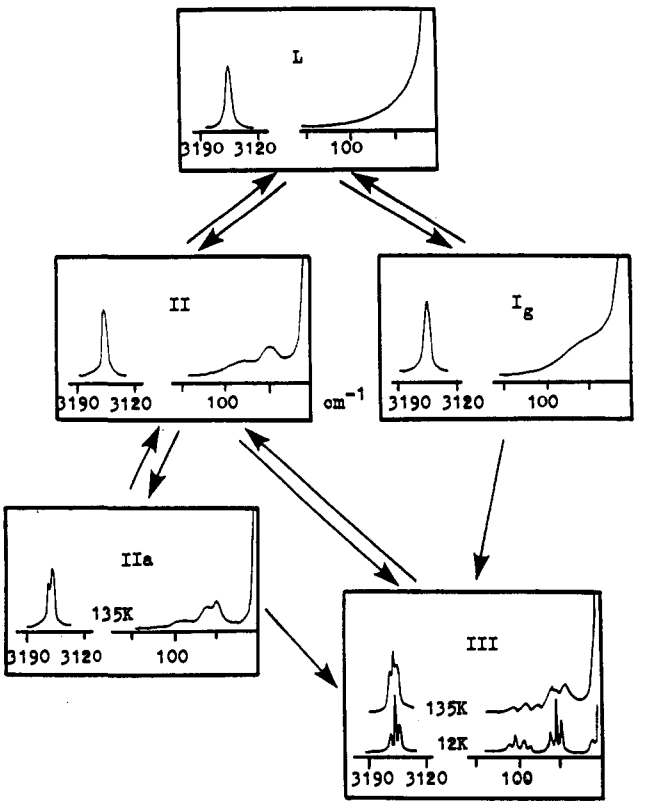

Figure 32. Phase transformations of 1,5-dicarba-*closo*-pentaborane according to temperature evolution of its Raman spectrum in the low-frequency and CH-stretching regions: L, liquid; Ig, glass; II, plastic phase; IIa, metastable "glassy crystal"; and III, ordered crystal.

at room temperature was also demonstrated by X-ray findings.[112]

Thus, a stretched medium carborane turned out to have only one plastic phase, apparently with anisotropic molecular reorientations. The single broad weak band observed in the low-frequency region of its Raman spectrum seems to correspond to the libration around the preferred axis.

2. 1,5-Dicarba-closo-pentaborane

In an analogous study of a small stretched carborane, *p*-$C_2B_3H_5$ (see Figure 23), almost the same results were obtained, but the phase transformations of this substance are somewhat complicated.[112,133,134]

The substance is a gas at ambient temperature, its boiling point being 269 K while the melting point is 150 K. All experiments were carried out with the sample in a sealed ampule. The temperature evolution of the Raman spectrum of this carborane in the low-frequency and ν(CH) regions is presented in Figure 32 together with the spectral interpretation.

The liquid *p*-$C_2B_3H_5$ exhibits a wide Rayleigh wing in the low-frequency Raman. On solidification of the substance this wing disappears, being substituted by two weak broad features, while the spectrum of intramolecular vibrations does not significantly change. Hence, it is clear that a plastic phase is formed on solidification, which is analogous to the phase II of the icosahedral carboranes and to the single plastic phase of the medium carborane studied. By analogy, anisotropic molecular reorientations were assumed in this plastic phase. It is noticeable that, on going from the

liquid to the plastic phase, the frequency of the CH stretching band shifts abruptly from 3154 to 3152 cm^{-1}. The plastic phase does not exist over a long temperature interval. Under equilibrium conditions (slow cooling) at 135 K, it transforms into an ordered crystal with a clear-cut phonon spectrum and narrow lines, corresponding to internal modes. The ν(CH) band splits into four Davydov peaks.

However, the small carborane in question does not always turn from the liquid into a plastic phase. When rapidly cooled, the liquid often glassifies (see phase Ig in Figure 32). On subsequent cooling, phase Ig spontaneously transforms into an ordered crystal phase III. On fast cooling, the plastic phase sometimes suddenly turns into a "glassy-crystalline" modification, analogous to phase IIa of icosahedral *o*-carborane. It is easy to distinguish between the plastic phase and the "glassy crystal", because they differ substantially in the ν(CH) Raman region (see Figure 32).

The "glassy-crystalline" modification of *p*-$C_2B_3H_5$ turns into an ordered crystal on its own, each time at a different temperature.

The phase transitions Ig–III and IIa–III are monotropic and the modifications Ig and IIa are metastable, because the ordered crystal phase III on heating always transforms only into the plastic phase.

Thus, the small carborane *p*-$C_2B_3H_5$, like the medium carborane *p*-$C_2B_8H_{10}$, forms only one plastic phase, apparently, with anisotropic reorientations. It is remarkable that both molecules are stretched. Besides, *p*-$C_2B_3H_5$ tends to form metastable modifications. As in the case of the icosahedral *o*-carborane, the phase state of *p*-$C_2B_3H_5$ is again not a single-valued function of the temperature, but depends on the thermal history of the sample.

3. 1,6-Dicarba-closo-hexaborane

A similar study of another small carborane, *p*-$C_2B_4H_6$ (Figure 22) with its quasispherical octahedral molecule, has shown that this substance, a liquid at room temperature, forms on solidification at 241 K a plastic phase with a Rayleigh wing in the low-frequency Raman region, i.e. with isotropic molecular motion.[112,133] This is the only plastic phase of this substance; it turns into an ordered crystal phase on subsequent cooling.

The results obtained for the phase transformations of medium and small *p*-carboranes are summarized as phase diagrams in Figure 33. Only the equilibrium phases are presented for the smallest *p*-$C_2B_3H_5$.

D. General Remarks on *closo*-Carborane Phase Diagrams

Comparative analysis of the data obtained by Bukalov and Leites for $C_2B_nH_{n+2}$ carboranes of different size and shape allowed these authors to formulate the following main conclusions:

(1) All the carboranes studied form plastic phases because of their globular shape and weak intermolecular forces.

(2) There exist two types of plastic phases (type I and type II), which differ in the degree of dynamic orientational disorder and in the mechanism of the molecular reorientational motion. In plastic phases of type I, the reorientational motion is isotropic and seems to be a kind of rotational diffusion, like that in simple liquids.

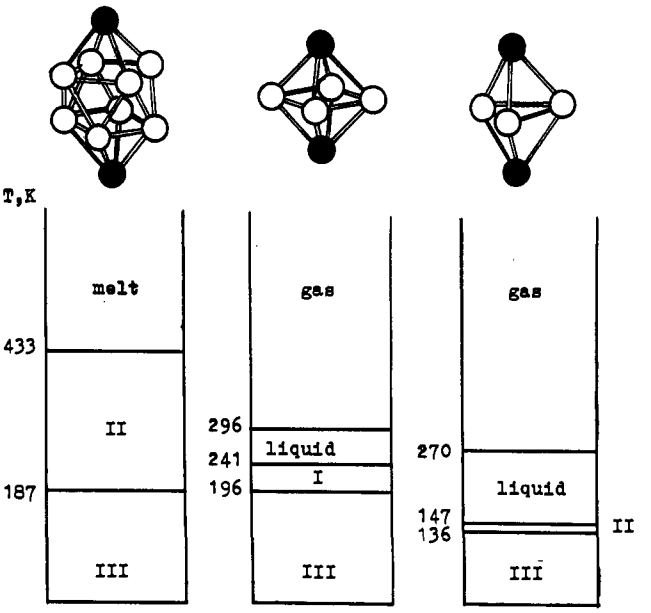

Figure 33. Phase diagrams of "medium" 1,10-dicarba-*closo*-decaborane and "small" 1,6-dicarba-*closo*-hexaborane and 1,5-dicarba-*closo*-pentaborane: I, plastic phase of type I; II, plastic phase of type II; and III, ordered crystal.

In plastic phases of type II, the reorientational motion is anisotropic and shows itself as reorientational jumps about the preferred axes.

(3) These two types of plastic phases can be easily distinguished by the low-frequency region of the Raman spectrum. A broad Rayleigh wing corresponds to the plastic phase of type I, while broad weak features are indicative of a plastic phase of type II. The Rayleigh wing is formed by isotropic molecular motion, while the broad weak bands might be assigned to librations about the preferred axes, broadened by fast reorientational jumps.

(4) A globular substance can form either only plastic phase of type I (like quasispherical *p*-$C_2B_4H_6$), or only plastic phase of type II (like stretched molecules *p*-$C_2B_8H_{10}$ and *p*-$C_2B_3H_5$), or both plastic phases in succession (like three isomers of $C_2B_{10}H_{12}$), depending on the size, shape, and symmetry of the molecule.

(5) The temperature interval of the plastic phase existence is related to molecular size and structure, being the least (10 K) for *p*-$C_2B_3H_5$ and the largest for icosahedral *o*-carborane (403 K). *o*-Carborane is an absolute champion in this respect among all globular molecules.

It should be emphasized here that the study of carborane molecular mobility is not simply a "Glassperlenspiel", using the term of Hermann Hesse.[135] The results of such investigations could be very useful in solid-state chemistry. The kinetics of solid-phase reactions, now attracting wide interest, are directly related to the rate and mechanism of molecular motions.[136]

Another quite unexpected application of plastic-phase studies is as follows. The most powerful method of molecular structure determination is X-ray analysis, which requires the use of a perfect crystal. If a substance forms a plastic crystal at ambient temperature, it is impossible to elucidate its molecular structure because in this case the X-ray reflections are diffuse and small in number due to the reorientational dynamics

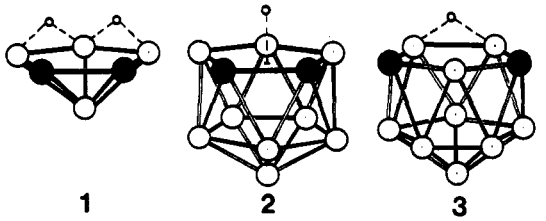

Figure 34. *nido*-Carboranes studied by Raman and IR spectroscopy: 1, 4,5-dicarba-*nido*-hexaborane(8); 2, 7,8-dicarba-*nido*-undecaborate; 3, 7,9-dicarba-*nido*-undecaborate. Terminal hydrogen atoms are omitted.

in a crystalline sample. Raman spectroscopy, being diagnostic, can immediately show whether the crystalline sample is plastic or ordered.

1-Boraadamantane will be presented as an example; this compound can to some extent, formally, be regarded as a carborane. In spite of the fact, that 1-boraadamantane was synthesized as early as 1974,[137] its molecular structure has not yet been determined. Numerous attempts to carry out X-ray analysis proved to be unsuccessful due to the small number of diffuse reflections obtained, even from crystals that seemed perfect at first sight. The Raman spectrum of this substance at ambient temperature revealed a Rayleigh wing in the low-frequency region, which is indicative of a plastic phase. Temperature investigations of the Raman spectrum[138] have also shown that the transition to an ordered crystal phase occurs on cooling to 183 K. Thus, it is clear now that good X-ray results for this substance can be obtained only in low-temperature experiments below 183 K.

VI. Vibrational Spectra of nido-Carboranes and π-Dicarbollyl Complexes

Scanty vibrational data on *nido*-carboranes are available. Full Raman and IR spectra can be found only for the small carborane $C_2B_4H_8$ and for several isomers of the dicarba-*nido*-undecaborate anion $C_2B_9H_{12}^-$ and derivatives.

A. 4,5-Dicarba-*nido*-hexaborane(8) $C_2B_4H_8$

There is a comprehensive study on 4,5-dicarba-*nido*-hexaborane(8) (see Figure 34) and its deuterated and methylated derivatives. IR spectra of $C_2B_4H_8$ and its bridge-, C-, and B-deuterated analogues have been published by Onak et al.[139] and those of the *C*-methyl derivatives of Grimes et al.[140] Full vibrational data on $C_2B_4H_8$ and its mono- and di-*C*-methyl derivatives have been presented by Jotham et al.[141] An assignment has been also given in ref 141 on the basis of the IR and Raman band intensities, qualitative state of polarization, gas-phase IR band structures, and comparison with the data for deuterated molecules.

The $C_2B_4H_8$ molecule is of low symmetry (C_s), so all its vibrations are IR and Raman active. The spectrum of the small *nido*-carborane exhibits some interesting features, which distinguish it from small *closo*-carboranes.[96]

The $C_2B_4H_8$ molecule contains two adjacent CH bonds, like 1,2-$C_2B_{10}H_{12}$ (*o*-carborane). However, in contrast to *o*-carborane, the spectrum of $C_2B_4H_8$ shows two bands at 3032 and 3042 cm^{-1} (in both Raman and IR), which can be readily assigned to the asymmetrical and symmetrical CH stretching modes. This is the first case in carborane spectroscopy, when two CH oscillators are coupled! For *closo*-carboranes we always see one ν(CH) band for two CH bonds.

The significant decrease in the ν(CH) band frequencies observed for the small *nido*-carborane as compared to those of *closo*-carboranes is also striking. In contrast, the frequencies of the CH in-plane deformations situated near 1330 cm^{-1} are more than 100 cm^{-1} higher than those for *o*-carborane. These peculiarities may be partly attributed to an unusually short (1.43 Å) C–C distance in $C_2B_4H_8$.[141]

The terminal BH_t stretches of the *nido*-molecule in question are subdivided into apical and equatorial modes, the frequency of the former is 2624 cm^{-1}, higher than those of the latter, 2610 and 2592 cm^{-1}. So it is clear that the apical BH bond is the strongest of the BH terminal bonds. The average value of the $\nu(BH_t)$ frequencies is 2604 cm^{-1}, which is about 40 cm^{-1} lower than those of small *closo*-carboranes.

The stretching vibrations of the two BHB bridges of $C_2B_4H_8$ are situated in the region of 1980–1500 cm^{-1}. The symmetrical BHB stretching mode appears in the Raman spectrum as a weak broad band in the region 1980–1850 cm^{-1}, exhibiting a structure with many peaks, all of which are polarized. This spectral pattern is characteristic of BHB bridges and is explained by extensive Fermi resonance. A detailed discussion of this phenomenon in the methyldiborane spectra can be found in ref 79.

The assignment of the polyhedron stretching modes given in ref 141 seems to be tentative. It is obvious that the BB and BC stretching and BH deformation coordinates are mixed. The skeletal symmetrical stretches could be characterized by the set of the most intense polarized Raman lines, which are situated at 1106, 1070, 1034, and 889 cm^{-1} for $C_2B_4H_8$. Concerning these modes, the authors[141] have come to the conclusion that the framework of the small *closo*-carboranes appears to be significantly more strongly bound than that of the *nido*-carborane studied. They have also assumed that the *nido*-carborane CH and BH stretching frequencies are lowered because the open framework is not such a strong electron-attracting system as the *closo*-carborane cages.

It is also notable that low-frequency Raman bands are reported[141] for 4,5-$C_2B_4H_8$ (180 cm^{-1}, w) and its *C*-methyl derivatives (226 and 260 cm^{-1}, vw), which are assigned as cage deformation.[141] If this were really so, it would be of great importance as an indication of nido cluster flexibility. However, weak bands at ca. 250 cm^{-1} in the spectra of the *C*-methyl derivatives could be alternatively assigned to methyl torsional modes and the only weak feature at 180 cm^{-1} is too weak to be the basis of such an important conclusion.

B. Dicarba-*nido*-undecaborates $C_2B_9H_{12}^-$ and Their Derivatives

1. Terminal BH, Stretching and Bending CH, and Cage Modes

Already in the first papers devoted to the alkaline degradation reactions of the icosahedral *closo*-carborane cage, Hawthorne et al.[142,143] paid attention to the ν(BH) band shift to lower frequencies by about 50 cm^{-1} on

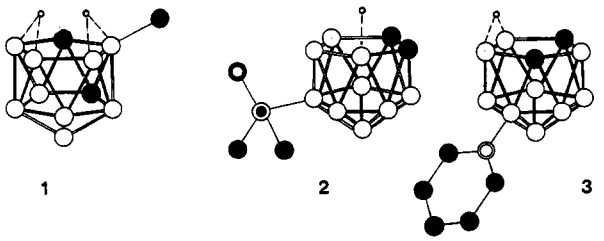

Figure 35. *nido*-Carboranes studied by Raman and IR spectroscopy: 1, 11-Me-2,7-$C_2B_9H_{12}$; 2, 5(6)-Me_2SO-7,8-$C_2B_9H_{11}$; 3, 6-C_5H_5N-7,9-$C_2B_9H_{11}$. Terminal hydrogen atoms are omitted. The symbols are as follows: ◉, sulfur atom; ●, oxygen atom; and ◎, nitrogen atom.

going from *o*- or *m*-carboranes to the 7,8- or 7,9-dicarba-*nido*-undecaborate anions, respectively (see Figure 34). The broad IR ν(BH) band with its center of gravity at ca. 2550 cm^{-1} is characteristic of all dicarba-*nido*-undecaborate anions and is well-known to carborane chemists.

The IR spectra of $C_2B_9H_{12}^-$ anions and their derivatives in a limited region are given in a few papers (see, e.g., refs 142–146). Their Raman spectra have been published only by Leites et al.[147–149] The analysis of the full vibrational spectra of the salts M[$C_2B_9H_{12}$], M = K, Cs, is presented in ref 30.

These spectra are rather complicated compared to those of *closo*-carboranes since the icosahedron symmetry is no longer effective. 7,8- and 7,9-$C_2B_9H_{12}^-$ anions belong to the C_s point symmetry group, their vibrations are allocated to 32 A′ and 24 A″ symmetry species, both species being active in the Raman and in the IR. In spite of the complicated nature of the spectrum, its overall pattern is retained. The intense Raman lines corresponding to cage breathing in the region 700–800 cm^{-1} continue to be the most prominent, as in the spectra of *closo*-carboranes.

Full vibrational spectra are also available for dicarba-*nido*-undecaborate zwitterions with *B*-dimethylsulfoxonium and *B*-pyridinium groups, 5(6)-Me_2SO-7,8-$B_9C_2H_{11}$ and 6-C_5H_5N-7,9-$B_9C_2H_{11}$,[149] and also for a neutral molecule 11-Me-2,7-$C_2B_9H_{12}$.[148] The structures of these compounds are given in Figure 35.

A detailed analysis of the spectra of dicarba-*nido*-undecaboranes mentioned above and their μ-deutero analogues leads to the conclusion that the stretching frequencies of all σ-bonds situated in the open face of the nido polyhedron are lowered as compared to those in the closed part of the molecule. Thus, the observed shift of the ν(BH) band center of gravity to lower frequencies is a result of the three BH bonds located in the open face. The stretching frequencies of the CH bonds located in the open face of the polyhedron are also lowered to ca. 3040 cm^{-1}. Two ν(CH) bands are observed for the 7,8-$C_2B_9H_{12}^-$ ion which has adjacent CH bonds. The same phenomenon has been observed by Jotham et al.[141] for the small *nido*-carborane $C_2B_4H_8$.

It is of interest to compare the frequencies of the CH in-plane deformation modes for the three species with adjacent CH bonds: *o*-carborane, 7,8-dicarba-*nido*-undecaborate, and 4,5-dicarba-*nido*-hexaborate(8), bearing in mind the substantial shortening of the C–C distances in this series (1.68, 1.58, and 1.43 Å, respectively[141,150]). These frequencies increase gradually and are 1215 and 1150 cm^{-1} for 1,2-$C_2B_{10}H_{12}$,[10] 1265 and 1185 cm^{-1} for 7,8-$C_2B_9H_{12}^-$,[30,149] and 1348 and 1323 cm^{-1} for $C_2B_4H_8$.[141]

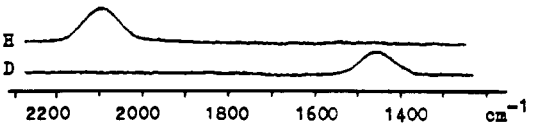

Figure 36. The extra-hydrogen band in the Raman spectra of 7,8-dicarba-*nido*-undecaborate and its μ-D derivative.

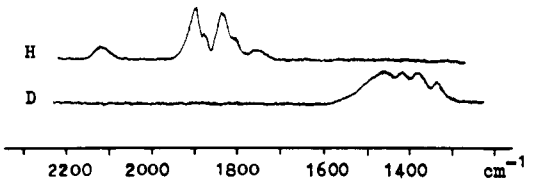

Figure 37. The extra-hydrogen bands in the Raman spectra of 7,9-dicarba-*nido*-undecaborate and its μ-D derivative.

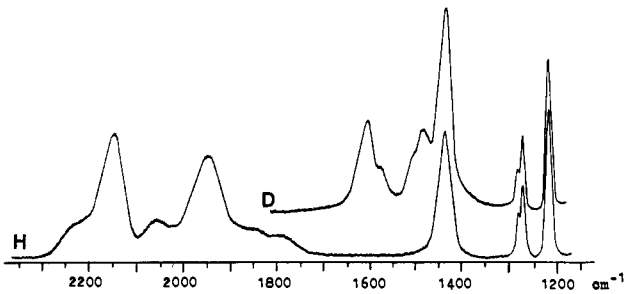

Figure 38. The extra-hydrogen bands (along with δCH bands) in the Raman spectra of 11-Me-2,7-$C_2B_9H_{12}$ and its μ-D_2 derivative.

It is important to note that the dicarba-*nido*-undecaborates studied exhibit no low-frequency modes, like the *closo*-carboranes. This means that the *nido*-polyhedron continues to be rigid.

2. "Extra-Hydrogen" Manifestations

The most challenging problem in dicarba-*nido*-undecaborane spectroscopy is the localization of the so-called "extra hydrogen". In the course of an alkali degradation reaction of the cage, one of boron atoms leaves the carborane molecule, but all 12 of the hydrogen atoms remain. It is the 12th hydrogen atom, the "extra hydrogen", whose position in the molecule is a point of discussion. X-ray investigations put this extra hydrogen above the open face of the polyhedron, its distances to all five atoms of the open face being reported as almost equal.[150–153] However, NMR data place the extra hydrogen near the boron atoms as a BHB bridge.[144,154]

In the IR spectrum of the 7,9-$C_2B_9H_{12}^-$ anion, Hawthorne et al.[144] observed weak bands in the region of 1600–1900 cm^{-1}. On deuteration of the extra hydrogen these bands disappeared and three very weak bands in the region of 1200–1300 cm^{-1} appeared instead. On this basis they were assigned as vibrational modes with extra-hydrogen participation. No similar bands were observed by the same authors in the IR spectrum of the 7,8-$C_2B_9H_{12}^-$ anion.

Leites et al. succeeded in detecting the extra hydrogen in the Raman spectra of all *nido*-carboranes studied.[147–149] The extra-hydrogen stretching mode manifests itself as a weak broad polarized feature in the region 1700–2350 cm^{-1}. This interval is typical of BHB bridges in the spectra of boranes (see, e.g., refs 79, 155, and 156) and also of a small *nido*-carborane.[141] Hence, an inference can be drawn that the extra hydrogen also

forms a BHB bridge on the open face of a given nido polyhedron.

Deuteration of the extra hydrogen shifts the broad Raman feature to the interval 1300–1700 cm^{-1} with a normal isotopic ratio of 1.35 (see Figures 36–38). Both ν(BHB) and ν(BDB) Raman bands are very weak. To detect them, it is sometimes necessary to increase the electron gain of the detector by 1 order of magnitude.

Some thought should be given to the unusual shape of the ν(BHB) bands presented in Figures 36–38. For the 7,9-$C_2B_9H_{12}^-$ anion and its derivatives studied as well as for 11-Me-2,7-$C_2B_9H_{12}$ a broad Raman band with fine structure is observed (Figures 37 and 38). Deuteration of the extra hydrogen proves that all the peaks of this structure originate from an extra-hydrogen vibration, because all these peaks disappear on deuteration, being replaced by a corresponding ν(BDB) band also exhibiting fine structure. This fine structure cannot be explained by crystal effects because it remains in the spectra of solutions. It is remarkable that the patterns of the corresponding ν(BHB) and ν(BDB) bands are not identical.

It is obvious from these experimental findings that the structure of the extra-hydrogen stretching band is due to extensive Fermi resonance with overtones and combinations of skeletal modes, situated in the region ca. 1000 cm^{-1}. As mentioned above, the same pattern has been reported and detailed for the symmetrical ν(BHB) modes in the Raman spectra of methyldiboranes[79] and the small *nido*-carborane $C_2B_4H_8$.[141]

Quite a different spectral pattern is observed in the Raman spectrum of the 7,8-$C_2B_9H_{12}^-$ anion and its derivative studied.[147,149] In this case the extra-hydrogen stretching mode shows itself as a single broad symmetrical Raman band without structure (see Figure 36).

It is of interest to note that this broad smooth Raman feature has no IR counterpart (in accordance with the IR data of Hawthorne et al.[144]), while some weak IR coincidences can be found for the Raman band with Fermi resonance structure. However, not all these IR peaks disappear on deuteration of the extra hydrogen, so their origin is doubtful.

What is the reason for the specific extra-hydrogen behavior in the 7,8-$C_2B_9H_{12}^-$ anion? We believe that it may be explained by extra-hydrogen dynamics. Indeed, in this case the open face has the following structure with the single extra hydrogen migrating between the two equivalent positions:

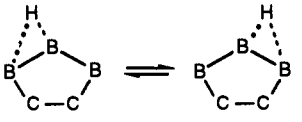

Since the overall hydrogen motion is asymmetric relative to the polyhedron symmetry plane, its interaction with overtones is forbidden. This is one plausible reason why the ν(BHB) band and the corresponding ν(BDB) band have no Fermi resonance structure in this case. The unusual broadening of this band might also be due to intramolecular extra-hydrogen dynamics. NMR data[154] confirm the rapid motion of the extra hydrogen. However, this problem calls for further investigation.

In the case of the 7,9-$C_2B_9H_{12}^-$ anion and its derivatives and of the 11-Me-2,7-$C_2B_9H_{12}$ molecule with its two extra hydrogens, the open faces of the polyhedra have the following structures:

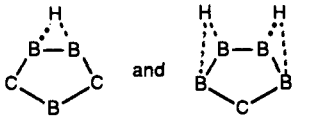

with fixed extra-hydrogen BHB positions. In these cases Fermi resonance interactions of the symmetrical BHB stretching mode with overtones are allowed in Raman.

It should be noted that in the case of the latter molecule the symmetrical vibration of the two extra hydrogens shows itself as a Raman band strong enough to be recorded without electronic gain increase (Figure 38). It is strange, however, that no strong IR band in the region of 1600–1500 cm^{-1}, characteristic of the antisymmetrical ν(BHB) mode,[79,156] was observed in this case.

The problem of the spectral manifestations of the BHB bridge is interesting and not yet clear. The peculiarities of the ν(BHB) Raman band, i.e., its broadening and Fermi resonance structure, seem to be characteristic not only of the BHB bridge stretching bands, but also of all vibrational bands associated with the doubly coordinated hydrogen stretching mode. For instance, the ReHRe bridge in a cluster exhibits the same spectral features in Raman.[157]

It is noticeable that deuteration of the extra hydrogen does not affect the ν(CH) and terminal ν(BH_t) frequencies but does significantly affect the spectral pattern in the "fingerprint" region. To rationalize this fact, one has to remember that the extra hydrogen is an equal and full participant in the cage formation, being involved in the united system of the polyhedron bonding. Deuteration of the extra hydrogen seems to change the eigenvectors of the skeletal modes with extra-hydrogen participation, causing anomalous isotope effects.[148]

3. *Dicarba-nido-undecaborate Group as a Substituent*

Investigations of C-derivatives of dicarba-*nido*-undecaborate[158] show that, unlike the *C-o*-carboranyl group, the *C*-7,8-dicarba-*nido*-undecaborate group is a strong donor of electrons, both by inductive and by resonance effects. This means that the *C*-7,8-dicarba-*nido*-undecaborate group might be capable of conjugation with π-electron systems. This conclusion was proved by the study of the UV absorption spectra of different phenylcarboranes.[159]

Unsubstituted *closo*-carboranes were shown not to absorb in the UV region studied (from 210 to 400 nm). In the spectra of all their phenyl derivatives, independent of the position to which phenyl group is attached [C-, B(9)-, or B(3)-substitution], the band in the region 240–280 nm, originating from the forbidden benzene A_{1g}–B_{2u} transition, retains a clear-cut vibronic structure, its peaks being only slightly shifted as compared to the spectrum of toluene (see Figure 39). This fact indicates that the *closo*-carboranyl substituent does not disturb the original electronic level system of the monosubstituted benzene and exerts only an inductive effect. A quite different pattern is observed in the UV spectrum of the *C*-phenyl-7,8-dicarba-*nido*-undecaborate anion (Figure 39). This substance exhibits a wide band at 260 nm without vibronic structure, the band

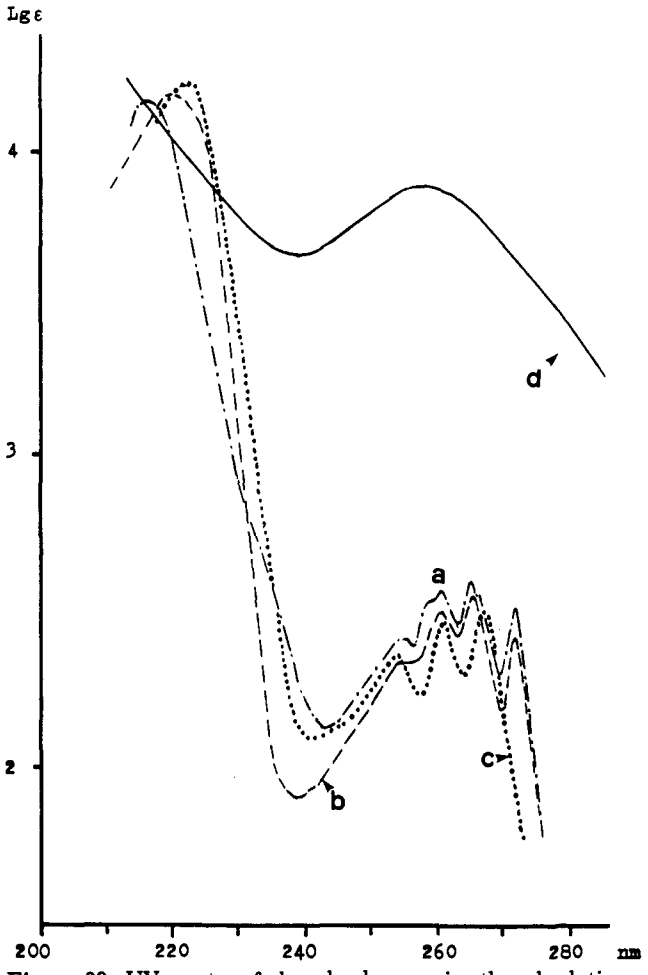

Figure 39. UV spectra of phenylcarboranes in ethanol solutions: (a) 1-phenyl-*o*-carborane; (b) 3-phenyl-*o*-carborane; (c) 9-phenyl-*o*-carborane; and (d) $Cs^+[7\text{-Ph-}7,8\text{-}C_2B_9H_{11}]^-$.

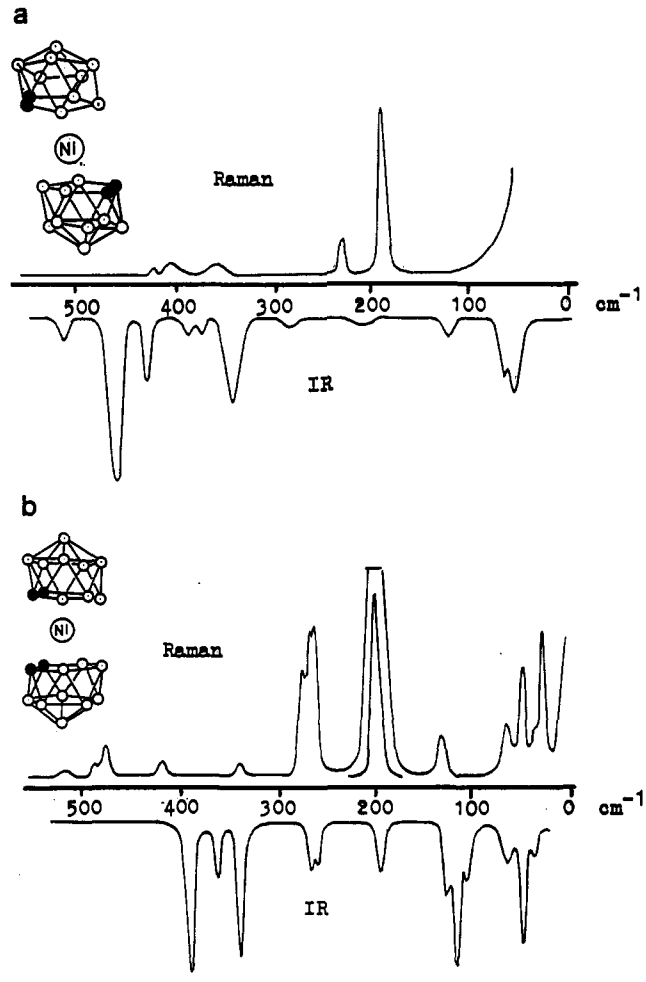

Figure 40. Structures and low-frequency vibrational spectra of bis(π-dicarbollyl) complexes of Ni: (a) $Cs[(C_2B_9H_{11})_2Ni^{III}]$; and (b) $(C_2B_9H_{11})_2Ni^{IV}$.

intensity being substantially enhanced, which suggests conjugation of the *nido*-polyhedron open face with the benzene ring.

Relevant data were also obtained from vibrational spectra. The *C*-dicarba-*nido*-undecaborate substituent was found to strongly affect the vibrational frequencies of attached functional groups when the latter were capable of π-conjugation.[30] In particular, the frequency of the carbonyl group bonded to the carbon atom of the dicarba-*nido*-undecaborate anion is lowered by about 50–70 cm^{-1} as compared to those of the corresponding *closo*-carborane C-derivatives.

The knowledge of "closo–nido" spectral transformation enabled the authors of refs 160 and 161 to follow the process of the thermal destruction of *m*-carborane-containing polyamides and to show that it is the 7,9-dicarba-*nido*-undecaborate group, formed on heating of the polyamide to 300 °C, which acts as an effective stabilizer of polyheteroarylenes.

C. π-Dicarbollyl Complexes of Transition Metals

It is well-known that 7,8- and 7,9-dicarba-*nido*-undecaborates easily eliminate the extra hydrogen to give rise to the $C_2B_9H_{11}^{2-}$ dicarbollide ion.[162] Interaction of the latter with transition metal salts gives π-dicarbollyl complexes of the type $(\pi\text{-}C_2B_9H_{11})_2M$ or $(\pi\text{-}C_2B_9H_{11})$-ML, where L is another π-ligand.

The IR spectra of most π-dicarbollyl complexes have been reported, but only in a limited region (without low frequencies) and more often merely as summaries in the experimental sections (see, e.g., refs 163 and 164). Full vibrational spectra of some π-dicarbollyl complexes of Fe, Co, and Ni are presented in ref 30; their salient features were published in ref 165. Most of these complexes are deeply colored and many of them decompose in the laser beam; thus it is not a trivial task to record their Raman spectra.

The main features of these spectra, like of those of other π-complexes,[166] are intense bands in the low-frequency region, originating from metal–ligand skeleton stretching modes. In the Raman spectrum, an intense polarized line, corresponding to the totally symmetrical metal–ligand stretching mode, is the most prominent and thus can be readily identified.

In the case of $(\pi\text{-}C_2B_9H_{11})_2M$ centrosymmetric complexes, this line is situated in the region 180–210 cm^{-1} and has no IR counterpart, while the IR band corresponding to antisymmetrical metal–ligand stretch and lying in the region 350–400 cm^{-1} is not active in the Raman. The frequencies of these modes depend insignificantly on the nature of the metal. As an example, the low-frequency spectral region of the centrosymmetric $[(\pi\text{-}1,2\text{-}C_2B_9H_{11})_2Ni^{III}]^-$ anionic complex is given in Figure 40, where it is confronted with the corresponding spectrum of the Ni^{IV} neutral complex $(\pi\text{-}1,2\text{-}C_2B_9H_{11})_2Ni^{IV}$. The latter molecule does not have a center of inversion but possesses the "cisoid" structure

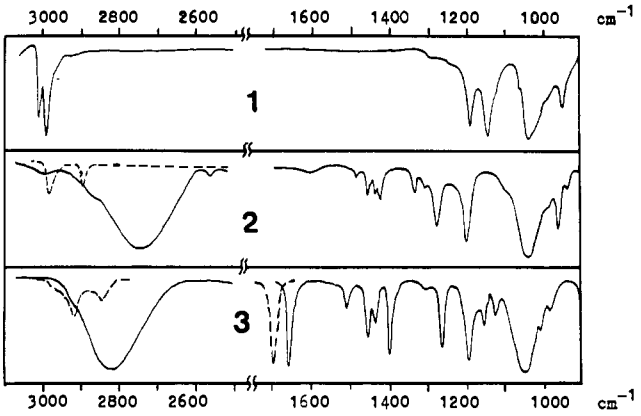

Figure 41. IR spectra of deca-*B*-chloro-*o*-carborane and its solid adducts with DMSO and DMFA: 1, deca-*B*-chloro-*o*-carborane; 2, adduct with DMSO (---, DMSO); 3, adduct with DMFA (---, DMFA).

of the C_{2v} symmetry point group; both symmetrical and antisymmetrical metal–ligand stretches are active in Raman and IR. Figure 40 demonstrates that the operating selection rules are in accord with the molecular structures. The second Raman line near 250 cm^{-1} belongs to the ligand tilt mode.

Recently a paper of Sobolev et al. has appeared,[167] where the Raman spectrum of another isomer of bis-(π-dicarbollyl)nickel(IV), (π-1,7-$C_2B_9H_{11})_2Ni^{IV}$, is presented and discussed. In contrast to the 1,2 isomer, this complex exhibits in the region ca. 180 cm^{-1} not a single intense line but a split pair, which is explained by the authors in terms of rotational isomerism (in solid!).

VII. Carboranes—A New Class of Proton Donors Forming Hydrogen Bonds of the Type C–H···Y

A. Introduction

In 1968 Zakharkin and Ogorodnikova[48] demonstrated that icosahedral deca-*B*-halo-*o*-carboranes and their *C*-alkyl derivatives react with dimethyl sulfoxide (DMSO) and dimethylformamide (DMFA) to form 1:1 crystalline adducts. Decahalo-*o*-carboranes are known to be strong acids; on the other hand, the decahalo-*o*-carborane nucleus is highly electron deficient. The structure of the adducts was therefore uncertain since several types of donor–acceptor interactions could lead to their formation.

The nature of the adducts was elucidated by Leites, Ogorodnikova, and Zakharkin by means of IR spectroscopy.[46] It was shown that it was strong hydrogen bonding of the type C–H···O that held the two molecules together in the adduct.

Figure 41 presents the IR spectra of 1:1 solid adducts of decachloro-*o*-carborane (*o*-DCC) with DMSO and DMFA as well as the spectra of the starting compounds. It is seen that on going from the *o*-DCC spectrum to the spectra of the adducts the sharp CH stretching bands near 3040 cm^{-1} (the splitting is crystalline because only one band is observed in the solution spectrum) disappear and are replaced by very broad intense absorption in the region 2600–2800 cm^{-1}. The CH deformation bands at 1140 and 1185 cm^{-1} are shifted in the spectra of the adducts to higher frequencies by about 50 cm^{-1}.

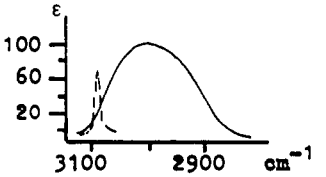

Figure 42. The CH stretching IR band of *o*-carborane in CCl_4 (---) and DMSO (—) solutions.

It is well-known that such spectral changes, namely, the shift to low frequencies, intensification and broadening of a stretching band, and the increase in frequency of a corresponding deformation band, are spectral criteria of hydrogen bond formation. Thus, it is the *o*-DCC C–H bond which serves as the proton donor in the adducts discussed.

Thus, IR spectroscopy was able to discover the ability of DCC to participate in hydrogen bonding. Later it was shown, also by IR spectroscopy, that all carboranes, not only DCC, are capable of forming H-complexes with various basic compounds Y.[46-49,90,168-171]

The existence of hydrogen bonds with CH group participation is well-known.[172,173] For instance, chloroform and other halogenated hydrocarbons as well as acetylenic compounds can serve as CH proton donors. However, their H-complexes exist only in solutions and the enthalpies of complex formation are usually lower than 3 kcal mol^{-1} even with strong proton acceptors.

After carboranes had been identified as a new class of proton donors in C–H···Y hydrogen bond formation, it was interesting to investigate them thoroughly from this point of view and to define their place among other CH proton donors. This was performed in a series of papers of Leites, Vinogradova et al.[158-171]

B. Carborane H-Complexes in Solution

Icosahedral deca-*B*-halocarboranes appeared to be the only representatives capable of forming solid adducts and then only with strong bases. All other carboranes studied, icosahedral and medium, closo and nido, were shown to form H-complexes in solution. The enthalpy of formation of carborane H-complexes with various bases in solution was measured also by means of IR spectroscopy.

Two types of measurements were performed: spectroscopic, using the well-known Iogansen's intensity and frequency rules,[174] which relate the enthalpy value ΔH to the increment of the IR integrated intensity ΔA and to the frequency shift $\Delta\nu$ of the ν(AH) band in an H-complex of the type A–H···Y:

$$-\Delta H = 2.9\Delta A^{1/2} \quad (1)$$

$$-\Delta H = \sqrt{0.1\Delta\nu} \quad (2)$$

and independent, according to the Van't Hoff equation. It should be noted that the intensity rule 1 has been proved universal and applicable to compounds of different classes while the relationship between the enthalpy and the ν(AH) frequency shift is approximate and can be used only for rough estimations. We used it in the simplified form 2.

The examples of IR spectra of carborane H-complexes in solution are given in Figures 42 and 43. Figure 42 presents the ν(CH) IR band of *o*-carborane, obtained for its solutions in neutral CCl_4 and in basic DMSO.[168] The low-frequency shift of the ν(CH) band

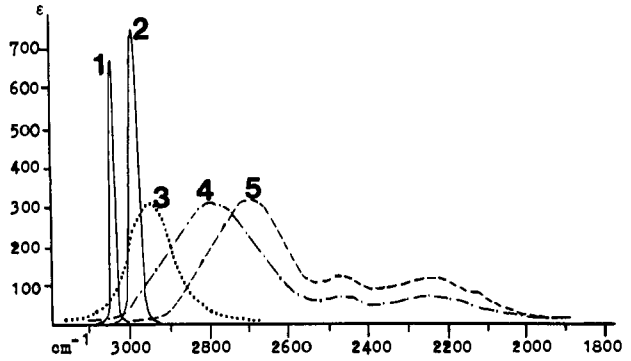

Figure 43. Evolution of the ν(CH) IR band of deca-*B*-chloro-*o*-carborane in solutions of basic solvents: 1, CCl_4; 2, C_6H_6; 3, CH_3CN; 4, DMFA; and 5, DMSO.

TABLE XIII. Characteristics of the ν(CH) Band in the IR Spectra of different Carboranes in Solution of Neutral (CCl_4) and Basic Solvents and the Enthalpy of Carborane H-Complex with Basic Solvent

compound	solvent	ν(CH)[a]	ν(1/2)[b]	$A \times 10^{-3}$ [c]	ΔH[d] according to eq 1
o-carborane	CCl_4	3076	13	1.6	
	DMSO	2995	154	18.7	2.8
m-carborane	CCl_4	3067	12	1.2	
	DMSO	3018	80	14.6	2.5
9-chloro-*o*-carborane	CCl_4	3079	13	2.5	
	DMSO	2975	140	36.0	4.0
9,12-dichloro-*o*-carborane	CCl_4	3080	12	3.1	
	DMSO	2975	186	42.2	4.4
deca-*B*-chloro-*o*-carborane	CCl_4	3046	10	10.0	
	C_6H_6	2990	23	27.0	1.9
	CH_3CN	2953	115	48.0	3.5
	THF	2750	213	105.0	6.5
	DMFA	2669	253	125.0	7.4
	DMSO	2532	233	143.0	8.1
deca-*B*-chloro-*m*-carborane	CCl_4	3037	9	8.4	
	DMFA	2740	225	107.0	6.8
	DMSO	2667	240	129.0	7.8

[a] ν(CH), frequency of the center of gravity of the ν(CH) band (cm^{-1}). [b] ν(1/2), estimated half-width (cm^{-1}) of the ν(CH) band. [c] *A*, IR integrated intensity (l mol^{-1} cm^{-2}) of the ν(CH) band (per one C–H bond). [d] ΔH, enthalpy (kcal mol^{-1}) of H-complex formation.

and its broadening and intensification on hydrogen bonding with DMSO are striking. Figure 43 shows the gradual evolution of the ν(CH) band of *o*-DCC in solution with the increase in solvent basicity in the series CCl_4, benzene, tetrahydrofuran (THF), acetonitrile, DMFA, and DMSO. The complicated pattern of the ν(CH) broad feature at its low-frequency side, observed for strong H-complexes, is due to Fermi resonance.[47,174]

Table XIII summarizes the data on the spectroscopic characteristics of the ν(CH) band and the H-bond enthalpy values.[168,169] The center of gravity positions and the IR integrated intensities of the ν(CH) bands were measured in the spectra of solutions in neutral and basic solvents, and then the ΔH values were estimated, using the relationships 1 and 2. It was shown that unsubstituted carboranes and their *C*-alkyl derivatives form a weak hydrogen bond. Even with strong bases, its ΔH values do not exceed 3 kcal mol^{-1}. They decrease in the order ortho > meta > para, in line with the CH acidity. Alkyl substituents affect the H-bond enthalpy insignificantly.

Introduction of halogen atoms to the boron atoms of the carborane nucleus successively increases the strength of the H-complexes, which reaches 6–8 kcal mol^{-1} for solutions of DCC in DMFA and DMSO. Thus, *o*-DCC appears to be just as strong a proton donor in hydrogen bonding as phenol[175] while *m*-DCC is only slightly weaker. It is notable that *o*-DCC forms a hydrogen bond in solution even with the weak π-base, benzene. Both *o*- and *m*-DCC have shown themselves as the strongest among all the other CH proton donors in hydrogen bonding.

TABLE XIV. Comparison of Enthalpy Values of *C*-Methyldeca-*B*-chloro-*o*-carborane H-Complexes with Different Bases (in Solution), Obtained According to the Iogansen Intensity Rule (1) and the van't Hoff Equation (3)[a]

solvent	ν(CH)	$A \times 10^{-4}$	ΔH according to eq 1	ΔH according to eq 3
CCl_4	3036	1.0		
$CH_3CN + CCl_4$	2962	3.4	2.6 ± 0.2	3.2 ± 0.3
CH_3CN	2948	5.1	3.8 ± 0.2	
$THF + CCl_4$	2845	5.7	4.1 ± 0.4	4.5 ± 0.6
THF	2730	10.4	7.3 ± 0.7	
$DMFA + CCl_4$	2767	7.2	4.9 ± 0.2	5.3 ± 0.4
DMFA	2640	12.6	8.0 ± 0.3	

[a] See designations of Table XIII.

The ability of other carboranes to form hydrogen bonds was also investigated. For instance, icosahedral phospha- and arsacarboranes of the general formulae $PCHB_{10}H_{10}$ and $AsCHB_{10}H_{10}$ were found to form weak H-bonds with the energy values close to those of the $C_2B_{10}H_{12}$ carboranes.[49] The medium carborane *p*-$C_2B_8H_{10}$ forms weaker H-complexes, their strengths (even with DMSO) not exceeding 2 kcal mol^{-1}.[90] For the examples of π-cyclopentadienyl-π-(3)-1,2-dicarbollyl complexes of Co and Fe, the CH bonds of the π-dicarbollyl group were shown to retain their ability to form hydrogen bonds, although they are weaker proton donors than the CH bonds of the corresponding *closo*-carboranes.[171]

The large ΔH values of DCC H-complexes with DMSO and DMFA, obtained in ref 169 from Iogansen's intensity rule 1, seemed to be unusually high for C–H···O hydrogen bonds. Hence these results called for verification of whether the empirical rule 1 is applicable to such peculiar systems as carboranes.

It is pertinent to mention here that there are some cases when the rule 1 gives exaggerated values of ΔH (e.g. H-complexes with aromatic N-heterocycles[176]). With this in mind, Vinogradova and Leites[177] have carried out an independent thermodynamic determination of ΔH, using Van't Hoff equation

$$R \ln K = -\Delta H/T + \Delta S \qquad (3)$$

Equilibrium constants for the reaction of the H-complex formation were measured by IR spectroscopy in CCl_4 solutions. *C*-Methyldeca-*B*-chloro-*o*-carborane, as having only one CH group, was chosen as a proton donor while acetonitrile, THF, and DMFA served as the proton acceptors.

The resulting ΔH values, given in Table XIV, appeared not to be lower but somewhat higher (within the limits of experimental error) than those, calculated from intensity rule 1, the linear correlation between ΔH and $\Delta A^{1/2}$ values being preserved. Thus, the applicability of rule 1 to carborane H-complexes was proved.

It is noticeable that ΔH values of the same H-complexes, when measured in triple solutions (with CCl_4),

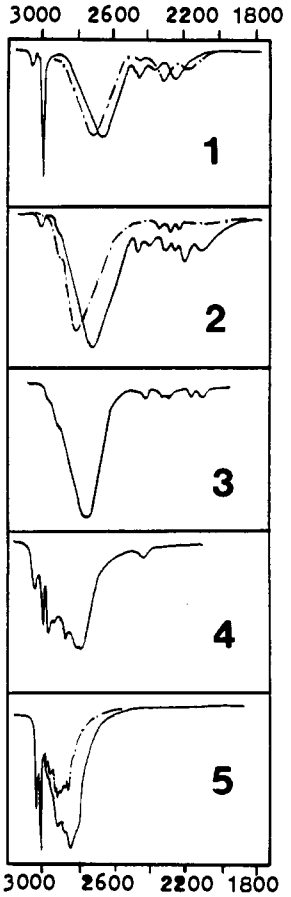

Figure 44. IR spectra in the ν(CH) region of solid 1:1 adducts of deca-*B*-chloro-*o*-carborane (—) and deca-*B*-chloro-*m*-carborane (···) with 1, TPPO; 2, DMSO; 3, DMFA: 4, THF; and 5, dioxane.

are significantly lower than those in binary mixtures (Table XIV), which is indicative of strong solvation effects.

C. Vibrational Spectra and Structure of Deca-*B*-chlorocarborane (DCC) Solid Adducts with Oxygen Bases

We have already mentioned the 1:1 solid adducts of DCC with DMFA and DMSO, in which two molecules are held together by strong C–H···O hydrogen bond.[46] DCC were found to form solid adducts also with other oxygen bases: dioxane, THF, and triphenylphosphine oxide (TPPO). The structures of these adducts were also investigated by IR and Raman spectroscopy.[46,47] All adducts were shown to be of the 1:1 type, though there are two CH bonds in *o*- and *m*-DCC molecules.

The IR spectra (see Figures 41 and 44) show an important difference since, in the case of adducts with dioxane and TPPO, the spectrum exhibits a narrow CH stretching band of the carborane CH bond above 3000 cm^{-1}, while in the spectra of DMFA and DMSO adducts only the broad ν(CH) band appears at much lower frequencies. The absence of a "free" CH bond in the latter case suggests the formation in the solid of conglomerates or chains with every oxygen atom participating in two hydrogen bonds. This does not happen in adducts with TPPO and dioxane, probably, for steric reasons. The X-ray investigation of the *o*-DCC adduct with DMSO[178] has confirmed the former suggestion and shown the adduct to be a cyclic centrosymmetric dimer (Figure 45) with shortened C···O distances (2.95 Å)

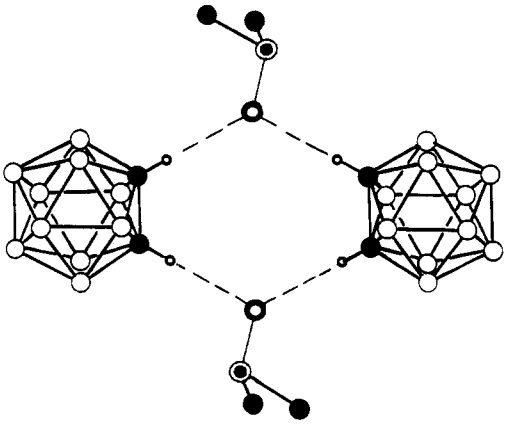

Figure 45. The structure of the crystalline deca-*B*-chloro-*o*-carborane adduct with DMSO. Chlorine and hydrogen atoms are omitted.

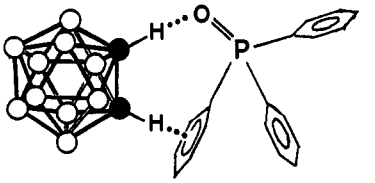

Figure 46. The structure of the deca-*B*-chloro-*o*-carborane adduct with TPPO, proposed on the basis of its IR spectrum.

compared to van der Waals radii sum 3.1 Å, which is also evidence for the strong C–H···O hydrogen bond.

However, the narrow ν(CH) band of the TPPO complex at 3003 cm^{-1} cannot be considered as really "free", because its frequency is lowered and close in value to that of *o*-DCC dissolved in benzene (2990 cm^{-1}). This may indicate a weak C–H···π hydrogen bond between *o*-DCC and one of the TPPO phenyl rings. Thus, according to the IR spectrum, we may assume two different hydrogen bonds in the *o*-DCC·TPPO adduct: a strong C–H···O and a weak C–H···π (see Figure 46).

The CH stretching frequency of *o*-DCC (measured as the center of gravity position) decreases from its "free" value of 3046 cm^{-1} (in CCl_4 solution) to 2860, 2840, 2740, and 2680 cm^{-1} on going to dioxane, DMFA, DMSO, and TPPO adducts, respectively, i.e. in the order of increasing basicity of the proton acceptor molecule. The relative shifts of the ν(CH) frequency of the *m*-DCC adducts with the same bases are lower, in line with the weaker acidity of *m*-DCC.

The CH bending frequencies of *o*-DCC increase from 1186 and 1141 cm^{-1} for the pure crystal to 1250 and 1180 cm^{-1} (1260 and 1180 cm^{-1}) for adducts with DMFA (DMSO). Similarly, the only δ(CH) frequency of *m*-DCC increases from 1154 to 1185 cm^{-1} in the DMSO complex.

The half-width $\nu(1/2)$ of the IR ν(CH) band of *o*-DCC increases from 5 cm^{-1} observed for a pure crystal component to 130, 180, and 200 cm^{-1} for dioxane, DMFA, and DMSO adducts, respectively. The Raman ν(CH) bands are generally narrower (see Figure 47), for instance, $\nu(1/2)$ = 120 cm^{-1} for DMSO adduct.

The low-frequency side of the broad ν(CH) band in the IR spectra of solid adducts with strong bases is complicated (as in solution spectra) due to Fermi resonance of overtones and combinations with the CH stretching fundamental. As is usual for systems containing relatively strong hydrogen bonds, strong over-

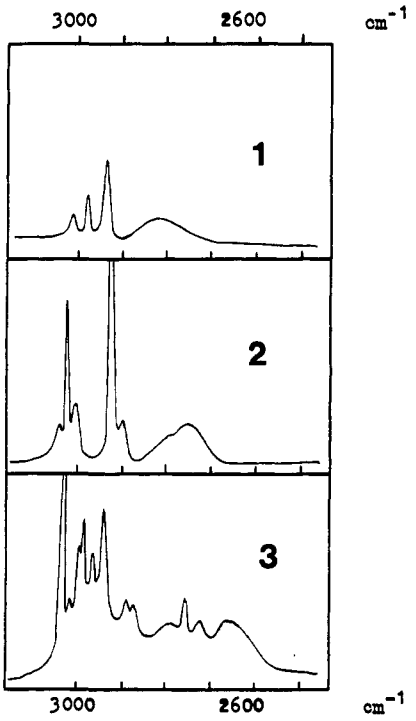

Figure 47. Raman spectra of the solid deca-*B*-chloro-*o*-carborane 1:1 adducts with DMFA (1); DMSO (2); and triethylamine (3).

tones and combinations are derived from fundamentals having more or less pronounced δ(CH) character (bands in the region 1100–1260 cm^{-1}).

The authors[47] succeeded in identifying the hydrogen bond C–H···O vibration among the low-frequency intermolecular vibrations by examining the IR and Raman spectra of solid adducts and their deuterated derivatives. A rather broad band at 133 cm^{-1} in the DMSO (126 cm^{-1} in DMFA) complex with *o*-DCC is assigned to this mode.

Recently, the dimerization of esters of *B*-carboranylphosphonic acids was established by IR spectroscopy, which is due to C–H···O=P hydrogen bonding.[179]

D. Vibrational Spectra and Structure of DCC H-Complexes with Nitrogen Bases

1. Pyridine

Solid *o*- and *m*-DCC complexes with pyridine (Py) were described[47,170] and their structures elucidated by IR and Raman spectroscopy. Two types of 1:2 complexes were isolated, designated as I and II, respectively, which substantially differ in their IR spectra (see Figure 48).

The spectrum of complex I is characteristic of a strongly C–H···N hydrogen-bonded adduct since the in-plane skeletal vibrations of pyridine in the 1400–1700-cm^{-1} region give rise to a pattern typical for pure[180] or hydrogen-bonded[181] pyridine. Much the same applies to the adduct of *o*-DCC with Py-d_5. The spectrum of the latter also allows us to identify the δ(CH) bands at 1275 and 1215 cm^{-1}. The CH stretching band, very strong and broad, is centered near 2500 cm^{-1}, its half-width is estimated to be about 500 cm^{-1} (Figure 48; 1 and 2). The band has a complicated structure which can be explained by Fermi resonance in much the same way as for C–H···O complexes.

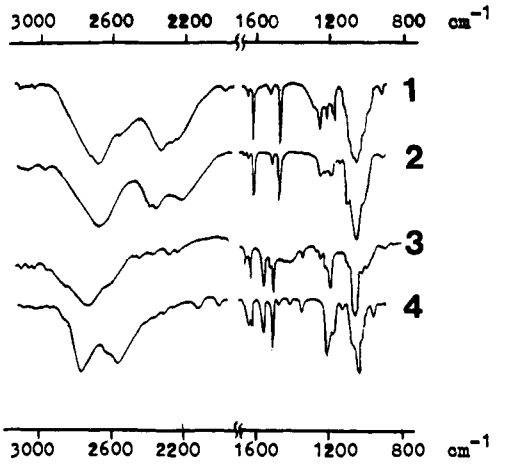

Figure 48. IR spectra of the solid deca-*B*-chlorocarborane complexes with pyridine: 1, *o*-DCC·2Py(I); 2, *m*-DCC·2Py(I); 3, *o*-DCC·2Py(II); and 4, *m*-DCC·2Py(II).

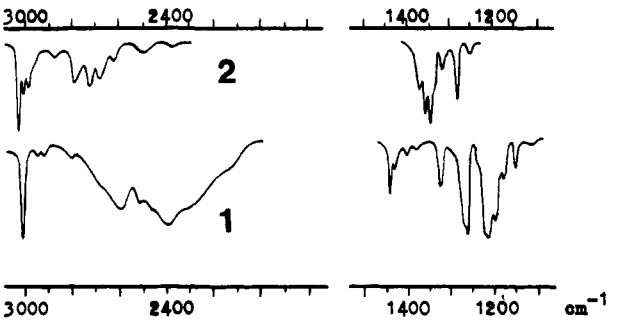

Figure 49. IR spectra of the solid deca-*B*-chloro-*o*-carborane 1:1 complexes with trimethylamine (1) and triethylamine (2).

The spectrum of DCC·2Py complex of the type II is entirely different (Figure 48; 3 and 4), in particular in the 1400–1700 cm^{-1} region. There are four strong bands which are characteristic of protonated pyridine. Their frequencies and relative intensities are very similar to those of solid pyridinium chloride.[182] Furthermore, the strong δ(CH) bands in the region 1200–1300 cm^{-1} disappear entirely from the spectrum. Thus, DCC adducts with Py of the type II contain a proton-transfer hydrogen bond of the type $N–H^+···C^-$. The corresponding ν(NH) stretching band centered near 2720 cm^{-1} for *o*-DCC and near 2600 cm^{-1} for *m*-DCC adducts has a structure which is quite different from that of the ν(CH) band of the complexes I. The lower ν(NH) frequency of the *m*-DCC complex can be correlated with the lower acidity of *m*-DCC and thus the higher basicity of the conjugated base.

It is significant that the isotopic substitution of Py by Py-d_5 changes the structure of the NH stretching absorption band in the same way as in the spectra of pyridinium halides.[182] Substitution of DMSO by DMSO-d_6 in the *o*-DCC·DMSO adduct, on the other hand, does not change the ν(CH) band shape at all.

2. Aliphatic Amines

DCC adducts with aliphatic amines were first described in ref 46. Their structures were elucidated by IR and Raman spectroscopy.[47] The IR spectra of *o*-DCC and *m*-DCC adducts with trimethylamine (TMA) and triethylamine (TEA) and of some deuterated derivatives have been studied; two of them are given in Figure 49. All these complexes are 1:1 adducts and

their spectra show a "free" ν(CH) carborane band near 3030 cm^{-1}.

The *o*-DCC·TMA complex contains a C–H···N hydrogen bond, similar to that of *o*-DCC·2Py complex I. The broad ν(CH) band center of gravity has a frequency near 2470 cm^{-1}, i.e. lower than any other C–H···Y hydrogen bonded adduct investigated (Figure 49; 1). This very low frequency and the band shape rule out the possibility of ascribing the broad and strong band to the NH stretching vibration of the Me_3NH^+ cation. The ν(NH) frequencies of trimethylammonium halides are considerably higher and the band structures are different.[183] Finally, a strong CH bending band near 1250 cm^{-1} can be identified in the spectrum of the *o*-DCC·TMA complex. Similar conclusions were drawn for an analogous adduct with *C*-monomethylated *o*-DCC.

The *o*-DCC·TEA adduct, however, shows a spectrum (Figure 49; 2) of the N–H^+···C^- proton transfer hydrogen bond. The average frequency of the NH stretching band triplet is found near 2720 cm^{-1}, i.e. higher than the ν(CH) frequency of the *o*-DCC·TMA complex. If there were a C–H···N hydrogen bond with TEA, its CH stretching vibration ought to absorb below 2500 cm^{-1} because TEA is more basic than pyridine. Furthermore, the ν(NH) band structure is widely different from that of the ν(CH) band but similar to that observed in the spectra of triethylammonium salts,[184,185] in particular of Et_3NHBr.

The same conclusion can be reached for the *m*-DCC·TEA complex. In this case the N–H^+···C^- hydrogen bond is, however, stronger as indicated by its lower (2550 cm^{-1}) ν(NH) frequency and lower ν(NH)/ν(ND) isotopic frequency ratio.[186] The reason must be the same as for pyridinium carboranides, *m*-DCC being a weaker acid than *o*-DCC. Finally, a comparison of the spectra of triethylammonium carboranides with their CD deuterated derivatives permits us to identify the δ(NH) bending band near 1450 cm^{-1}, which is close to the δ(NH) frequency of Et_3NHBr observed at 1432 cm^{-1}.

E. Enthalpies of Hydrogen Bonding in DCC Solid Adducts

Enthalpies of formation of DCC solid complexes can be estimated roughly from the shift of the AH stretching frequency (center of gravity of the broad structured band), using Iogansen's relationship 2, mentioned above.

In the cases of all amino complexes, ΔH values have been found to lie within the limits of 7–8 kcal mol^{-1}. This means that (energetically speaking) there is not much difference between the intermolecular C–H···N and the interionic C^-···$^+$H–N hydrogen bonds of the complexes studied and that molecular or ionic types of the hydrogen bond are determined in each particular case by secondary factors such as crystal packing, solvent, and temperature.

The formation of hydrogen-bonded molecular complexes or ion pairs and the existence of the equilibrium

$$A\text{–}H\cdots N \rightleftharpoons A^-\cdots{}^+H\text{–}N$$

have been studied for other systems in solution as a function of the solvent and amine concentration (see the review[187] and references therein). In the case of complexes of carboxylic acids with amines,[188] for instance, it has been shown that the equilibrium

$$O\text{–}H\cdots N \rightleftharpoons O^-\cdots{}^+H\text{–}N$$

is shifted entirely toward ion-pair formation when the corresponding enthalpy attains a value of ca. 11–13 kcal mol^{-1}. However, this conclusion is likely to be valid only for O–H···N systems and cannot be applied to C–H···N hydrogen bonds. For the latter the equilibrium is shifted toward the ion-pair side at considerably smaller enthalpy values as shown by the data[47,170] discussed above and also by NMR results obtained for other C–H···Y systems in solution.[189]

VIII. Regularities in Vibrational Spectra of Different Carboranes and Parent Boranes

Having presented all the spectral information available, it is now time to make some generalizations and to find regularities in the spectral behavior of carboranes.

A. Cage Rigidity Manifestation

The specific electronic structure of deltahedral *closo*-borate and *closo*-carborane clusters leads to cage rigidity which manifests itself in the high frequencies of the cage deformation modes and thus in the absence of low-frequency modes (lower than 450 cm^{-1}) from the vibrational spectra of all such molecules, irrespective of polyhedron size.[9,10,19,28,38,84,90,92,96] It is of interest that the spectra of unsubstituted dicarba-*nido*-undecaborates point to rigidity of these nido polyhedrons as well.[30]

In contrast, for small nido cluster $C_2B_4H_8$ a weak low-frequency Raman feature at 180 cm^{-1} is reported;[141] however, this fact alone is not enough to conclude that small nido polyhedrons are more flexible; this problem deserves further studies.

From the point of view of molecular vibrations, the cage rigidity leads to peculiar consequences. During the stretching vibration of the bond between the cage and the substituent X (whether it be a B–X or a C–X bond), the cage vibrates as a whole, as a pseudoatom. This vibration should be, in essence, looked upon not as a B–X or C–X but as a "cage–X" stretching motion. Such an approach allows us to consider this mode as a vibration of a quasidiatomic molecule and to rationalize its low frequency.[29,58,61–65,85,92,94] Thus, the spectrum of a substituted closo cluster appears to be divided in two parts, the first one consisting of the internal cage modes while the second consists of modes with substituent participation. This approach facilitates the spectral interpretation and enables an approximate estimation of the "cage–X" stretching frequencies. It was developed and successfully used for substituted icosahedral carboranes and octahedral borates. Its limitations are discussed in section III.D.

B. Spectral Regularities in the Series $B_nX_n^{2-}$; n = 6, 9, 10, 12, X = H, Cl, Br, I

Among the *closo*-borates $B_nX_n^{2-}$, only the vibrational spectra of $B_{12}X_{12}^{2-}$,[19,28] $B_{10}X_{10}^{2-}$,[84] and $B_6X_6^{2-}$[38,92] have been analyzed in any detail. The Raman and IR spectra of $B_9H_9^{2-}$ have been presented[43] only as pictures without precise frequency values and Raman polarization data.

TABLE XV. Salient Features (cm^{-1}) in the Spectra of *closo*-Carboranes and Parent *closo*-Borate Anions

borate		carborane[a]	
		$1,5\text{-}C_2B_3H_5$	
		ν(skel)	842
			1125
		ν(BH)	2622
		ν(CH)	3158
$B_6H_6^{2-}$		$1,6\text{-}C_2B_4H_6$	
ν(BB)	994	ν(skel)	986
			1096
ν(BH)	2448	ν(BH)	2660
		ν(CH)	3118
		$2,4\text{-}C_2B_5H_7$	
		ν(skel)	837
			889
			944
			983
		ν(BH)	2633
		ν(CH)	3096
$B_{10}H_{10}^{2-}$		$1,10\text{-}C_2B_8H_{10}$	
ν(BB)	741	ν(skel)	737
	836		875
			1120
ν(BH)	2471	ν(BH)	2600
		ν(CH)	3106
$B_{12}H_{12}^{2-}$		$1,12\text{-}C_2B_{10}H_{12}$	
ν(BB)	745	ν(skel)	765
			780
			1028
ν(BH)	2480	ν(BH)	2610
		ν(CH)	3060

[a] ν(CH), the frequency of the CH stretching band; ν(BH), the average frequency of all spectroscopically active ν(BH) modes; ν(skel), the frequencies of strong polarized Raman lines.

The polyhedrons mentioned above belong to different symmetry point groups: I_h, D_{4d}, O_h, and D_{3h}, respectively. While considering their symmetry species, one can see that, in spite of the facts, that the icosahedron contains twice as many boron atoms as octahedron and that the O_h group is not a subgroup of I_h, the selection rules allow the same number of modes of these two polyhedra to be active in Raman and IR. So the analogy here is straightforward (what was first noted in ref 38). The two other polyhedra are less symmetrical. Nevertheless, it is possible to compare the frequencies of related modes, close in symmetry and character. Some data on *closo*-hydroborates $B_nH_n^{2-}$ are given in Table XV (see also Tables II, XI, and XII), which demonstrate the similar frequency values of corresponding modes irrespective of the cage size. The same has been noted by Bragin et al.,[38] who compared the spectra of icosahedral and octahedral species, and by Brint et al.[43] The latter authors have concentrated on BH stretching bands in the spectra of the more extensive series $B_nH_n^{2-}$ (n = 6, 8–12) and inferred that the ν(BH) vibrations have much the same energy for the full range of cluster sizes. The recently established correlation between the ν(BH) frequency and the nominal boron atom hybridization[190] allowed them to assign sp^2 hybridization to all BH groups in the full set of anions. Indeed, the average ν(BH) frequency values, estimated for $B_{12}H_{12}^{2-}$, $B_{10}H_{10}^{2-}$, and $B_6H_6^{2-}$ on the basis of their spectroscopically active mode frequencies, are 2480, 2471, and 2448 cm^{-1}, respectively, still exhibiting an albeit small dependence on the cage size.

TABLE XVI. Some Principal Force Constants for *closo*-Borates and *closo*-Carboranes (mdyne $Å^{-1}$)

description	$B_6H_6^{2-}$ (ref 38)	$1,6\text{-}C_2B_4H_6$ (ref 38)	$B_{12}H_{12}^{2-}$ ref 24	$B_{12}H_{12}^{2-}$ ref 28	$C_2B_{10}H_{12}$ (ref 33)
BH stretch	3.2	3.8	3.4	3.08	4.0
BB stretch	3.4	3.8	1.4	1.16	0.66
BC stretch		3.9			1.04
CH stretch		5.3			5.53

Similar frequencies for the corresponding modes necessarily suggest similar force fields. The latter seems rather unexpected in view of the different boron coordination numbers, the different formal polyhedron edge bond orders, and the B–B distances.[191] Thus it is better to wait for normal coordinate calculations across the full series of anions, using the same internal coordinate basis, to be carried out, which will put all vibrational data on a common footing. The force constants available to date for $B_{12}H_{12}^{2-}$ [24,28] and $B_6H_6^{2-}$,[38] which can be found in Table XVI, are not comparable due to the different bases for the representation of the two potential functions.

We will comment on the behavior of totally symmetrical stretching modes of the cage, which show themselves as the most intense strongly polarized Raman lines. For the highly symmetrical $B_{12}H_{12}^{2-}$ and $B_6H_6^{2-}$, there is only one such vibration, being the in-phase breathing of the skeletal and hydrogen shells with respect to one another (with predominant ν(BB) participation.[28,38] For polyhedra of lower symmetry, there are two or more such skeletal modes, identified by their high intensity and low depolarization ratio in Raman. Table XV shows the obvious trend of these mode frequencies to increase with the decrease in cage size. This is evidently due to a kinetic energy effect, because a quite analogous situation is observed for the ring breathing mode of aromatic carbocyclic systems C_nH_n, although their spectra can be reproduced using one and the same force field.[192]

The spectral changes in the series X = H, Cl, Br, I were followed in Table XI for $B_{12}X_{12}^{2-}$ and $B_{10}X_{10}^{2-}$ and in Table XII for $B_6X_6^{2-}$. The comparison of these data shows analogous frequency and intensity behavior of related modes, close in symmetry and character. For instance, for $B_nX_n^{2-}$ where X = Cl the frequencies of the totally symmetrical ν_2 mode with ν(BCl) participation are 300, 303, and 328 cm^{-1} when n = 12, 10, and 6, respectively. Analogous values of ν(BBr) for X = Br are 194, 193, and 207 cm^{-1}; and for X = I analogous values of ν(BI) are much the same: 145, 145, and 151 cm^{-1}.

The similar frequency values of the corresponding modes are striking, pointing to similar force fields and thus to similar bonding in all $B_nX_n^{2-}$ *closo*-borates with the same X, regardless of cage size and shape, which is in keeping with their equally high stability.[193] However, we repeat that this conclusion will be strictly confirmed only after normal coordinate analysis produced on the full set of anions in one and the same coordinate basis.

C. From a *closo*-Borate to a Corresponding Carborane

We can follow the spectral changes observed on going from a *closo*-borate $B_nH_n^{2-}$ to an isoelectronic carborane

TABLE XVII. Some Spectral and Chemical Properties of the C-H Bond in *closo*-Carboranes

carborane	coordination number of carbon atom	ν(CH),[a] cm^{-1}	$A_{CH} \times 10^{-3}$,[b] l mol^{-1} cm^{-2}	ΔH,[c] kcal mol^{-1}	pK_a
1,5-$C_2B_3H_5$	4	3158	-		
1,6-$C_2B_4H_6$	5	3118	-		
2,4-$C_2B_5H_7$	5	3096	vw		
1,10-$C_2B_8H_{10}$	5	3106	0.70	1.7	27.3[d]
1,12-$C_2B_{10}H_{12}$	6	3060	0.75	2.2	26.8[d]
1,7-$C_2B_{10}H_{12}$	6	3065	1.2	2.5	25.6[d]
1,2-$C_2B_{10}H_{12}$	6	3075	1.6	2.8	22.0[d]
1,7-$C_2B_{10}Cl_{10}$	6	3037	8.4	7.8	9.19[e]
1,2-$C_2B_{10}Cl_{10}$	6	3046	10.0	8.1	6.89[e]

[a] ν(CH), frequency of the ν(CH) band (refs 96, 90, 41, and 47). [b] A_{CH}, integrated intensity of the IR ν(CH) band (in CCl_4 solution) (refs 90, 168, and 169). [c] ΔH, enthalpy of CH···O hydrogen bond formation with standard base DMSO (in solution) (refs 90, 168, and 169). [d] Kruglyak, L. I.; Kalinin, V. N.; Rys, E. G.; Zakharkin, L. I.; Shatenstein, A. I. *Zhurn. Obshch. Khim.* **1972**, *42*, 2670. [e] Reference 48.

$C_2B_{n-2}H_n$ also in the cases of the corresponding icosahedra (n = 12), Archimedian antiprisms (n = 10), and octahedra (n = 6). The latter case, namely, transformation of the *closo*-hexaborate anion $B_6H_6^{2-}$ into the 1,6-dicarba-*closo*-hexaborane $C_2B_4H_6$ has been investigated by Bragin et al.,[38] who not only compared their vibrational spectra but also produced normal coordinate calculations and presented principal force constants (Table XVI). Comparison of corresponding mode frequencies and force constants shows that substitution of BH^- by CH in the boron skeleton results in a stronger molecular bonding. Thus, the symmetrical ν(BH) frequency increases essentially from 2498 to 2667 cm^{-1}, the corresponding K_{BH} values being 3.2 and 3.8 mdyne/Å. The skeletal frequencies are not strictly comparable because of the different symmetry of the two molecules and the mixed character of the cluster cage modes. However, on going from the $B_6H_6^{2-}$ anion to the $C_2B_4H_6$ carborane the K_{BB} force constant increases from 3.4 to 3.8 and a new K_{BC} = 3.9 mdyne/Å appears, both leading to a strengthening of the polyhedron bond.

Unfortunately, for "large" and "medium" species we cannot compare force constants in the same way since the corresponding data are not available. Although normal coordinate analyses have been performed on both $B_{12}H_{12}^{2-}$ [28] and $C_2B_{10}H_{12}$,[33] the force constants obtained (Table XVI) are not comparable, again because of the different internal coordinate basis employed. However, a comparison of the corresponding related frequencies again reveals their increase, though the difference is not so pronounced as for the "small" species. For icosahedral polyhedra, the spectral transformation "borate–carborane" was followed in detail in section II.D.

Thus, vibrational spectra substantiate the conclusion that, on going from a *closo*-borate to a corresponding *closo*-carborane, all the bonds of the deltahedron undergo significant strengthening.

D. Carboranes of Different Size and Structure

Full vibrational data are available for the *closo*-carboranes $C_2B_{n-2}H_n$, n = 12, 10, 7, 6, 5, and the *nido*-carboranes $C_2B_4H_8$ and $C_2B_9H_{12}^-$.

The mean ν(BH) frequencies for *closo*-carboranes all lie in the range 2600–2660 cm^{-1}, being equal to 2611, 2600, 2633, 2660, and 2622 cm^{-1} for n = 12, 10, 7, 6, and 5, respectively, and thus showing no correlation either with the cage size, or with boron coordination number. It is noticeable that the ν(BH) value for 1,6-$C_2B_4H_6$ is the highest among the carboranes, while the corresponding value for $B_6H_6^{2-}$ is the lowest among the *closo*-borates (see above). A rough correlation between BH stretching frequency and BH NMR coupling constants has been reported for a number of boranes and carboranes;[96] however, these properties do not correlate with the BH bond length.[38]

While considering the strange ν(BH) behavior it is pertinent to remember that substitution of two BH^- groups in $B_{12}H_{12}^{2-}$ either by two more electronegative CH groups, or by two more electropositive CH_3–Si groups[51] each leads to the increase in the average ν(BH) frequency (2611 and 2550 cm^{-1}, respectively, compared to 2480 cm^{-1}).

On going to nido structures, the ν(BH) overall band moves to lower frequencies with respect to the parent *closo*-carborane, which was first noted by Hawthorne et al.[143] for $C_2B_9H_{12}^-$ anions.

It is not of much use to compare the skeletal mode frequencies presented in Table XV because these vibrations are of mixed origin, having different displacement eigenvectors in different polyhedra. Unfortunately, comparable data on the corresponding force constants are not available (see above).

As repeatedly emphasized above, the most informative feature in the vibrational spectrum of a carborane is a pure, well-localized CH stretching mode, its characteristics being extremely sensitive to all intra- and intermolecular effects. The behavior of the ν(CH) stretch in the carborane series in question will be the last, but not least important point of our discussion. Relevant data are outlined in Table XVII.

The position of the ν(CH) band obviously depends on the coordination number of the carbon atom.[194] The highest frequency, 3160 cm^{-1}, is observed for the smallest carborane 1,5-$C_2B_3H_5$ with its four-coordinated carbon atoms. If the coordination number increases by 1, the ν(CH) frequency decreases by about 50 cm^{-1}. Indeed, all carboranes with five-coordinated carbon atoms exhibit ν(CH) values near 3100 cm^{-1}, irrespective of their size: 1,6-$C_2B_4H_6$, 3118 cm^{-1}; 2,4-$C_2B_5H_7$, 3096 cm^{-1}; and 1,10-$C_2B_8H_{10}$, 3106 cm^{-1}. All icosahedral carboranes in which carbon atoms occupy six-coordinate positions exhibit the ν(CH) band in the region 3040–3080 cm^{-1}, its exact frequency depending on the molecular structure and the substitution (see sections II.E. and III.E).

A similar dependence of the ^{13}C NMR chemical shifts of carboranes on the coordination number of the carbon atoms was noted by Todd.[195]

If we apply the well-known correlation between the ν(CH) frequency and the s character of carbon atom to carboranes we could infer that the carbon atom hybridization in carboranes is close to sp^2. The same qualitative conclusion can be drawn in terms of the polyhedron external BCH angle values taken as a measure of s character. Spin coupling constants in the ^{13}C NMR spectra of icosahedral carboranes are also close to those observed for molecules with sp^2 carbon atoms,[196] while the NQR spectra of icosahedral chlorocarboranes point to sp^3 carbon atoms.[197]

Jotham and Reynolds have argued that high carborane ν(CH) frequencies reflect the high electron-withdrawing power of the whole carborane nucleus.[96] However, this is not the case, because B-chlorination of icosahedral carboranes, leading to a significant increase in electron-withdrawing power, results in the decrease of the ν(CH) frequency from ca. 3070 to ca. 3040 cm^{-1}.[10]

Only one ν(CH) frequency is observed for all *closo*-carboranes, even if two CH groups are adjacent, due to the weak coupling of CH oscillators.[41] The different frequency values for Raman and IR ν(CH) bands reported for $C_2B_5H_7$[96] (3096 and 3110 cm^{-1}) were obtained in different phase states and are not strictly comparable since the ν(CH) frequency is extremely sensitive to the phase state.

However, in *nido*-carboranes with two adjacent CH groups in the open face of the polyhedron,[30,141] CH coupling becomes appreciable and two ν(CH) bands are observed in both Raman and IR, the spacing being 10 cm^{-1}. Their frequencies are lowered by 30–50 cm^{-1} with respect to the parent closo species.

Some other carborane C–H bond properties were shown[194] to be connected with polarity. These are the integrated intensity of the ν(CH) IR band A_{CH}, the CH groups ability to hydrogen bond (measured as enthalpy ΔH of H-complex formation with the standard base DMSO), and CH acidity pK_a (see Table XVII). The ν(CH) IR band is not observable in the spectra of the "small" 1,5-$C_2B_3H_5$ and 1,6-$C_2B_4H_6$,[95,96,98,100] its intensity is "very-very weak" for 2,4-$C_2B_5H_7$,[96] has normal values for "medium" and "large" carboranes, and reaches very high values for icosahedral deca-*B*-chlorocarboranes (see Table XVII). The values of ΔH and pK_a follow this trend. Moreover, the A_{CH}, ΔH, and pK_a values were shown to be linearly interrelated,[194] this is reasonable because all these properties are determined by the charge on carbon and hydrogen atoms (the references to charge distribution in carboranes can be found in a recent paper by Ott and Gimarc[198]).

The regularities found in the ν(CH) spectral behavior can help in solving particular structural problems and allow useful predictions to be made in the field of carborane C–H bonds properties.

References

(1) Onak, T. In *Comprehensive Organometallic Chemistry*; Wilkinson, G., Ed.; Pergamon Press: New York, 1982; Vol. 1, p 411.
(2) Grimes, R. N. *Carboranes*; Academic Press: New York, 1970.
(3) Schroeder, H.; Heying, T. L.; Reiner, J. R. *Inorg. Chem.* **1963**, *2*, 1092. Alexander, R. P.; Schroeder, H. *Inorg. Chem.* **1963**, *2*, 1107.
(4) Fein, M. M.; Bobinski, J.; Mayes, N.; Schwartz, N.; Cohen, M. S. *Inorg. Chem.* **1963**, *2*, 1111.
(5) Grafstein, D.; Dvorak, J. *Inorg. Chem.* **1963**, *2*, 1128.
(6) Papetti, S.; Heying, T. L. *J. Am. Chem. Soc.* **1964**, *86*, 2295.
(7) Zakharkin, L. I.; Stanko, V. I.; Bratzev, V. A.; Chapovski, Yu. A. *Dokl. Akad. Nauk SSSR* **1964**, *157*, 1149.
(8) Bukalov, S. S.; Leites, L. A.; Alexanyan, V. T. *Izv. Akad. Nauk SSSR, Ser. Khim.* **1968**, 929.
(9) Leites, L. A.; Vinogradova, L. E.; Bukalov, S. S.; Alexanyan, V. T. *Izv. Akad. Nauk SSSR, Ser. Khim.* **1975**, 566.
(10) Leites, L. A.; Vinogradova, L. E.; Alexanyan, V. T.; Bukalov, S. S. *Izv. Akad. Nauk SSSR, Ser. Khim.* **1976**, 2480.
(11) Leites, L. A.; Bukalov, S. S. *J. Raman Spectrosc.* **1978**, *7*, 235.
(12) Bukalov, S. S.; Leites, L. A. *Chem. Phys. Lett.* **1982**, *87*, 327.
(13) Bukalov, S. S.; Leites, L. A.; Blumenfeld, A. L.; Fedin, E. I. *J. Raman Spectrosc.* **1983**, *14*, 210.
(14) Blumenfeld, A. L.; Bukalov, S. S.; Fedin, E. I.; Leites, L. A. *Khim. Fizika* **1985**, *4*, 191.
(15) Leites, L. A.; Vinogradova, L. E.; Kalinin, V. N.; Zakharkin, L. I. *Izv. Akad. Nauk SSSR, Ser. Khim.* **1968**, 1016.
(16) Hoard, J. L.; Haghes, R. E. In *The Chemistry of Boron and its Compounds*; Muetterties, E. L., Ed.; Wiley & Sons: New York, 1967; p 25.
(17) Muetterties, E. L.; Merrifield, R. E.; Miller, H. C.; Knoth, W. H.; Downing, J. R. *J. Am. Chem. Soc.* **1962**, *84*, 2506.
(18) Abdul-Fattah, M.; Butler, I. S. *Can. J. Spectrosc.* **1977**, *22*, 112.
(19) Leites, L. A.; Bukalov, S. S.; Kurbakova, A. P.; Kagansky, M. M.; Gaft, Yu. L.; Kuznetsov, N. T.; Zakharova, I. A. *Spectrochim. Acta* **1982**, *38A*, 1047.
(20) Muetterties, E. L.; Balthis, J. H.; Chia, Y. T.; Knoth, W. H.; Miller, H. C. *Inorg. Chem.* **1964**, *3*, 444.
(21) Kuznetsov, N. T.; Klimchuk, G. S.; Kanaeva, O. A.; Solntsev, K. A. *Zhurn. Neorg. Khimii* **1976**, *21*, 927.
(22) Knoth, W. H.; Miller, H. C.; Sauer, J. C.; Balthis, J. H.; Chia, Y. T.; Muetterties, E. L. *Inorg. Chem.* **1964**, *3*, 159.
(23) Kuznetsov, N. T.; Kulikova, L. N.; Zhukov, S. T. *Zhurn. Neorg. Khim.* **1976**, *21*, 96.
(24) Weber, W.; Thorpe, M. F. *J. Phys. Chem. Sol.* **1975**, *36*, 967.
(25) Boyle, L. L.; Parker, Y. M. *Mol. Phys.* **1980**, *39*, 95.
(26) Cyvin, S. I.; Cyvin, B. N. *Spectrosc. Lett.* **1984**, *17*, 125.
(27) Cyvin, S. I.; Brunvoll, J.; Cyvin, B. N. *Spectrosc. Lett.* **1984**, *17*, 569.
(28) Cyvin, S. I.; Cyvin, B. N. *Spectrochim. Acta* **1986**, *42A*, 985.
(29) Srebny, H.-G.; Preetz, W.; Marsmann, H. C. *Z. Naturforsch.* **1984**, *39b*, 189.
(30) Leites, L. A. Dr. Sci. Thesis, Institute of Organo-Element Compounds, Moscow, 1987.
(31) Cyvin, S. I. Private communication.
(32) Woodward, L. A.; Hall, J. R.; Dixon, R. N.; Sheppard, N. *Spectrochim. Acta* **1959**, *15*, 249.
(33) Klimova, T. P.; Gribov, L. A.; Stanko, V. I. *Opt. Spektroskop.* **1974**, *35*, 1112.
(34) Gribov, L. A.; Klimova, T. P.; Raichstatt, M. M. *J. Mol. Spectr.* **1979**, *56*, 125.
(35) Lipscomb, W. N. *Boron Hydrides*; Amsterdam, 1963.
(36) Gordy, W. *J. Chem. Phys.* **1946**, *14*, 305.
(37) Koetzle, T. F.; Lipscomb, W. N. *Inorg. Chem.* **1970**, *9*, 2743.
(38) Bragin, J.; Urevig, D. S.; Diem, M. *J. Raman Spectr.* **1982**, *12*, 86.
(39) Kochikov, I. V.; Kuramshina, G. M.; Pentin, Yu. A. *Zhurn. Fiz. Khim.* **1987**, *61*, 865.
(40) Tallant, D. R.; Aselage, T. L.; Campbell, A. N.; Emin, D. *Phys. Rev. B* **1989**, *40*, 5649.
(41) Leites, L. A.; Bukalov, S. S. *Izv. Akad. Nauk SSSR, Ser. Khim.* **1989**, 2263.
(42) Bartet, B.; Freymann, R.; Gandolo, D.; Mathey, G. et al. *C. R. Acad. Sci. Paris* **1974**, *279B*, 283.
(43) Brint, P.; Sangchakr, B.; Fowler, P. W.; Weldon, V. J. *J. Chem. Soc., Dalton Trans.* **1989**, 2253.
(44) Plešek, J.; Hanslík, T.; Hanousek, F.; Heřmánek, S. *Coll. Czech. Chem. Commun.* **1972**, *37*, 3403.
(45) Zakharkin, L. I.; Stanko, V. I.; Klimova, A. I. *Izv. Akad. Nauk SSSR, Ser. Khim.* **1966**, 1946.
(46) Leites, L. A.; Ogorodnikova, N. A.; Zakharkin, L. I. *J. Organomet. Chem.* **1968**, *15*, 287.
(47) Leites, L. A.; Vinogradova, L. E.; Belloc, J.; Novak, A. *J. Mol. Struct.* **1983**, *100*, 379.
(48) Zakharkin, L. I.; Ogorodnikova, N. A. *J. Organomet. Chem.* **1968**, *12*, 13.
(49) Vinogradova, L. E.; Kyskin, V. I.; Leites, L. A.; Zakharkin, L. I. *Izv. Akad. Nauk SSSR, Ser. Khim.* **1972**, 2436.
(50) Seyferth, D.; Büchner, K.; Rees, W. S., Jr.; Davis, W. M. *Angew. Chem.* **1991**, in press.
(51) Seyferth, D.; Leites, L. A.; Bukalov, S. S. Unpublished results.
(52) Fontal, B.; Spiro, T. G. *Inorg. Chem.* **1971**, *10*, 9.
(53) Dernova, V. S.; Kovalev, I. F. *Kolebatel'nye Spektry Soedineniy Elementov IV B Gruppy (Vibrational Spectra of IV B Group Element Compounds)*; Izdatelstvo Saratovskogo Universiteta (Saratov University Press) Saratov, 1979; p 154.
(54) Bregadze, V. I.; Chumaevski, N. A.; Shkirtil, E. V. *Dokl. Akad. Nauk SSSR* **1968**, *181*, 910.

(55) Klimova, T. P.; Bratzev, V. A.; Anorova, G. A.; Gol'tyapin, Yu, V.; Stanko, V. I. *Zhurn. Prikl. Spektr.* **1974**, *21*, 874.
(56) Klimova, T. P.; Stanko, V. I.; Gribov, L. A. *Zhurn. Prikl. Spektr.* **1974**, *20*, 1049.
(57) Nikitin, V. S.; Grigos, V. I.; Pechurina, S. Ya. *Zhurn. Obshch. Khim.* **1976**, *46*, 1508.
(58) Vinogradova, L. E.; Leites, L. A.; Bukalov, S. S.; Kovredov, A. I.; Zakharkin, L. I. *Izv. Akad. Nauk SSSR, Ser. Khim.* **1977**, 2337.
(59) Hall, L. H.; Perloff, A.; Mauer, F. A.; Block, S. *J. Chem. Phys.* **1965**, *43*, 3911.
(60) Dorofeeva, O. V.; Mastryukov, V. S.; Vilkov, L. V.; Karimov, A. S. 9th Austin Symposium on Molecular Structure, Austin, TX, 1982, p 69.
(61) Leites, L. A.; Bukalov, S. S. *Organomet. Chem. USSR*, in press.
(62) Leites, L. A.; Vinogradova, L. E.; Bukalov, S. S.; Kampel, V. Ts.; Bregadze, V. I. *Izv. Akad. Nauk SSSR, Ser. Khim.* **1981**, 2035.
(63) Usiatinsky, A. Ya.; Bregadze, V. I.; Godovikov, N. N.; Vinogradova, L. E.; Leites, L. A.; Yanovsky, A. I.; Struchkov, Yu. T. *Izv. Akad. Nauk SSSR, Ser. Khim.* **1984**, 2009.
(64) Leites, L. A.; Vinogradova, L. E.; Bukalov, S. S.; Garbuzova, I. A.; Petriashvili, M. V.; Kampel, V. Ts.; Bregadze, V. I. *Organomet. Chem. USSR* **1989**, *2*, 337.
(65) Leites, L. A.; Vinogradova, L. E.; Bregadze, V. I.; Kampel, V. Ts.; Usiatinsky, A. Ya. *Inorg. Chim. Acta* **1978**, *31*, 467.
(66) Maslowsky, E. *Vibrational Spectra of Organometallic Compounds*; Wiley & Sons: New York, 1977.
(67) Mink, J.; Pentin, Yu. A. *Sovremennye Problemy Fisicheskoi Khimii, MGU (Modern Problems of Physical Chemistry, Moscow State University)* **1973**, *7*, 224.
(68) Barraclough, C. G.; Berkovic, G. E.; Deacon, G. B. *Austr. J. Chem.* **1977**, *30*, 1905.
(69) Goggin, P. L.; Kemeni, G.; Mink, J. *J. Chem. Soc., Faraday Trans.* 2 **1976**, *72*, 1025.
(70) Deacon, G. B.; Green, J. H. S.; Kunaston, W. *J. Chem. Soc. A* **1967**, 158.
(71) Lee, A. G. *Quart. Rev.* **1970**, *24*, 310.
(72) Grushin, V. V.; Bregadze, V. I.; Kalinin, V. N. *Organomet. Chem. Rev.* **1988**, *20*, 1.
(73) Clark, R. J. H.; Davies, A. G.; Puddephatt, R. J. *J. Chem. Soc. A* **1968**, 1828.
(74) Herzberg, G. *Infrared and Raman Spectra of Polyatomic Molecules*; Van Nostrand: Princeton, NJ, 1945; p 215.
(75) Leites, L. A.; Vinogradova, L. E.; Bukalov, S. S.; Lebedev, V. N.; Balagurova, E. V.; Zakharkin, L. I. *Metalloorg. Khim.* **1991**, *4*, 1073.
(76) Grushin, V. V.; Polyakov, A. V.; Yanovsky, A. I.; Struchkov, Yu. T.; Bukalov, S. S.; Leites, L. A. *Metalloorg. Khim.* **1991**, *4*, 828.
(77) Vinogradova, L. E.; Leites, L. A.; Gedymin, V. V.; Kalinin, V. N.; Zakharkin, L. I. *Izv. Akad. Nauk SSSR, Ser. Khim.* **1973**, 2817.
(78) Leites, L. A.; Vinogradova, L. E.; Bukalov, S. S.; Olshevskaya, V. A.; Kovredov, A. I.; Zakharkin, L. I. *Organomet. Chem. USSR* **1989**, *2*, 705.
(79) Carpenter, J. H.; Jones, W. J.; Jotham, R. W.; Long, L. H. *Spectrochim. Acta* **1970**, *26A*, 1199; **1971**, *27A*, 1721.
(80) Carroll, B. L.; Bartell, L. S. *Inorg. Chem.* **1968**, *7*, 219.
(81) Hoffman, R.; Lipscomb, W. N. *J. Chem. Phys.* **1962**, *36*, 2179; 3489.
(82) Volkov, V. V.; Posnaya, I. S.; Grankina, Z. A. *Izv. S. O. Akad. Nauk SSSR, Ser. Khim.* **1977**, 115.
(83) Volkov, V. V.; Posnaya, I. S. *Izv. Akad. Nauk SSSR, Ser. Khim.* **1980**, 400.
(84) Leites, L. A.; Kurbakova, A. P.; Kagansky, M. M.; Gaft, Yu. L.; Zakharova, I. A.; Kuznetsov, N. T. *Izv. Akad. Nauk SSSR, Ser. Khim.* **1983**, 2284.
(85) Preetz, W.; Srebny, H.-G.; Marsmann, H. C. *Z. Naturforsch.* **1984**, *39b*, 6.
(86) Zakharova, I. A. *Coord. Chem. Rev.* **1982**, *43*, 313.
(87) Zakharova, I. A.; Gaft, Yu. L.; Kuznetsov, N. T.; Salyn, Ya. V.; Leites, L. A.; Kurbakova, A. P.; Kagansky, M. M. *Inorg. Chim. Acta* **1981**, *47*, 181.
(88) Garret, P. M.; Smart, J. C.; Ditta, G. S.; Hawthorne, M. F. *Inorg. Chem.* **1969**, *8*, 1907.
(89) Garret, P. M.; Ditta, G. S.; Hawthorne, M. F. *Inorg. Chem.* **1970**, *9*, 1947.
(90) Leites, L. A.; Vinogradova, L. E.; Bukalov, S. S.; Alexanyan, V. T.; Rys, E. T.; Kalinin, V. N.; Zakharkin, L. I. *Izv. Akad. Nauk SSSR, Ser. Khim.* **1975**, 1985.
(91) Atavin, E. G.; Mastryukov, V. S.; Golubinsky, A. V.; Vilkov, L. V. *J. Mol. Struct.* **1980**, *65*, 259.
(92) Preetz, W.; Fritze, J. *Z. Naturforsch.* **1984**, *39b*, 1472.
(93) Kohlrausch, K. W. F. *Ramanspektren*, Leipzig, 1943; I, Section 4.
(94) Fritze, J.; Preetz, W. *Z. Naturforsch.* **1987**, *42b*, 293.
(95) Shapiro, I.; Keilin, B.; Williams, R. E.; Good, C. D. *J. Am. Chem. Soc.* **1963**, *85*, 3167.
(96) Jotham, R. W.; Reynolds, D. J. *J. Chem. Soc. A* **1971**, 3181.
(97) Urevig, D. S. M. S. Thesis, California State University, Los Angeles, 1974.
(98) Shapiro, I.; Good, C. D.; Williams, R. E. *J. Am. Chem. Soc.* **1962**, *84*, 3837.
(99) Grimes, R. N. *J. Am. Chem. Soc.* **1966**, *88*, 1895.
(100) Onak, T.; Dunks, G. B.; Beaudet, R. A.; Poynter, R. L. *J. Am. Chem. Soc.* **1966**, *88*, 4622.
(101) Köster, R.; Rotermund, G. W. *Tetrahedron Lett.* **1964**, *25*, 1667.
(102) Ebsworth, E. A. V.; Rankin, D. W. H.; Cradock, S. *Spectral Methods in Inorganic Chemistry*; Blackwell Sci. Publications: Oxford, 1987; p 178.
(103) Kitaigorodski, A. I. *Molecular Crystals and Molecules*; Academic Press: New York, 1973.
(104) *Physics and Chemistry of Organic Solid State*; Fox, D., et al., Eds.; Interscience Publishers J. Wiley & Sons: New York, 1965.
(105) *The Plastically Crystalline State*; Sherwood, J. N., Ed.; J. Wiley & Sons: New York, 1979.
(106) Parsonage, N. G.; Stavely, L. A. K. *Disorder in Crystals*; Clarendon Press: Oxford, 1978.
(107) Timmermans, J. *J. Chem. Phys.* **1938**, *36*, 331.
(108) Bukalov, S. S.; Leites, L. A. *Izv. Akad. Nauk SSSR, Ser. Fiz.* **1989**, *53*, 1715.
(109) Leites, L. A.; Bukalov, S. S. *Proc. Int. Conf. Raman Spectros.* **1990**, *12*, 428.
(110) Bukalov, S. S.; Leites, L. A. *Proc. Int. Conf. Raman Spectros.* **1976**, *5*, 554.
(111) Blumenfeld, A. L.; Fedin, E. I. *Proc. Congr. AMPERE* **1979**, *20*, 584.
(112) Bukalov, S. S. Ph.D. Thesis, Leningrad State University, Leningrad, 1986.
(113) Zhizhin, G. N.; Losovik, Yu. E.; Moskaleva, M. A.; Usmanov, A. *Dokl. Akad. Nauk SSSR* **1970**, *190*, 301.
(114) Bertie, J. E.; Sunder, S. *J. Chem. Phys.* **1973**, *59*, 3853.
(115) Zhizhin, G. N.; Krasyukov, Yu. N.; Mukhtarov, E. I.; Rogovoy, V. N. *Pis'ma v ZhETF* **1978**, *28*, 465.
(116) Mukhtarov, E. I.; Rogovoy, V. N.; Krasyukov, Yu. N.; Zhizhin, G. N. *Opt. Spektroskop.* **1979**, *46*, 920.
(117) Beckman, P.; Leffler, A. J. *J. Chem. Phys.* **1980**, *72*, 4600.
(118) Selim, M.; Capderroquez, G.; Freymann, R. *C. R. Acad. Sci. Paris* **1975**, *281*, sB, 33.
(119) Baughman, R. H. *J. Chem. Phys.* **1970**, *53*, 3781.
(120) Beckman, P.; Wendel, A. *J. Chem. Phys.* **1980**, *73*, 3514.
(121) Westrum, E. F.; Henriquez, S. *Mol. Cryst. Liq. Cryst.* **1976**, *32*, 31.
(122) Leffler, A. J.; Alexander, M. N.; Sagalin, P. L.; Walker, N. *J. Chem. Phys.* **1975**, *63*, 3971.
(123) Reynhardt, E. C.; Watton, A.; Petch, U. E. *J. Magn. Reson.* **1982**, *46*, 453.
(124) Gal'chenko, G. L.; Martynovskaya, L. N.; Stanko, V. I. *Dokl. Akad. Nauk SSSR* **1969**, *186*, 1328; *188*, 587.
(125) Hones, M. J.; Shaw, D. E.; Wunderlich, F. J. *Spectr. Lett.* **1973**, *6*, 483.
(126) Adachi, K.; Suga, N.; Seki, S. *Bull. Chem. Soc. Jpn.* **1968**, *41*, 1073.
(127) Adachi, K.; Suga, N.; Seki, S. *Bull. Chem. Soc. Jpn.* **1970**, *43*, 1916.
(128) Haida, O.; Suga, N.; Seki, S. *Chem. Lett.* **1973**, 79.
(129) Eguchi, T.; Soda, G.; Chihara, H. *J. Magn. Reson.* **1975**, *23*, 55.
(130) Clark, T.; McKervey, M. A.; Mackle, H.; Booney, J. J. *J. Chem. Soc., Faraday Trans. 1* **1974**, *70*, 1279.
(131) Clark, T.; McKnox, T.; Mackle, H.; McKervey, M. A. *J. Chem. Soc., Faraday Trans. 1* **1977**, *73*, 1224.
(132) Bukalov, S. S.; Leites, L. A. *J. Raman Spectr.* **1985**, *16*, 326.
(133) Leites, L. A.; Bukalov, S. S. In *Spectroscopiya Molekul i Kristallov (Spectroscopy of Molecules and Crystals)*; Naukova Dumka: Kiev, 1978; p 117.
(134) Bukalov, S. S.; Leites, L. A. *Proc. USSR Conf. Raman Spectros.* **1986**, *3*, 125.
(135) Hesse, H. *Das Glassperlenspiel*; Switzerland, 1943.
(136) Emanuel, N. M.; Roginsky, V. A.; Buchachenko, A. L. *Uspekhi Khim.* **1982**, *51*, 361.
(137) Mikhailov, B. M.; Smirnov, V. N. *Izv. Akad. Nauk SSSR, Ser. Khim.* **1973**, 2165.
(138) Bukalov, S. S.; Leites, L. A.; Bubnov, Yu. N.; Gurski, M. E.; Potapova, T. V. *Izv. Akad. Nauk SSSR, Ser. Khim.* **1989**, 483.
(139) Spielman, J.; Warren, R.; Dunks, G.; Scott, J.; Onak, T. *Inorg. Chem.* **1968**, *7*, 216. Onak, T.; Dunks, G. *Inorg. Chem.* **1966**, *5*, 439.
(140) Grimes, R. N.; Bramlett, C. L.; Vance, R. L. *Inorg. Chem.* **1968**, *7*, 1066.
(141) Jotham, R. W.; McAvoy, J. S.; Reynolds, D. J. *J. Chem. Soc., Dalton Trans.* **1972**, 473.
(142) Wiesboeck, R. A.; Hawthorne, M. F. *J. Am. Chem. Soc.* **1964**, *86*, 1642.

(143) Hawthorne, M. F.; Young, D. C.; Garrett, P. M.; Owen, D. A.; Schwerin, S. G.; Tebbe, F. N.; Wegner, P. A. *J. Am. Chem. Soc.* **1968**, *90*, 862.
(144) Howe, D. V.; Jones, C. J.; Wiersema, R. J.; Hawthorne, M. F. *Inorg. Chem.* **1971**, *10*, 2516.
(145) Knyazev, S. P. Ph.D. Thesis, Moscow State University, Moscow, 1979.
(146) Janoušek, Z.; Heřmánek, S.; Plešek, J.; Štíbr, B. *Collect. Czech. Chem. Commun.* **1974**, *39*, 2363.
(147) Leites, L. A.; Bukalov, S. S.; Vinogradova, L. E.; Kalinin, V. N.; Kobel'kova, N. I.; Zakharkin, L. I. *Izv. Akad. Nauk SSSR, Ser. Khim.* **1984**, 954.
(148) Leites, L. A.; Bukalov, S. S.; Vinogradova, L. E.; Knyazev, S. P.; Strelenko, Yu. A. *Izv. Akad. Nauk SSSR, Ser. Khim.* **1986**, 1801.
(149) Leites, L. A.; Bukalov, S. S.; Grushin, V. V. *Izv. Akad. Nauk SSSR, Ser. Khim.* **1989**, 2639.
(150) Yanovsky, A. I.; Struchkov, Yu. T.; Kalinin, V. N.; Zakharkin, L. I. *Zhurn. Strukt. Khim.* **1982**, *23*, 77.
(151) Churchill, M. R.; DeBoer, B. G. *J. Am. Chem. Soc.* **1974**, *96*, 6310.
(152) Grushin, V. V.; Tolstaya, T. P.; Yanovsky, A. I.; Struchkov, Yu. T. *Izv. Akad. Nauk SSSR, Ser. Khim.* **1984**, 855.
(153) Vinas, C.; Butler, W. M.; Teixidot, F.; Rudolph, R. W. *Inorg. Chem.* **1986**, *25*, 4369.
(154) Heřmánek, S.; Jelinek, T.; Plešek, J.; Štíbr, B.; Fusek, J.; Mareš, F. In Boron Chemistry. *Proceedings of the 6th IMEBORON*, Bechyne, Czecho-Slovakia, World Scientifici London, 1987; p 26.
(155) Idelmann, P.; Müller, G.; Scheidt, W. R.; Schüssler, W.; Köster, R. *Angew, Chem.* **1984**, *23*, 153.
(156) Hanousek, F.; Stíbr, B.; Heřmánek, S.; Plešek, J. *Collect. Czech. Chem. Commun.* **1973**, *38*, 1312.
(157) Jayasooviya, U. A.; Stotesbury, S. J.; Grinter, R.; Powell, D. B.; Sheppard, N. *Inorg. Chem.* **1986**, *25*, 2853.
(158) Adler, B. A.; Hawthorne, M. F. *J. Am. Chem. Soc.* **1970**, *92*, 6174.
(159) Leites, L. A.; Vinogradova, L. E.; Kalinin, V. N.; Zakharkin, L. I. *Izv. Akad. Nauk SSSR, Ser. Khim.* **1970**, 2596.
(160) Korshak, V. V.; Danilov, V. G.; Komarova, L. G.; Bekasova, N. I.; Leites, L. A. *Vysokomolekulyarnye Soedineniya* **1971**, *13A*, 1517.
(161) Leites, L. A.; Katz, G. A.; Bukalov, S. S.; Komarova, L. G. *Izv. Akad. Nauk SSSR, Ser. Khim.* **1991**, 371.
(162) Hawthorne, M. F.; Dunks, G. B. *Science* **1972**, *178*, 462.
(163) Warren, L. F.; Hawthorne, M. F. *J. Am. Chem. Soc.* **1970**, *92*, 1157.
(164) Plešek, J.; Baše, K.; Mareš, F.; Hanousek, F.; Stíbr, B.; Heřmánek, S. *Collect. Czech. Chem. Commun.* **1984**, *49*, 2776.
(165) Leites, L. A.; Vinogradova, L. E. *Tezisy Dokl. I Vses. Konf. Metalloorg. Khim.* **1979**, II, 184.
(166) Alexanyan, V. T.; Lokshin, B. V. *Kolebatel'nye Spektry π-Kompleksov Perekhodnykh Metallov (Vibrational Spectra of Transition Metals π-Complexes)* Itogi Nauki i Techniki, 5, VINITI, Moscow, 1976.
(167) Sobolev, E. V.; Kradenov, K. V.; Volkov, V. V.; Vasil'eva, S. G. *Organomet. Chem. USSR* **1989**, *2*, 658.
(168) Vinogradova, L. E.; Leites, L. A.; Kalinin, V. N.; Zakharkin, L. I. *Izv. Akad. Nauk SSSR, Ser. Khim.* **1969**, 2847.
(169) Leites, L. A.; Vinogradova, L. E.; Ogorodnikova, N. A.; Zakharkin, L. I. *Zhurn. Prikl. Spektr.* **1972**, *16*, 488.
(170) Leites, L. A.; Vinogradova, L. E.; Zakharkin, L. I.; Novak, A.; Belloc, J. *Izv. Akad. Nauk SSSR, Ser. Khim.* **1980**, 696.
(171) Vinogradova, L. E.; Leites, L. A.; Bikkineev, R. Kh.; Kobak, V. V.; Zakharkin, L. I. *Izv. Akad. Nauk SSSR, Ser. Khim.* **1976**, 2641.
(172) Green, R. D. *Hydrogen Bonding by CH Groups*; McMillan Press: New York, 1974.
(173) Pogorely, V. K.; Vishnyakova, T. B. *Uspekhi Khim.* **1984**, *53*, 1985.
(174) Iogansen, A. V. In *Vodorodnaya Svyaz (Hydrogen Bonding)*; Sokolov, N. D., Ed.; Nauka: Moscow, 1981.
(175) Iogansen, A. V. *Teor. Eksp. Khim.* **1971**, *7*, 302.
(176) Kurkchi, G. A. *Zhurn. Prikl. Spectr.* **1967**, *6*, 829.
(177) Vinogradova, L. E.; Leites, L. A. *Zhurn. Prikl. Spektr.* **1975**, *23*, 260.
(178) Yanovsky, A. I.; Struchkov, Yu. T.; Vinogradova, L. E.; Leites, L. A. *Izv. Akad. Nauk SSSR, Ser. Khim.* **1982**, 2257.
(179) Bregadze, V. I.; Kampel, V. Ts.; Matrosov, E. I.; Antonovich, V. A.; Yanovsky, A. I.; Struchkov, Yu. T.; Godovikov, N. N.; Kabachnik, M. I. *Dokl. Akad. Nauk SSSR* **1985**, 285; 1127.
(180) Fax, B. J.; Corsin, L.; Lord, R. C. *J. Chem. Phys.* **1953**, *21*, 1170.
(181) Takahashi, H.; Mamola, K.; Plyler, E. K. *J. Mol. Spectrosc.* **1966**, *21*, 217.
(182) Foglizzo, R.; Novak, A. *J. Chim. Phys.* **1969**, *66*, 1539; *J. Chem. Phys.* **1969**, *50*, 5366.
(183) Huong, P. V.; Schlaak, M. *Chem. Phys. Lett.* **1974**, *27*, 111.
(184) Shenon, B.; Sandorfy, C. *Can. J. Chem.* **1958**, *36*, 1181.
(185) Glazunov, V. P.; Mashkovsky, A. A.; Odinokov, S. E. *J. Chem. Soc., Faraday Trans. 2* **1974**, *4*, 629.
(186) Novak, A. *Struct. Bonding* **1974**, *18*, 177.
(187) Gur'yanova, E. N.; Goldshtein, I. P.; Perepelkova, T. I. *Uspekhi Khim.* **1976**, *45*, 1568.
(188) Odinokov, S. E.; Mashkovsky, A. A.; Glazunov, V. P.; Iogansen, A. V.; Rassadin, B. V. *Spectrochim. Acta* **1976**, *32A*, 1335.
(189) Golubev, N. S.; Denisov, G. S. In *Mol. Spektrosk.* **1977**, *4*, 62.
(190) Brint, P.; Sangchakr, B.; Fowler, P. W. *J. Chem. Soc., Faraday Trans.* **1989**, *2*, 29.
(191) Wade, K. *Adv. Inorg. Chem. Radiochem.* **1976**, *18*, 1.
(192) Garbusova, I. A.; Garkusha, O. G.; Lokshin, B. V.; Mink, J. *Izv. Akad. Nauk SSSR, Ser. Khim.* **1988**, 2519.
(193) Jemmis, E. D.; Pavankumar, P. N. V. *Proc. Indian Acad. Sci. (Chem. Sci.)* **1984**, *93*, 479.
(194) Leites, L. A.; Vinogradova, L. E. *J. Organomet. Chem.* **1977**, *125*, 37.
(195) Todd, L. J. *Pure Appl. Chem.* **1972**, *30*, 587.
(196) Fedin, E. I.; Antonovich, V. A.; Rys, E. G.; Kalinin, V. N.; Zakharkin, L. I. *Izv. Akad. Nauk SSSR, Ser. Khim.* **1975**, 801.
(197) Stanko, V. I.; Semin, G. K.; Babushkina, T. *Dokl. Akad. Nauk SSSR* **1975**, *221*, 1129.
(198) Ott, J. J.; Gimarc, B. M. *J. Am. Chem. Soc.* **1986**, *108*, 4303.